Friedrich-Alexander University

of Erlangen-Nuremberg

Department of Materials Science

Glass and Ceramics

ANNUAL REPORT

2011

Preface

The year 2011 was characterized by an all-time high of staff number of more than 55 with 20% coming from abroad. New laboratory facilities in the new Department building at Fuerth (Pratum) provide about 150 m² laboratory and office spaces for research projects of the glass group. The research activities in the field of energy related materials were intensified. A large grant from the Bavarian State Government supports the establishment of the "Energy Campus Nuremberg". The five years project coordinated by Prof. L. Wondraczek aims on the development of glasses, ceramics and metals to be applied in solar thermal power systems. Furthermore, new research projects funded by DFG, "Neue Werkstoffe Bayern" as well as international industrial companies in Europe and overseas started in 2011. Coordinated by Prof. L. Wondraczek a new priority program funded by DFG "Topological Engineering of Ultra-Strong Glasses" was approved.

In 2011 a total number of 35 B.Sc., M.Sc., Dipl.-Ing Thesis and PhD Thesis were finished. Dr. N. Travitzky successfully completed his habilitation on "Ceramic-Metal Composites". Dr. C. Zollfrank accepted a call on a professorship "Biogenetic fiber composites" at the TU Munich and left the institute by the end of September 2011. A number of seminars and conferences were organized by our colleagues including "Characterization in Ceramics Processing: From Powders to green Bodies" (A. Roosen), "Glass strengthening" (L. Wondraczek), 4th Advanced Training Course on "Tape Casting and Ceramic Multilayer Technology" (A. Roosen). In November 2011 the second German-Japanese Seminar on "Advanced Ceramic Materials" involving more than 20 contributions from young researchers from the Department of Materials Sience Erlangen and the Nagoya Institute of Technology (NITech) took place at the institute.

Peter Greil, Andreas Roosen, Lothar Wondraczek

Team of the chair of glass and ceramics at the annual outing in front of Crailsheim castle

OUTLINE

1. INSTITUTE OF GLASS AND CERAMICS

Staff

Faculties

Prof. Dr. Peter Greil	Head of Institute
Prof. Dr. Andreas Roosen	Functional Ceramics
Prof. Dr. Lothar Wondraczek	Glass
PD Dr. Cordt Zollfrank*	Bioengineered Ceramics
PD Dr. Nahum Travitzky	Ceramics Processing

Secretaries

Candice Iwai	Evelyne Penert-Müller
Karin Bichler	Ursula Klarmann

Senior Research Staff

Dr.-Ing. Ulrike Deisinger	Ceramic Multilayer Processing
Dr.-Ing. Tobias Fey	Simulation and Cellular Ceramics

Research Staff

Advanced Engineering Ceramics and Rapid Prototyping

M.Sc. Benjamin Dermeik	Dipl.-Ing. Lorenz Schlier
Dipl.-Ing. Björn Gutbrod†	Dipl.-Ing. (FH) Tobias Schlordt
Dipl.-Ing. (FH) Christian Heiss†	

* Now Professor at the TU München

† Now in Industry

Bioengineered Ceramics

Dipl.-Ing. (FH) Kai Gutbrod*

Dipl.-Min. Sabine Gruber*

Dipl.-Ing. Daniel Van Opdenbosch

Biomaterials

Dipl.-Min. Anne-Kathrin Maier*

Dipl.-Ing. Birgit Joana Pedimonte

Functional Ceramics

Dipl.-Ing. Michael Beck

Dipl.-Ing. Armin Dellert*

Dipl.-Ing. (FH) Ingo Götschel

M. Sc. Torsten Schüler

Dipl.-Ing. Nadja Kölpin

Simulation and Cellular Ceramics

Dr. rer. nat. Andrea Dakkouri-Baldauf

Dipl.-Ing. Michael Götz

Dr. Young Jae Kang

M.Sc. Bruno Ceron Nicolat

M. Sc. Nataliya Müller*

Glass

Dr. rer. nat. Quentin Coulombier*

M.Sc. Ning Da

M. Sc. Guojun Gao

Dipl.-Ing. Sebastian Krolikowski

M. Sc. Na Liu*

M.Sc. Wenjie Li*

Dipl.-Ing. (FH) Robert Meszaros

Dr. Doris Möncke

M.Sc. Karsten Nielsen

Dipl.-Min. Sindy Reibstein

Dr. Sergey Sirotkin

Dipl.-Ing. Birgit Stolte

M. Sc. Weijuan Zhang*

Dipl.-Ing. Anja Winterstein

* Now in Industry

Technical Staff

Sabine Brungs

Evelyn Gruber

Dipl.-Ing. (FH) Helmut Hädrich

Beate Müller

Timotheus Barreto-Nunes

Heike Reinfelder

Peter Reinhardt

Alena Schenkel-Rybar

Eva Springer

Dipl.-Ing. Alfons Stiegelschmitt

Hana Strelec

Andreas Thomsen

Graduates

Student Research Projects

Dil, Roman

Design of a pressing tool

Kaiser, René

Calculation of packing densities of multi-modal powders

Khosravani, Arman

Manufacturing of celllular ceramics with periodic pore structures

Schkutow, Andreas

Residual stresses in polymer-derived laminate ceramics

Schumacher, Moritz

Solid free form fabrication of SiSiC precombustion nozzle

Zierath, Bodo

Glass formation in the systems P_2O_5-SiO_2-ZnO and P_2O_5-SnO-MgO

Bachelor Thesis

Artes, Galina

Influence of sintering atmosphere on the properties of PZT-multilayer actors

Brandl, Franziska

Optimization of drying thin ceramic films

Borchardt Rudolf

Efficiency optimization of a biomass reactor by means of spectral light conversion

Dil, Roman

Design of a pressing tool with variable powder filling

Dörnhöfer, Andrea

Influence of heat-treatment on the structure of micro-porous silica-based gels

Eichhorn, Franziska

Piezoelectrics with textured pore structures

Eckert, Denise

Fabrication of ultra-thin and transparent oxide layers

Friedrich, Bernhard

Formation and characterization of biomorphous iron carbides

Huber, Richard

Crystallization of glass fibres

Hammerbacher, Ruth

Mineralization of biotemplates

Herbst, Jonas

Formation of nanoscale metal particles in ionic glasses

Lenhart, Marita

Anisotropy of shrinkage and orientation texture of particles in tape cast foils

Lorenz, Hannes

Reduction of porosity of sintered oxide ceramic tapes

Lutz, Christian

Formation and processing of electical ceramic pastes

Müller, Matthias

Liquid phase deposition of ZnO-layers

Schiele, Christian

Transparent Pb-Ge-glasses for IR-laser applications

Seemann, Benjamin

Formation and characterization of spectral light converting foils for bioreactors

Scheiner, Simon

Influence of spectral light conversion on the growth kintics of *Haematococcus pluvialis*

Schweizer, Peter

Increase of biomass production by spectral light

Stumpf, Martin

Fabrication of cellular alumina with hierarchical microstructure

Teichert, Sebastian

Actuation of cellulose based composites

Weiß, Lukas

3D Printing of FeSiCr/SiC ceramic composites

Diploma and Master Thesis

Fu, Zongwen

Manufacturing of Si-based ceramics by means of 3D printing

Johannes, Maren

Formation of photonic microstructures from preceramic polymers

Jakobsen, Daniel

Microstructure formation in piezo ceramics during sintering

Kaiser, René

DEM simulation of 3D powder printing process

Manske, Tamara

Formation of Ca-phosphate biocermics with gradient pore structure

Walter, Florian

Tape casting of transparent ITO layers

Winkel, Alexander

Sintering of bioactive glass-apatite composites

Winterstein, Anja

Development of optically active germanate glasses for photonic crystal fibers

Zhao, Rong

Mechanical properties of glass-silicone-glass laminate composite

Girl's Day

Young girls exploring experimental science

Ph.D.-Thesis

Marcel Hagymasi

Densification of magnetic and dielectric glass ceramic systems

Cornelia Treul

Packing density optimization and sintering of ceramic powder bodies

Dr. Cornelia Treul receiving her personalized doctoral cap.

Thomas Soller

Texture formation of lead free K-Na-Nb based piezoceramics

Martin Rauscher

Processing and printing of In-Sn-oxide nano powders

Dr. Martin Rauscher after successful Ph.D. examination

Visiting Students and Scientists

Kotaro Hattori (November 2011 – January 2012)
Nagoya Institute of Technology, Nagoya, Japan

Akinobu Kawai (September – November 2011))
Nagoya Institute of Technology, Nagoya, Japan

Dr. Steferson Luiz Stares (September 2011 – February 2013)
Federal University of Santa Catarina, UFSC, Brazil

Elisabeth Bertelson (May - August 2011)
Iowa State University of Science and Technology

Nicolay Jordanov (November – December 2011)
Bulgarian Academy of Sciences, Sofia, Bulgaria

Chao Te Liu (July 2011)
National Taiwan University, Taipei, Taiwan

Dr. Janaina Accordi Junkes (April 2011 – March 2012)
Federal University of Santa Catarina, UFSC, Brazil

M. Sc. Verónica Moreno Argüello (April 2011)
Federal University of Santa Catarina, UFSC, Brazil

Stefan Karlsson (June – July 2011)
Linnaeus University, Växjö, Sweden

Keitaro Kioka (October 2010 – January 2011)
Nagoya Institute of Technology, Dep. of Material Science and Engineering, Nagoya, Japan

Masashi Tabe (July 2011)
Nippon Electric Glass

Simon Striepe (February 2011)
Clausthal University of Technology, Clausthal-Zellerfeld, Germany

Teaching

The Department of Materials Science and Engineering offers a Bachelor and a Master programme. The bachelor course is a three years programme (six semesters) which qualifies for the master programme (three semesters).

The curriculum consists of the "*Grundstudium*" during the first 2 years, devoted to the fundamental scientific education. It introduces the student very early into materials science and engineering concepts by offering courses on materials structures, properties, thermodynamics, kinetics, chemistry, processing, product manufacturing, analysis and testing as well as practical training. Examinations follow immediately after each semester.

The subsequent advanced programme in the 5th and 6th semester broadly deepens the entire field of materials science and engineering. Courses on economics, management and other soft skills are obligatory. This period ends with a Bachelor Thesis of nine weeks duration. Additionally, the student has to perform an industrial internship of 12 weeks.

The Master programme in the 7th and 8th semester is devoted to specialisation in a selected "*Kernfach*" (core discipline), including corresponding seminars. The student has to select an additional "*Technisches Schwerpunktfach*" (special technical discipline) which offers the possibility of specialisation. Finally, the programme is completed by a Master Thesis of six months.

In addition to this Materials Science and Engineering programme, the Institute of Glass and Ceramics is involved in the new programme “Nanotechnology” of the Department of Materials Science and Engineering. We also contribute to Bachelor programmes “Energy Technology”, “Medical Technology” and the Elite course “Advanced Materials and Processes”.

Courses offered by the faculties of the Glass and Ceramics Institute

1. Semester

- Introduction to Inorganic Non-metallic Materials, P. Greil

3. Semester

- Materials Characterisation and Testing, A. Roosen

4. Semester

- Solid-state Kinetics, L. Wondraczek

5. Semester

- Processing and Applications of Glasses, L. Wondraczek
- Processing and Applications of Ceramics, A. Roosen

Major Courses 7. and 8. Semester

- Biomimetic Engineering Materials and Processes, C. Zollfrank
- Ceramic Materials in Medicine, P. Greil
- Computational calculation of crack probabilities, T. Fey
- Diffusion and Heat Transfer, L. Wondraczek
- Electroceramics I + II, A. Roosen
- Engineering Ceramics, P. Greil
- Glassceramics, L. Wondraczek
- Innovative Processing Techniques for Advanced Ceramic Materials, P. Greil
- Mechanical Testing, T. Fey
- Non-destructive Testing, T. Fey
- Physics and Chemistry of Glasses and Ceramics: I. Thermodynamics of condensed systems, P. Greil
- Powder Synthesis and Processing, A. Roosen
- Properties of Optical Glasses, L. Wondraczek
- Rapid Prototyping, N. Travitzky
- Silicate Ceramics: From Natural Raw Materials to Modern Applications, N. Travitzky
- Special Glasses, L. Wondraczek
- Stresses and Mechanical Strength, T. Fey

Laboratories

Technical hall (600 m²): equipped with facilities for advanced processing and shaping, heat treatment and analysis.

Main Equipment

Laboratories

- Biomaterials laboratory
- Ceramography workshop
- Functional ceramics laboratory
- Glass laboratories
- Mechanical testing laboratory
- Multilayer laboratory
- Polymer processing laboratory
- Powder characterization laboratory
- Processing workshop
- Rapid Prototyping laboratory
- SEM/AFM laboratory
- Simulation laboratory
- Technical hall
- X-ray charcterization laboratory

Analysis

Thermal analysis

- 3-dimensional optical dilatometer
- Push rod dilatometers (up to 1800 °C)
- Thermal analysis (DTA/TGA/DSC/TMA)
- Thermal conductivity device
- Viscometry (beam bending)

Powder characterization

- ESA acoustophoretic analyser (Zeta-meter)
- Gas absorption analyser (BET)
- Laser scattering particle size analyser
- X-ray diffractometers (high-temperature)

Optical analysis

- FT-IR spectrometer
- High-resolution fluorescence spectrometer (Fluorolog-3, Horiba Jobin Yvon)
- Light Microscopes (digital, polarization, in-situ hot stage)
- Scanning electron microscope (variable pressure, ESEM and high temperature with EDX)
- UV-VIS-NIR spectrometers

Mechanical testing

- High precision mechanical testing with optical tracking system (EXAKT)
- Impulse Excitation Measurement (buzz-o-sonic)
- Micro hardness tester
- Servo hydraulic mechanical testing systems (also high temp.)
- Single fibre tensile testing machine
- Viscosimeter and elevated-temperature viscosimeter

Structural analysis

- 2D laser scanning microscope (UBM)
- 3D Laser scanner
- Atomic force microscope (AFM)
- Electron paramagnetic resonance spectroscopy
- He-pycnometer
- High accuracy weighing scales
- Mercury porosimeter
- Micro-CT Sky scan 1172
- Microwave and ultrasonic devices for non-destructive testing
- Raman-microscope with two excitation lasers

Chemical analysis

- High-pressure liquid chromatograph
- ICP-OES (Spectro Analytical Instruments)

Processing

Powder and slurry processing

- Attrition mills
- Disc mill
- Intensive mixers (Eirich, powder and inert gas/slurry)
- Jaw crusher
- Overhead mixer
- Planetary ball mills
- Planetary centrifugal mixer (Thinky)
- Rotary evaporators
- Sieve shakers
- Single ball mill
- Thermo kneader
- Three-roll mill
- Tumbling mixers
- Ultrasonic homogenizer

Shaping

- 3D printers
- Advanced screen printing device
- Calender
- CNC High speed milling machine
- Cold isostatic press
- Electrospinning machine
- Flaring cup wheel grinding machine
- Fused deposition modelling device (FDM)
- High precision cutting device
- Hot cutting device
- Laminated object manufacturing devices (LOM)
- Lamination presses
- Langmuir–Blodgett trough
- Lapping and polishing machines
- Low-pressure injection moulding machine
- Precision diamond saws
- PVD coaters
- Robot-controlled device
- Roller coater
- Sheet former
- Spin coater
- Tape caster
- Textile weaving machine
- Twin screw extruder
- Ultrasonic drill
- Vacuum infiltration device

Heat treatment

- Autoclave
- Dryers
- Furnaces (air, N_2, Ar, Vac, High-Vac, forming gas) up to 2500 °C for sintering, glass melting, infiltration, debindering, pyrolysis
- Gradient furnace
- High-temperature spray furnace

2. RESEARCH

Survey

Research centres on basic aspects of ceramics, glasses and composites. Materials for applications in microelectronics, optics, energy, automotive, environmental, chemical technologies and medicine were investigated. Research was carried out in close cooperation with partners from national and international universities and industries.

Research Projects (in alphabetical order)	**Funding**	**Principal Investigator**
Accelerated glass durability testing	ECN	Prof. Wondraczek
Bioinspired design of functional optical structures	DFG	PD Dr. Zollfrank
Biomineralisation of vegetable plant structures for bone regeneration scaffolds	EU	Prof. Greil
Biomorphous ceramic scaffolds for bone regeneration	DFG	Prof. Greil
Bismuth activated glasses with IR luminescence for broad band amplifier applications in laser technology	DFG	Prof. Wondraczek
Cellular ceramics for heat absorbers	ECN	Prof. Greil
Deformation and sintering behaviour of preceramic papers	DFG	Dr. Travitzky
Disperse systems for electronic manufacturing	DFG	Prof. Roosen
Eu^{2+} doped glasses with broad band luminescence behaviour	DFG	Prof. Wondraczek
Experimental study and simulation of anisotropic effects in cast green tapes	DFG	Prof. Roosen
Flexible manufacturing of preceramic paper based refractory components	DFG	Prof. Greil

Research Projects (in alphabetical order)	Funding	Principal Investigator
Glass melt filled photonic fibers	DFG	Prof. Wondraczek
Hierarchical cellular ceramics and composites	DFG	Prof. Greil
Hierarchically structured porous ceramics templated by plant cell walls	DFG	PD Dr. Zollfrank
Highly resistant multilayer systems	BFS	Prof. Wondraczek
Lightweight cellular ceramics	EC	Prof. Greil
Lightweight ceramics	AIF	Dr. Travitzky
Long time stability of glasses	BFS	Prof. Wondraczek
Manufacturing of multilayer refractories by tape casting	DFG	Prof. Roosen
Manufacturing of transparent ceramic substrates	BMBF	Prof. Roosen
Mechanochemical properties of nitridaded glasses	DFG	Prof. Wondraczek
Microstructuring of metal-oxide-based nano-composites	DFG	PD Dr. Zollfrank
Molecular design templated by nanotube assemblies	DFG	PD Dr. Zollfrank
New glasses for photonic crystal fibers	EC	Prof. Wondraczek
Optics-Optoelektronics	ECN	Prof. Wondraczek
Polymer derived ceramics for bearing applications	IN	Dr. Travitzky
Relaxation behaviour of compressed inorganic glasses	DFG	Prof. Wondraczek
Self healing MAX phase ceramics	DFG	Prof. Greil
Tape on Ceramic Technology	BMBF	Prof. Roosen
Transparent glass foams	EC	Prof. Wondraczek

Funding organisations:

AIF: Industrial research Cooperation

BFS: Bavarian Science Foundation

BMBF: Federal Ministry of Education and Research

DFG: German Science Foundation

EC: Cluster of Excellence (“Engineering of Advanced Materials”)

EU: European Union

IN: Industry

Selected Research Highlights

Ceramics with Periodical Meta-Structures

Michael Götz, Tobias Fey, and Peter Greil

Objectives

Ceramics with a three-dimensional periodic structure such as photonic crystals have found increasing interest for a variety of application fields including sensors, electromagnetic wave guides, circuits, filters, cavities, laser, antenna, and absorbers. While the properties of an individual periodic element (thereafter called building block) are dominated by its microstructure (porosity, grain size, phase content, etc.), the behaviour of the bulk material will strongly be influenced by the three-dimensional arrangement of the periodic elements (thereafter denoted meta-structure). This work aims to explore the self-assembly process of space filling alumina cubes to form two- and three-dimensional meta-structures of regular translational periodicity with dimensions orders of magnitude larger (1000 µm) than the particle size (0.1–10 µm). However, falling in a transition region between the conventional micromachining techniques and the micro/nano-fabrication methods site specific control of periodic meta-structure formation is a great challenge during fabrication process.

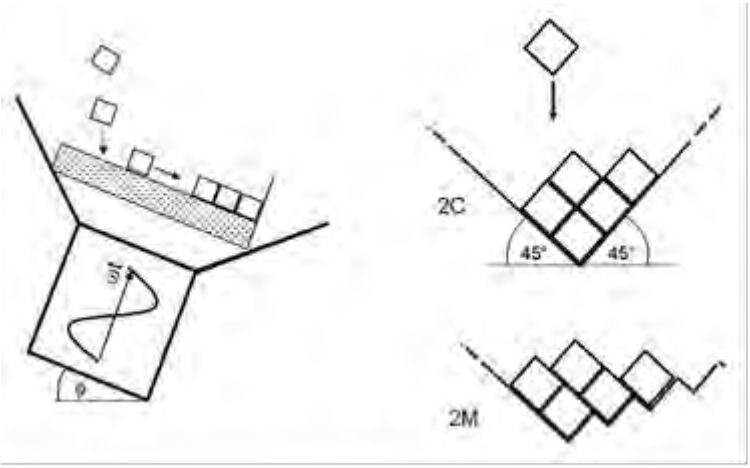

Fig. 1: Vibration assisted self gravitational assembling: experimental configuration (left) and side wall configuration for 2D layer assembly structure formation (right).

Experimental Procedure

A vibration assisted assembling process driven by gravity was used to achieve forced configuration of space-filling building blocks (regular cubes) under geometrically constrained boundary condition. The process of transfer-moulding and sintering was applied in this work to manufacture regular alumina cubes with an edge length of 1.34 ± 0.04 mm. Orientation of the building blocks in three dimensional space was achieved by self assembling of two-dimensional cube layers which subsequently were stacked layer-by-layer to form three-dimensional arrays. The assembly element

(configuration frame) was equipped with periodic side walls that place the alumina cubes in the designated positions of minimum potential energy configuration on the substrate. The configuration frame was mounted on a vibration table connected to the membrane of a large amplitude (± 6 mm) low band loud-speaker with a diameter of 25 cm and a power input of 110 W (WS 25 E 8 OHM 37 Hz – 6 kHz, Visaton GmbH, Haan, Germany). The vibration table was operated at a constant vibration frequency of 50 Hz (longitudinal vibration mode perpendicular to the configuration plane).

Results

Two-dimensional and three-dimensional periodic assembly structures of different unit cell symmetry were prepared. Unlike to colloidal crystallization which suffers from a high degree of packing defects, vibration assisted gravitational assembly of space filling building blocks offers a high potential for achieving periodic assembly structures with quasi-crystalline order, high packing densities and low defect content. Vibration assisted formation of periodic assembly structures may be separated into two steps:

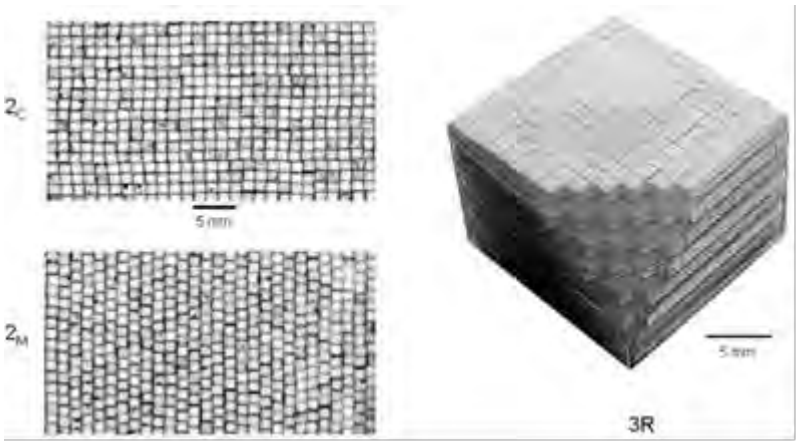

Fig. 2: Al_2O_3/Al-building bloc assemblies prepared: 2D-layers of cubic and monoclinic unit cells (left) and 3D-assembly of rhomboedric unit cell (right).

i. sliding of the feeded alumina cubes along the inclined configuration plane and **ii.** attachment of the cube to the growing interface of the ordered assembly structure. Critical conditions to overcome frictional drag during sliding may be derived from force balance acting on a single alumina cube during harmonic oscillations of the inclined configuration plane. Fig. 2 shows examples of periodic building block structures (2C, 2M and 3R) manufactured by vibration assisted self assembling (2C: $\gamma = 90$ ° and $a = b$ and (cubic 2D unit cell); 2M: $\gamma = 63°$ (= arctan 2) and $b = a/0.89$ (monoclinic unit cell); 3R: $\alpha = \beta = \gamma = 63°$ and $a, b = c = a/0.89$ (rhombohedric 3D unit cell). Furthermore, 3C and 3M periodical assembly structures were generated (not shown) (3C: $\alpha = \beta = \gamma$ and $a = b = c$ (cubic 3D unit cell); 3M: $\alpha = \beta = 90°$, $\gamma = 63°$ and $a = b$, $c = a/0.89$ (monoclinic 3D unit cell)).

Future Work

Compared to self assembling techniques based on electrostatic, van der Waals and molecular surface interaction, the driving force in our approach is gravity. Unlike to colloidal crystallization which suffers from a high degree of packing defects, vibration assisted gravitational assembly of space filling building blocks with sizes ranging from approximately 10 to 1000 µm offers a high potential for achieving periodic assembly structures with high packing densities and low defect content. Processing of regular periodic assembly structures of space filling building blocks is particularly attractive for achieving net shape capability e.g. minimized shape and volume changes upon consolidation. Interface bonding by infiltration of a liquid (preceramic) polymer, a sol, or a metal melt which upon proper heat treatment may form a reactive bonding phase between the building blocks should allow to obtain significantly lower dimensional change (linear shrinkage << 1 %) as compared to conventional sintering techniques (> 10–15 %). Depending on the periodic pattern symmetry a pronounced enhancement of surface area may be beneficial in the case of interface controlled crack propagation for triggering crack deflection and crack bridging phenomena. Furthermore, building blocks with a complex internal microstructure such as particle, fibre or multi-layer composites, may extend the approach to hierarchical periodic materials which might be of particular interest for development of advanced materials for emerging engineering as well as functional applications.

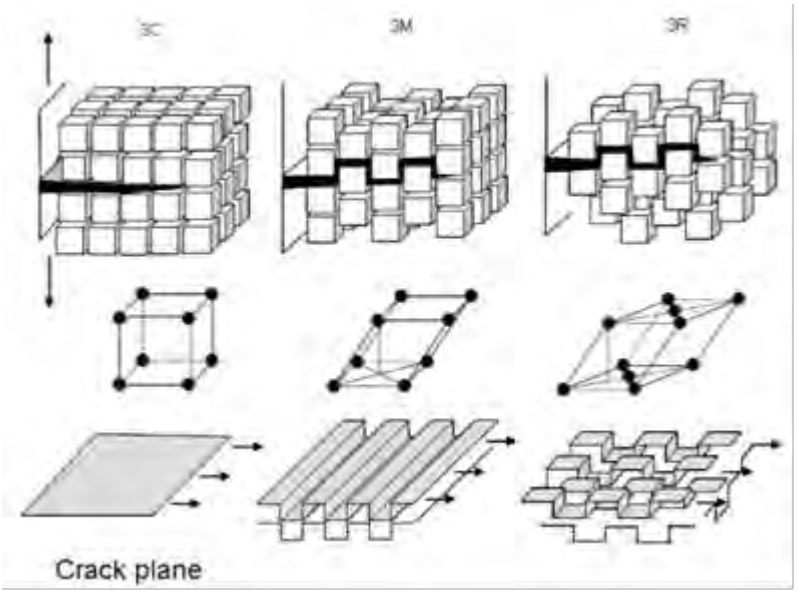

Fig. 3: Interface fracture and area enhancement of 3D periodic assembly structures.

Reference

M. Götz, T. Fey, P. Greil: Vibration Assisted Self-Assembly Processing of Ceramic-Based Composites with Modular Meta-Structure *J. Am. Ceram. Soc. 95 (2012) 95–101*

Multilayer Structures

Ulrike Deisinger and Andreas Roosen

Objectives

Multilayer structures are widely used in functional ceramic applications such as capacitors, highly integrated circuits, sensors or actuators. Research in the multilayer group covers all process steps from tape casting, structuring, metallization, stacking and laminating to binder burnout and co-firing of the laminates. One special focus is set on the structuring and lamination of ceramic green tapes in order to integrate large voids or channels.

Experimental procedure

Ceramic green tapes (LTCC tapes) were applied to manufacture multilayer devices. The tapes were structured using a milling plotter with a high frequency spindle (10 000–100 000 rpm). The design of the tape structure was generated by CAD software. The diameter of the milling cutter was varied in high resolution from 0.1 to 3 mm and the travelling speed of the milling cutter reached up to 40 mm/s. After structuring the green tapes were laminated. As lamination by thermo-compression would destroy large cavities the so-called cold low pressure lamination (CLPL) was applied. CLPL is based on the connection of two adjacent green tapes by the means of a thin double-sided adhesive tape. The adhesive tape was mounted at ambient conditions (i.e. room temperature) onto the green tape by a soft roller. The three dimensional device was generated by alternate stacking of green tapes and adhesive tapes without applying elevated temperature or pressure. After binder burn-out, laminates of LTCC ceramics were sintered at 870 °C for 20 min.

Results

Single and laminated green tapes were structured arbitrarily using the milling plotter. Various internal (e.g. cooling channels) and external geometries (e.g. gear wheels) were realised in high accuracy (*Fig. 1*). Channels were milled with a channel width of ≥ 0.4 mm, while drill holes had a diameter of ≥ 0.1 mm. Large cavities from 2.5 x 20 mm² to 15 x 20 mm² were realised without sagging of the top layer (*Fig. 2*).

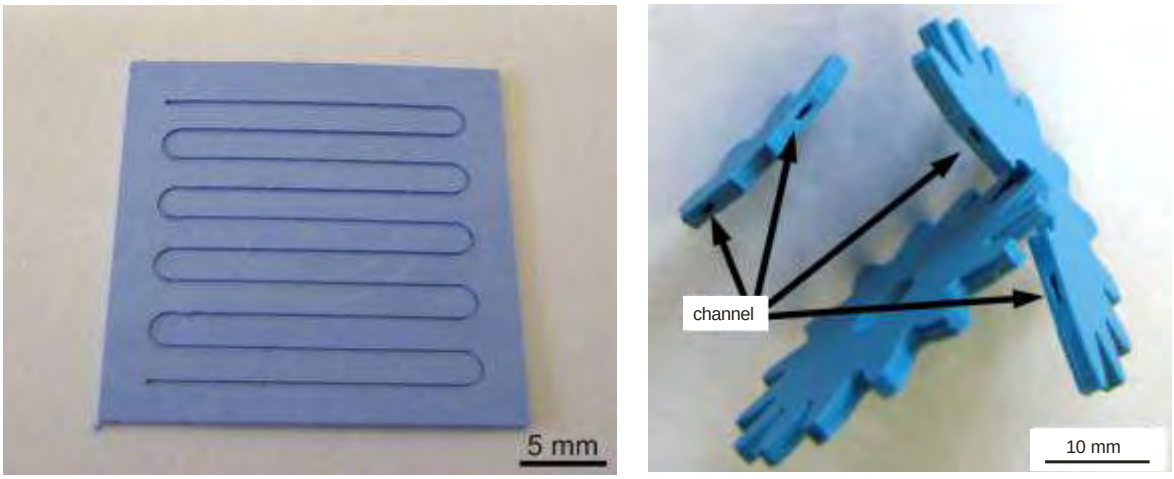

Fig. 1: Various LTCC parts, structured by a milling plotter.

After sintering the initial interfaces separating the individual tapes could not be detected anymore and a homogeneous bulk ceramic was formed. A thorough investigation of the binder burn-out and sintering processes revealed that the ceramic tapes approach each other due to a combination of

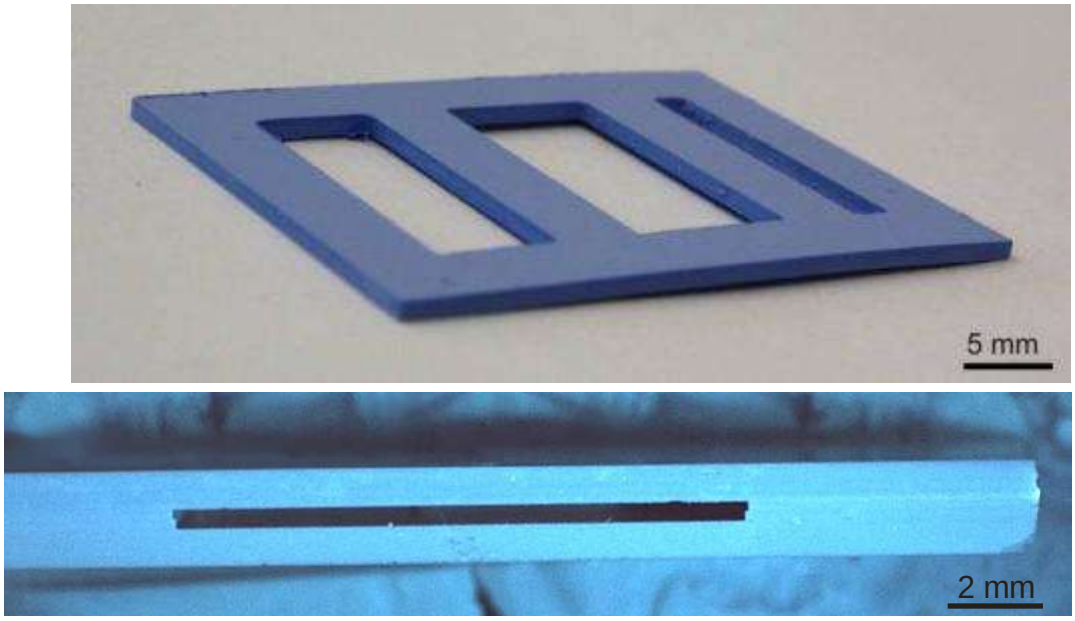

Fig. 2: Internal cavities in LTCC ceramic. During CLP-lamination and sintering no sagging of the top layer occurred.

adhesive and capillary forces during burn-out of the double-sided adhesive tape. With CLPL the same sintered density of ceramic parts could be achieved as with thermo-compression lamination. This work showed the high potential of the multilayer ceramic technology combined with cold low pressure lamination for the fabrication of complex ceramic structures.

Future work

The multilayer technology including the cold low pressure lamination together with the precise structuring of the green tapes using a milling plotter will be adapted to other ceramic materials and applications. In microelectronics internal cooling channels or top layer cavities for surface mounting of other devices are of interest. Further applications can be found in micro electro mechanical systems (MEMS) and in micro fluidic devices. Since a high resolution of small dimensions can be achieved easily this technique offers a high potential for micro-reactor fabrication. Another promising application will be the realisation of bioreactors for culturing specific tissue cells. Furthermore, bioreactors applied in tissue engineering or for analysis of the interaction of living cells with certain toxic elements or medication will be processed.

References

K. Schindler, A. Roosen: Manufacture of 3D structures by cold low pressure lamination of ceramic green tapes, *J. Eur. Ceram. Soc. 29 (2009) 899–904*

Cellular Ceramics

Tobias Fey, Bruno Ceron-Nicolat, Nataliya Myuller, Nahum Travitzky and Peter Greil

Objectives

Research in the cellular ceramics group centers on design, processing, engineering and property evaluation of tailored cellular ceramics distinguished by uniform, gradient or hierarchical pore structures. Ceramics with stochastic foam structures as well as those with periodical cell arrangement were processed and the mechanical behaviour was analyzed. Cellular ceramics with improved stiffness and failure tolerance at low weight are envisaged for applications in energy, environment and medicine fields.

Experimental procedure

An open-cellular PU foam template was coated with a primary SiC slurry. Cross-linking of a polysiloxane binder at resulted in a SiC filled reticulated thermoset foam (1st generation). Subsequently, this matrix foam was infiltrated with a second slurry of slightly different polysiloxane composition which upon heating to 290 °C caused bubble nucleation and formation of a 2nd generation foam filling the cell space in the matrix foam skeleton.

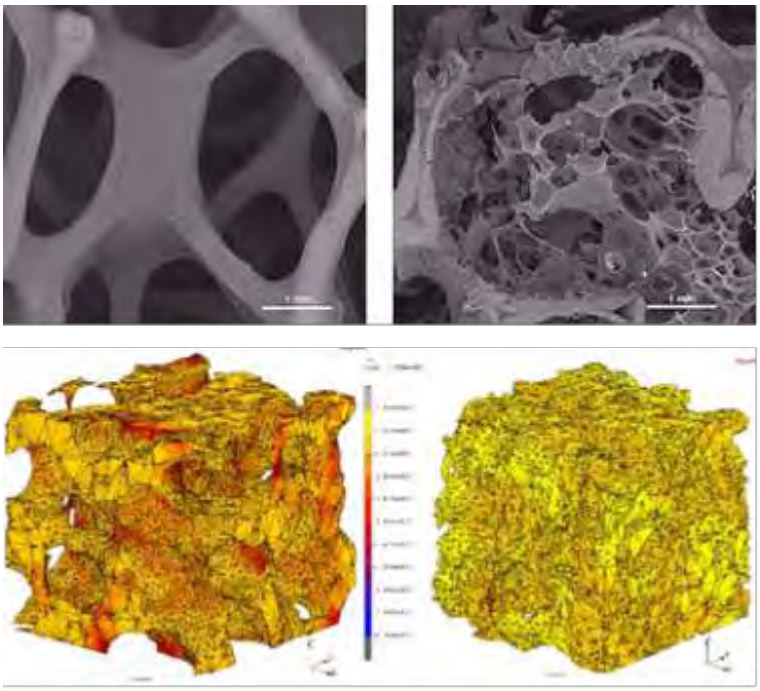

Fig. 1: Polymer derived hierarchical SiC-based foam (top) and FE-calculation of principal tensile stress distribution in the foam microstructure.

Advanced generative manufacturing techniques including 3D printing, fused deposition molding, laminated object manufacturing and robocasting were established and applied to manufacture ceramics with periodical cellular structures. The cellular microstructure was analyzed by X-ray µ-CT and FE calculations were applied to simulate the global and local mechanical response when subjected to directional loading.

Results

Silicon carbide based cellular ceramics characterized by a hierarchical pore structure and a fractional density of 0.3 were processed, Fig. 1. While the matrix foam skeleton provides control of macroscopic shape as well as density distribution in component single- or multistep foam infiltration may offer a high potential for improving the properties of hierarchical cellular materials. FE calculations of µ-CT structure reconstructions shows mean equivalent stress at a strain of 20 % to be reduced by −9 % in the direction parallel and −33 % perpendicular to the compression loading direction.

Strut lattice structures of reaction bonded silicon infiltrated silicon carbide ceramics (RB-SiSiC) for air-fuel mixture formation and for non-stationary lean-burn applications were fabricated by indirect three-dimensional printing, Fig. 2. Compressive strength values of 618 MPa and 82 MPa for the single strut (diameter 1.5 mm and length 2–8 mm) and the macro-cellular lattice structure with a porosity of > 80 %, respectively, were measured. It was shown, that preignition processes in the porous reactor are much faster than in a free combustion, especially at lower temperatures. Interaction of high velocity diesel jets with cylindrical strut ligaments of the SiSiC lattice structure offers new possibility for quick and efficient fuel distribution (multi-jet splitting) in space.

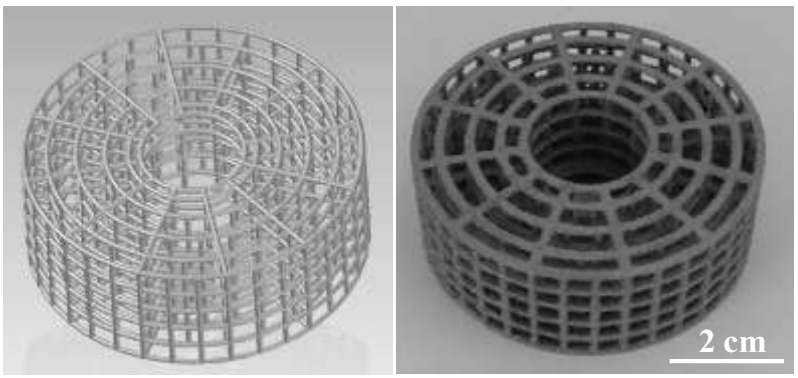

Fig. 2: CAD model (left) and 3D-printed SiC/Si lliagement structure for

Future work

Design and processing of ceramics with periodical cellular structure ("meta-structure") will be explored. Incorporation of an oriented pore network in piezoelectric ceramic micro-structure will be used as a variable for tuning specific properties such as hydrostatic strain coefficient, electrical charge density, and permittivity which might result in improved impedance matching, signal sensitivity, and signal-to-noise ratio of piezoceramic devices. Coupling piezoelectric properties with auxetic deformation behaviour of periodical lattice structures, Fig. 3, may offer novel functional modules distinguished by improved stress and strain sensing behaviour as well as capability for harvesting of vibration energy. The electrical, mechanical and thermal properties of these materials will be analyzed. The work addresses fundamental aspects of design, processing and property optimization of novel piezoelectric materials which might be of particular relevance for applications as sensors, actuators and electro-mechanical devices.

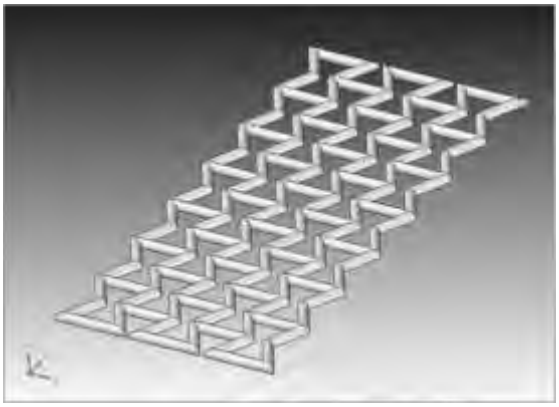

Fig. 3: Example of an auxetic lattice (PZT) fabricated by robo-casting.

References

B. Ceron-Nicolat, T. Fey, P. Greil: Processing of Ceramic Foams with Hierarchical Cell Structure *Adv.Eng. Mat. 12 (2010) 884–892*

L. Schlier, W. Zhang, N. Travitzky, J. Cypris, M. Veclas, P. Greil: Macro-Cellular Silicon Carbide Reactors for Nonstationary Combustion Under Piston Engine-Like Conditions, *Int. J. of App. Cer. Tec. 8 (2011) 1237–1245*

Biotemplating of Functional Materials from Cellular Plant Tissue

Mariya H. Kostova[1], Miroslaw Batentschuk[2], Friedlinde Goetz-Neunhoeffer[3], Sabine Gruber[1], Albrecht Winnacker[2], Peter Greil[1], and Cordt Zollfrank[1]

[1]Department of Materials Science (Glass and Ceramics)

[2]Department of Materials Science (Materials for Electronics and Energy Technologies)

[3]Geo-Centre Northern Bavaria, Mineralogy

University of Erlangen-Nuernberg, Erlangen, Germany

Objectives

Patterned phosphor materials have gained increasing interest for high-resolution screen and imaging devices. Recently, a new approach demonstrated that needle-structured phosphors could improve conventional powder phosphors. However, processing involves evaporation *in-vacuo* that requires sophisticated equipment and is difficult to control. For X-ray imaging systems based on image plates (IP), BaFBr doped with Eu^{2+} exhibit optimum storage and read-out properties along with a high-temperature stability and decreased sensitivity towards humidity. Biotemplating techniques provide a simple and facile route for patterning inorganic materials which take advantage of the structural features of biological tissue anatomy to create novel types of well-defined inorganic hierarchically organised architectures.

Experimental Procedure

Templates of pine wood (*Pinus sylvestris*) were consecutively infiltrated with two solutions. The first precursor solution was prepared by dissolving stoichiometric amount of NH_4F in distilled water and methanol. The second solution was composed of hydrated $BaBr_2 \cdot 2H_2O$ and $EuCl_3 \cdot 6H_2O$ dissolved in methanol. Multiple vacuum-assisted infiltrations enhanced the yield of material. The oxidation of the infiltrated template was performed in an electrically heated furnace up to 800 °C. The biomorphous BaFBr:Eu^{3+} specimens were annealed for 2 h under reducing atmosphere (95 % N_2, 5 % H_2) at 800 °C. The final materials were characterised by powder X-ray diffraction together with Rietveld refinement. The microstructure was characterised by scanning electron microscopy (SEM). In order to generate the F-centres the samples were irradiated with an x-ray dose of 0.6 Gy utilizing a medical X-ray tube. The photostimulated luminescence (PSL) was realised by monochromatic light obtained from a 150 W Xe lamp dispersed through a double monochromator.

Results

Axial sections of pine-templated BaFBr:Eu^{2+} sintered at 800 °C are shown in Fig. 1. While the wood cell morphology in the latewood region was replicated, pronounced deformations of the struts with minor changes of cellular anatomy were observed in the earlywood regions. Since the BaFBr sub-micrometer precipitate was not uniformly dispersed through a single cell wall variation in strut thickness may give rise for differences in sintering behaviour between late wood (small pore size and large strut thickness) and early wood regions (large pore size and small strut thickness). Compared to the original cell morphology the mean pore diameters of the early- and latewood tracheids for the sintered sample were reduced and attained values of 12 µm and 6 µm, respectively.The mean strut thickness for the early and latewood cells also decreased to values of 1.5–3.5 µm. Using the SEM micrographs of the axial sections of pine-templated BaFBr:Eu 65 % open porosity was estimated.

The photoluminescence excitation and emission spectra of the biotemplated BaFBr:Eu^{2+} phosphor at room temperature showed a broad peak at 275 nm with a shoulder at 265 nm. A single emission band with maximum at 390 nm was observed. The band is ascribed to the 4f65d1→4f7 transition of the Eu^{2+} activator ion. No additional presence of a long wavelength shifted emission band assigned to Eu^{3+} or O^{2-} PL was observed while exciting at 250 nm (host lattice) or 265 nm. We concluded that oxygen was not incorporated into the lattice, which would lead to the creation of PSL-inactive O^{2-}-based hole traps which decreases the PSL efficiency.

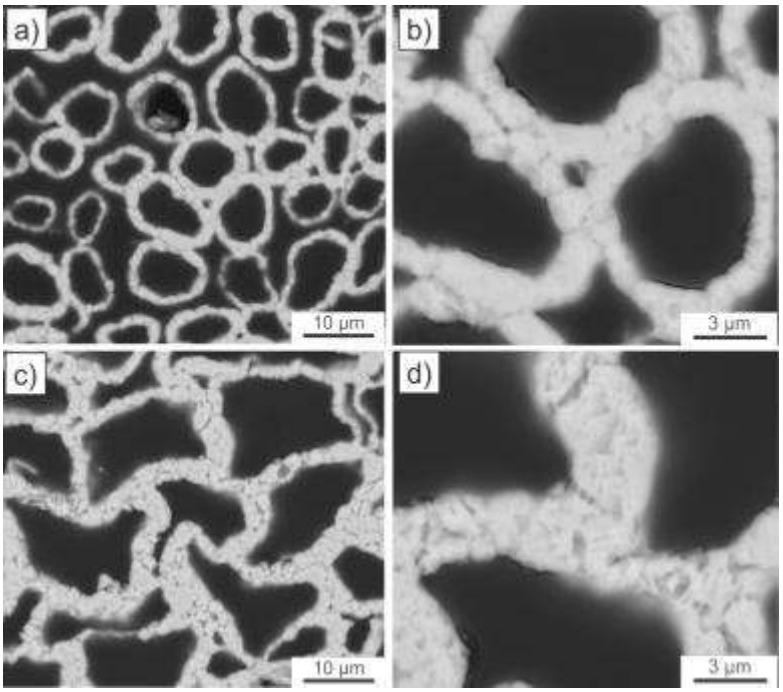

Fig. 1: SEM micrographs of the axial sections of pine-templated BaFBr:Eu^{2+} samples sintered at 800 °C (a, b) latewood, (c,d) earlywood regions.

The PSL spectrum of the solid-state powder of BaFBr:Eu^{2+} prepared with fluorine excess for comparison purposes exhibits the typical double peak structure of F(Br−)-colour centres, Fig. 2. For the biotemplated BaFBr:Eu^{2+} which contains small amounts of Ca (0.95 mol %), no shift in the

stimulation maxima compared to the BaFBr:Eu^{2+} sample was observed, Fig. 2. The broadening of the PSL spectrum is ascribed to fraction of barium ions substituted by calcium ions in the lattice and formation of FA(Br−, Ca^{2+})-centre. The assessment of the image quality is obtained experimentally by means of a test object. The image quality evaluation was performed using a compact storage phosphor scanner. The images of biotemplated BaFBr:Eu^{2+} embedded in epoxy resin obtained after X-ray irradiation and following removing the lead foil is illustrated in the inset in Fig. 2. We can clearly see the four holes and the edges of the lead mask. The sharp edges of the X-irradiated areas are spread due to scattering in lateral direction.

Future Work

Biomorphous BaFBr:Eu^{2+} with a structure mimicking the cellular anatomy of pine wood (*Pinus sylvestris*) was prepared using in-filtration of submicrometer BaFBr:Eu^{2+} precipitate. In contrast to minimizing particle size of densely packed phosphor powder our novel approach using biotemplate control might offer an elegant way for generating highly oriented and optically isolated µm- and sub-µm arrays of phosphor material to significantly attain improved spatial resolution for X-ray image storage systems.

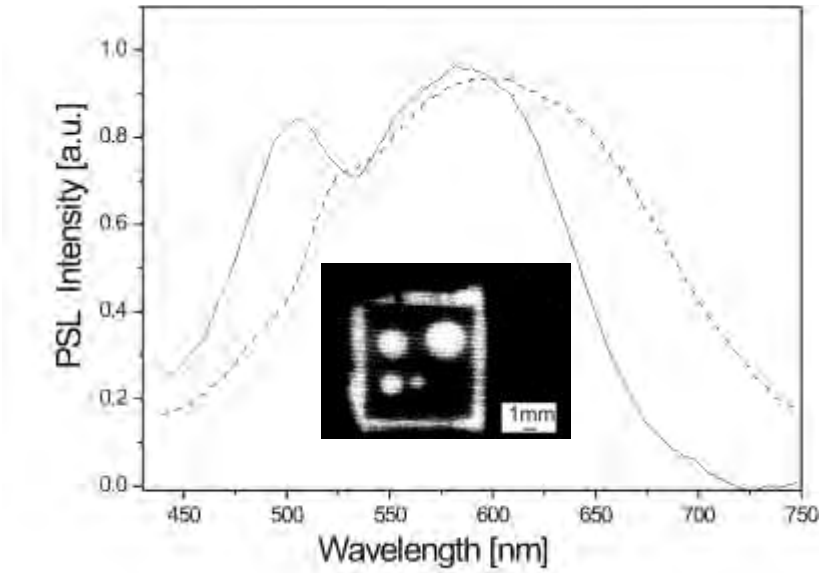

Fig. 2: PSL spectra of solid-state prepared powder of BaFBr:Eu^{2+} (solid-line) and biotemplated BaFBr:Eu^{2+} (dashed-line); inset: Read-out image of biotemplated BaFBr:Eu^{2+} obtained using a compact storage phosphor scanner.

References

M.H. Kostova, M. Batentschuk, F. Goetz-Neunhoeffer, S. Gruber, A. Winnacker, P. Greil, C. Zollfrank: Biotemplating of BaFBr:Eu^{2+} for X-ray storage phosphor applications. *Materials Chemistry and Physics 123 (2010) 166–171*

Polymer Filler Derived Ceramics

Lorenz Schlier, Nahum Travitzky and Peter Greil

Objectives

Preceramic polymers based on Si-containing polycarbosilanes, -silazanes, or -siloxanes, can be chemically functionalised to yield ceramic materials with a wide range of compositions (Fig. 1) and properties. Reactive fillers which upon reaction with the decomposition products of the polymer may compensate the volume changes associated with the polymer-to-ceramic transition offer a high potential for achieving net shape capability as well as optimizing mechanical and electrical proper-ties. Control of thermally induced molecular rearrangement and microstructure formation, however, is a great challenge in order to develop the processing chain for polymer derived ceramic manufacturing. Microcomposite materials for brake systems and bearings offering enhanced wear and fatigue resistance are being developed.

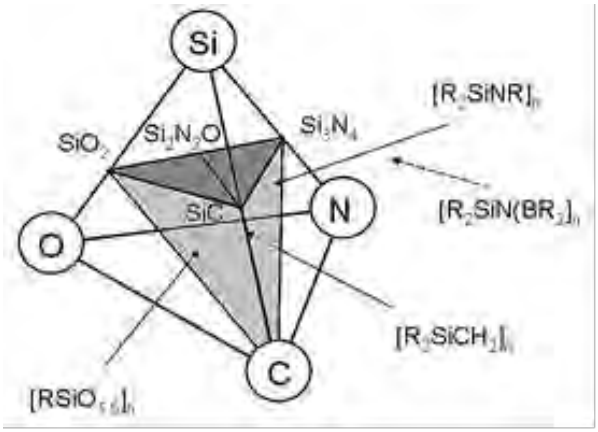

Fig. 1: Basic component tetrahedra of Si-containing preceramic polymer compositions.

Experimental Procedure

Multilayer Si-O-C composites were fabricated from Si- and SiC-filler loaded polymethyl-silsesquioxane based polymer solutions by tape casting and lamination. Filler fraction and filler particle size were varied and different stacking designs were prepared (gradient and sandwich type). Laminated object manufacturing (LOM) was applied for shaping. Cylindrical rods were fabricated by extrusion. The shaped preforms were pyrolyzed in nitrogen at 1000–1400 °C. Residual stress profiles were derived by means of strain relaxation method.

Results

A rate controlled pyrolysis scheme was developed to facilitate and accelerate the polymer to ceramic conversion. Heating rate was controlled to achieve a linear weight loss with heating time (0.003 %/min) at minimum residual porosity. The mechanical properties of the multilayer composites exhibit a pronounced variation of bending strength and fracture tough-ness with different stacking design, Fig. 2. Compared to homogeneous stacks the sandwich stacks with higher Si-filler content in the outer layer compared to the core achieved an increase of 100 % and 120 % of fracture stress and toughness, respectively. Tribo-logical measurements revealed a high coefficient of friction and a pronounced improvement of wear resistance compared to monolithic materials.

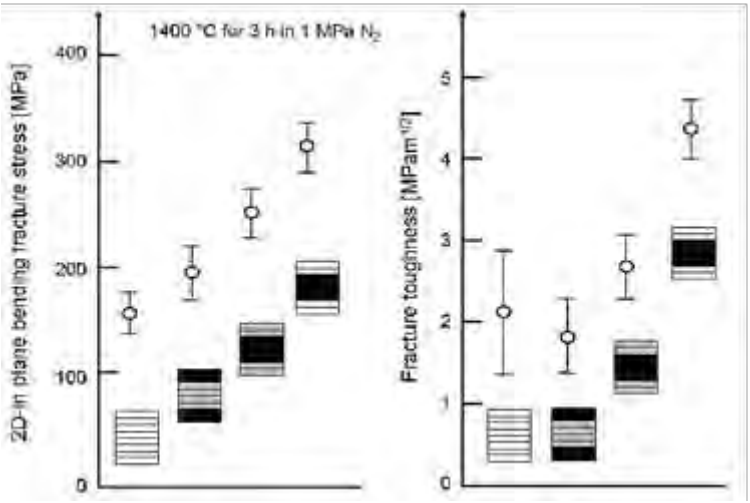

Fig. 2: Bending strength and fracture toughness of multilayer Si-O-C ceramic composites fabricated from SiC-loaded polysiloxane tapes of various stacking design.

Measurement of residual stress profile (Fig. 3) by strain relaxation method revealed a compression stress prevailing on the surface layer of sandwich stacking design which gave rise for a pronounced increase in bending fracture strength.

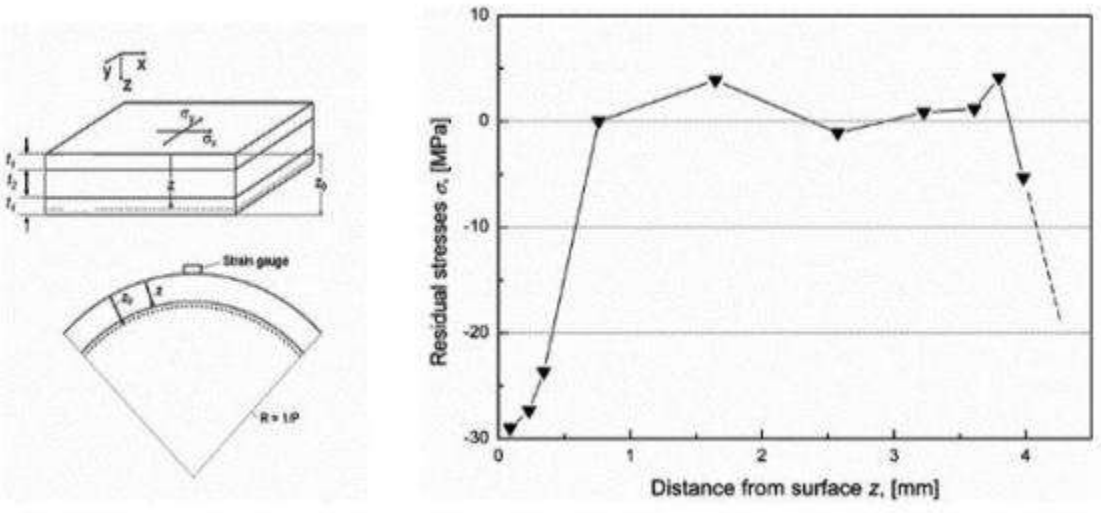

Fig. 3: Distribution of residual stress over the multilayer stack thickness.

Extrusion of Si and SiC loaded bearing components was successfully demonstrated (Fig. 4). Nitridation reaction forming Si_2N_2O and Si_3N_4 caused the porosity in the surface layer to be reduced significantly resulting in an enhanced Young´s modulus and improved wear resistance as confirmed by bearing wear tests. Furthermore, linear bearings were fabricated by high speed cutting of cured performs. Upon reactive pyrolysis excellent shape retention and high compression loading capacity was obtained.

Fig. 4: Silicon carbide based roller bearings manufactured by extrusion of Si- and SiC-loaded polysiloxane polymer.

Future Work

Future work will be directed to minimization of residual porosity by post-annealing in reactive N_2-atmosphere. Furthermore, enhancement of residual stress formation for strengthening and toughening will be explored by experimental work as well as transient stress simulation calculations.

References

M. Steinau, N. Travitzky, T. Zipperle, P. Greil: Functionally Graded Ceramics Derived from Preceramic Polymers, *Advances in Polymer Derived Ceramics and Composites, edt. P. Colombo, R. Raj, Ceram. Trans. 213, Wiley, NY (2010) 61–71*

L. Schlier, M. Steinau, N. Travitzky, J. Gegner, P. Greil: FeSiCr Filled Polymer Derived Ceramics, *Int.J.Appl Ceram.Techn. 6 (2011) 8, 1509–1516*

Preceramic Paper Derived Lightweight Ceramics

B. Gutbrod, N. Travitzky, and P. Greil

Objectives

Preceramic paper offers a novel approach to process ceramics with high versatility of chemical composition and flexibility in shaping and lightweight product design. While the cellulose fiber network generated during papermaking provides excellent machinability, filler loading controls the paper-to-ceramic conversion via sintering or reaction infiltration. Compositional diagram (volume fractions) showing the range of preceramic paper compared to common writing paper. Arrows indicate compositional change upon paper-to-ceramic conversion; initial fiber fraction may transform to fiber template porosity upon sintering in air (Fig. 1). This work aims to investigate the influence of partial replacement of bioorganic pulp fibers in Al_2O_3-loaded preceramic paper by inorganic short ZrO_2 fibers on the pre-ceramic paper processing and mechanical properties of the resulting ceramics. Substitution of pulp fibers by ceramic fibers may reduce large, elongated pores templated by the bioorganic pulp fibers and thus, enhance design possibilities, improve microstructure and properties of the ceramic composites. The challenge is to find the limits of pulp fiber substitution by inorganic zirconia fibers which do not deteriorate the flexibility of the paper web required for paper processing and machining while improving the properties of the sintered ceramic products.

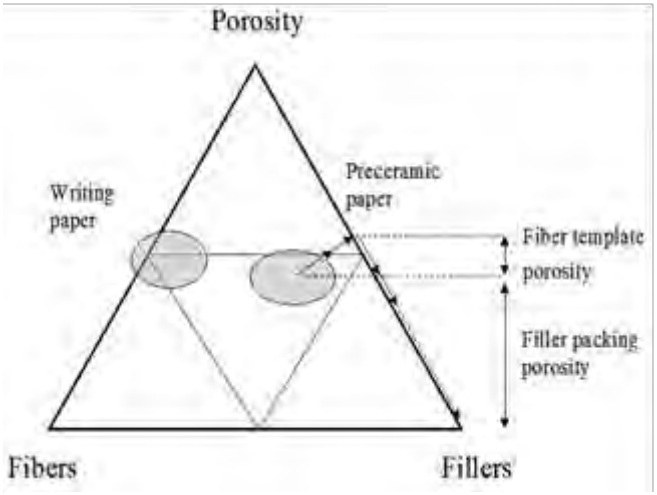

Fig. 1: Composition of preceramic paper.

Experimental Procedure

Preceramic paper processing includes the preparation of an aqueous feedstock, filtration of the feedstock, and drying of the wet fiber web. Controlled flocculation in the feedstock suspension is induced by addition of retention aid chemicals in order to promote the formation of a filter cake during dewatering of the aqueous feed-stock. Single sheets of preceramic paper with a thickness of 300–450 µm and loaded with 20–30 vol. % of a sub-micron ceramic filler (Al_2O_3) and short fibers

(ZrO_2) were prepared from low concentrated aqueous suspensions. External pressure was applied to increase the packing density of the sheet. Lightweight structures of multilayer, corrugated and sandwich type were processed from the preceramic paper sheet and finally sintered in air at 1600 °C for 2 h (Fig. 2).

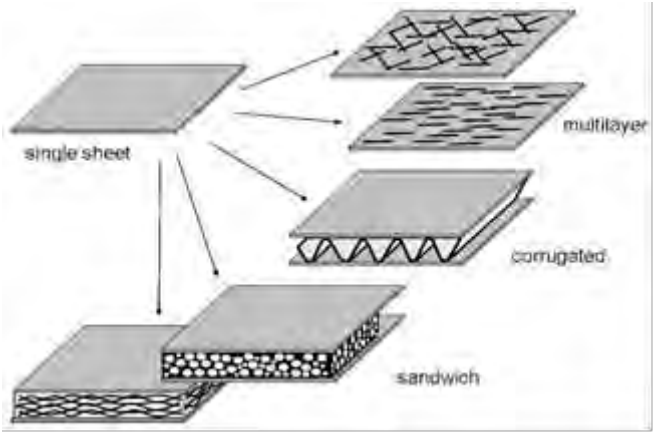

Fig. 2: Lightweight structure design processed from preceramic paper.

Results

Powder packing density in the paper sheet decreased with increasing amount of non-deformable zirconia fibres for highly deformable pulp fibres. Despite of the high stiffness of the inorganic ceramic fiber compared to the bioorganic pulp fiber the excellent shaping properties of the preceramic paper were retained. The fibres are uniformly distributed over the sheet cross section with the fibres preferentially orientated in the

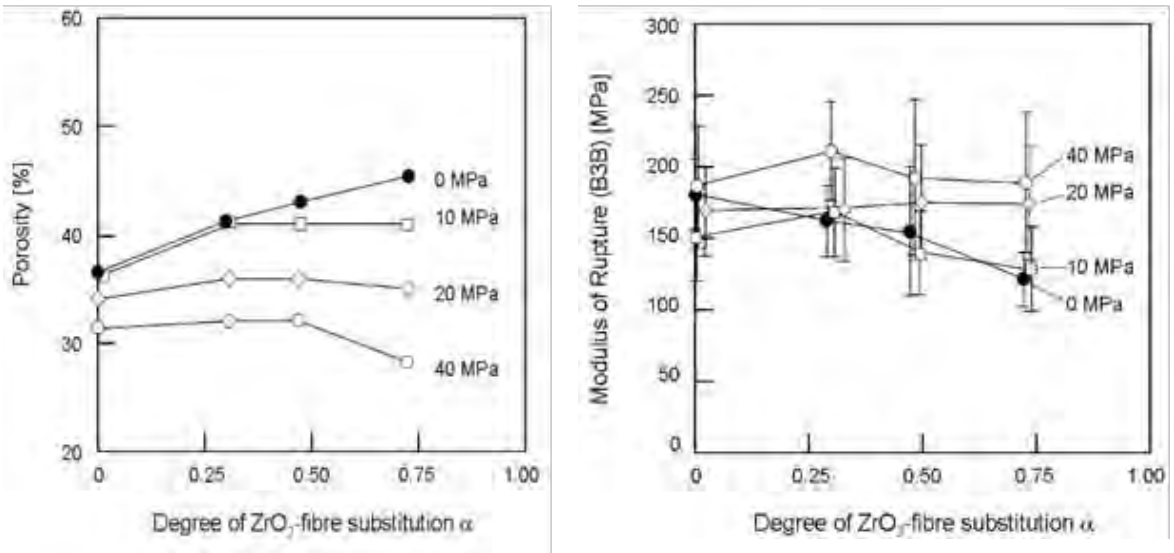

Fig. 3: Porosity of the sintered ceramic sheet versus degree of zirconia fibre substitution in the pre- ceramic paper web consolidated with external pressure (left). Modulus of rupture measured by ball-on-three-ball 2D bending test (right).

sheet plane (x-y plane). Post-pressing was demonstrated to achieve improved paper consolidation and a reduction of porosity which ultimately led to improved mechanical properties of the sintered ceramic products (Fig. 3). Thus, preceramic paper containing a zirconica fibre volume fraction of 19 % sintered at 1600 °C attained a rupture strength measured by ball-on-three-ball loading of 137 ± 19 MPa (porosity 44 %) which after pressure consolidation of the paper increased to 200 ±

54 MPa (porosity 28 %). Anisotropic shrinkage variation has mainly been associated with spatial variation of powder packing density, the orientation of the pore/solid interface, the alignment of anisotropic particles and the introduction of joining and bonding interfaces in multilayer packages. Substitution of pulp fibres by rigid ZrO_2-fibers caused a reduced in-plane-shrinkage of 19 % while out-of-plane shrinkage perpendicular to the paper plane increased slightly to 34 %.

Future Work

It was shown, that porosity in the preceramic paper is a key factor for tailoring of the mechanical properties of the sintered ceramic product. Enhancement of porosity upon substitution of compliant pulp fiber by rigid ceramic fiber, can be compensated by applying external pressure which may significantly improve the packing density of the preceramic paper preform. Ceramic fiber loaded preceramic paper might offer a versatile and economic approach to process light-weight ceramics with tailored macro- and microscopic porosities for a broad field of applications.

References

N. Travitzky, H. Windsheimer, T. Fey, P. Greil: Preceramic Paper-Derived Ceramics (Feature), *J. Am. Ceram. Soc. 91(11) (2008) 3477–3492*

B. Gutbrod, D. Haas, N. Travitzky, P. Greil: Preceramic Paper Derived Alumina/Zirconia Ceramics, *Adv. Eng. Mat., 13 (2011) 494–501*

Printed Electronics

Nadja Straue, Moritz Wegener and Andreas Roosen

Objectives

In the field of functional ceramics current research addresses colloidal processing of nano-sized powders for printed electronics based on particulate systems. Layers thicknesses and structure features of submicron size are desired, which cannot be achieved via screen printing process. Tape casting was used to generate very thin layers with thicknesses down to 500 nm and soft lithography and ink jet printing were tested to achieve miniaturized structures in the range of 10 µm and below. The combination of casting and printing was applied for the development of printed electronic devices like field effect transistors (FET) and electroluminescence lamps (EL). Transparent electrodes were processed from tin-doped indium oxide (ITO). Zinc oxide (ZnO) was used as a semiconductor.

Experimental Procedure

ITO and ZnO powders from Evonik Degussa GmbH, Germany with primary particle sizes below 20 nm and agglomerated structures up to 100 nm in size were transferred to deagglomerated dispersions by treating the powder-ethanol mixtures in a tumbling mixer for 24 h. A low molecular carbon acid (CA) was used as dispersing agent whose optimal concentration was determined by the measurement of adsorption isotherms and viscosity in dependence on CA-concentration. For the preparation of casting slurries with shear thinning behaviour binder and plasticizer were added to the highly concentrated dispersion. After homogenization in a tumbling mixer, the slurries were screened and degassed to remove any coarse residues and dissolved gases. The slurries were cast onto a moving polymer carrier film, using a profiled rod bar or a doctor-blade casting head. For inkjet and softlithographic printing, inks of Newtonian flow behaviour were prepared. Inkjet printing was performed with a Dimatrix printer (USA). FET and EL devices were manufactured by soft lithographic microprinting.

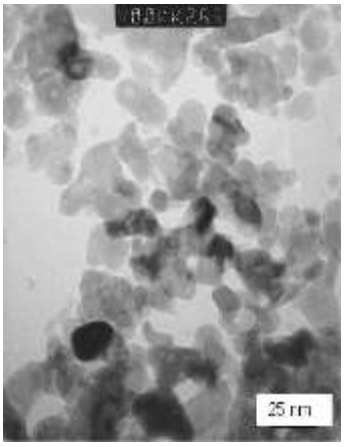

Fig. 1 TEM micrograph of ITO powder

Results

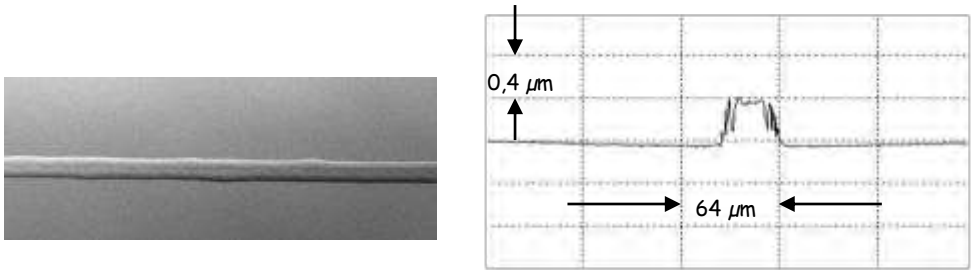

Fig. 2: Inkjet printed ITO lines. Left: line width: 30 µm. Right: profile of ITO line.

Fig. 2 shows the image and a confocal microscopy plot of inkjet printed lines. With a distance of 20 µm between each drop, a conductor line of ~ 30 µm in width and 40 nm in thickness could be obtained. On the right side a typical profile of a different line is shown, which demonstrates that the lines exhibit relatively low roughness. Smaller structures like line and spaces of 2 to 10 µm could be achieved via softlithographic printing (Fig. 3). With MiMiC fine structures with a clean background could be generated, whereas µCP resulted in particulate inhomogeneities of the background. ZnO green tapes of 550 nm thickness were cast with the profile rod technique (Fig. 4).

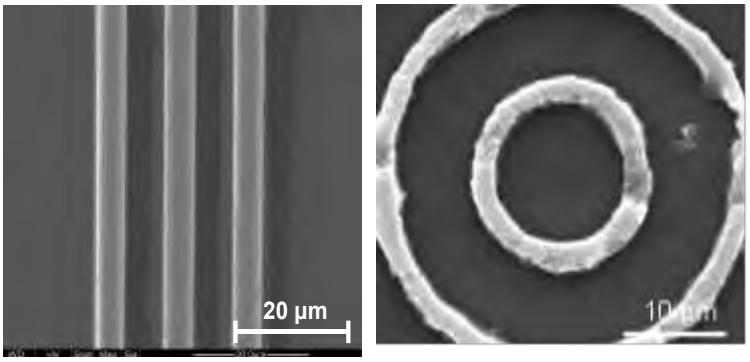

Fig. 3: Softlithographic printing of ITO lines. L: MiMiC. R: µCP.

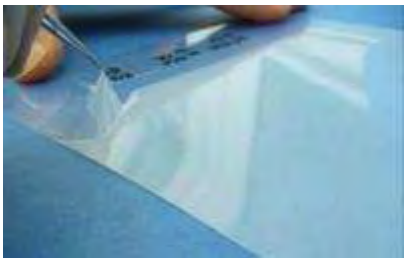

Fig. 4: Cast ZnO layer of 550 nm thickness (profiled rod technique)

FETs were manufactured by lamination of ZnO layer onto an oxidized silicon wafer and debindered at 500 °C to improve its conductivity. On top of this layer, source and drain were printed via MiMiC. These ITO structures exhibited a width of 30 µm, a gap of 5 µm and a thickness

Fig. 5: Schematic drawing of a FET

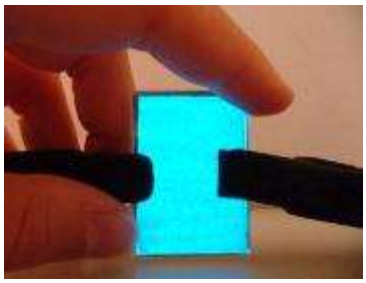

Fig. 6: EL (60 V, 600 Hz)

of 2.5 µm. Fig. 7 shows that the drain current can be controlled by the gate-source voltage, that the curves meet in 0-point, and that a plateau value is reached. The EL devices were manufactured by lamination of different green tapes onto a polymer sheet. Using the layer sequence PET film – ITO tape – ZnS:Cu tape (luminescence layer) – $BaTiO_3$ tape (dielectric layer) – ITO tape – PET film, a flexible EL lamp could obtained (Fig. 6).

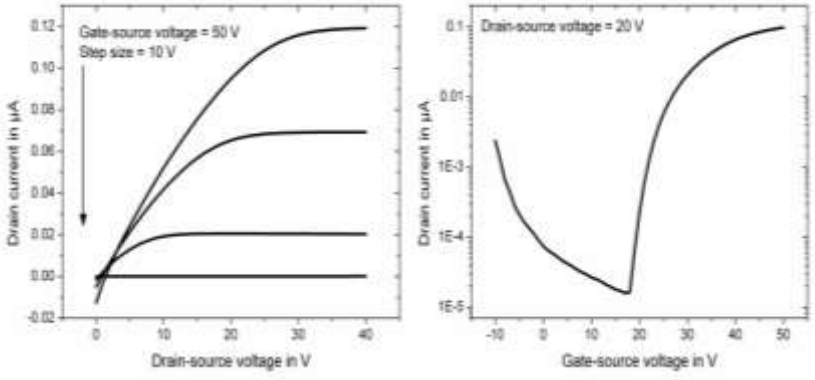

Fig. 7: Electrical characterization of printed FET. Left: output characteristics. Right: transfer characteristic.

Future Work

In case of FETs, the oxidized silicon wafer will be replaced by a ZnO layer and a polymer dielectric layer. Optimization of the EL refers to decrease of the voltage in order to improved performance of the different functional layers.

References

N. Straue, M. Rauscher, S. Walther, H. Faber, A. Roosen: Preparation and soft lithographic printing of nano-sized ITO-dispersions for the manufacture of electrodes for TFTs, *J. Mater. Sci. 44 (2009) 6011–6019*

N. Straue, S. Prado, S. Polster, A. Roosen: Profile rod technique: Continuous manufacture of ceramic green tapes and coatings with submicron thickness demonstrated for nano particulate ZnO powders. *J. Amer. Ceram. Soc. 94 (2011) 1698–1705*

N. Straue, M. Rauscher, M. Dressler, A. Roosen: Tape casting of ITO green tapes for flexible electroluminescence lamps. *J. Amer. Ceram. Soc. 95 (2012) 684–689*

3. PUBLICATIONS

Papers

(in alphabetical order)

01/11 **N. Da, A.A. Enany, N.Granzow, M.A. Schmidt, P.St.J. Russel, L. Wondraczek**
Interfacial reactions between tellurite melts and silica during the production of microstructured optical devices
Journal of Non-Crystalline Solids 357(2011) 1558–1563
DOI: 10.1016/j.jnoncrysol.2010.12.032

02/11 **N. Da, O. Grassmé, K.H. Nielsen, G. Peters, L. Wondraczek**
Formation and structure of ionic (Na, Zn) sulfophosphate glasses
Journal of Non-Crystalline Solids 357 (2011) 2202–2206
DOI: 10.1016/j.jnoncrysol.2011.02.037

03/11 **A. Dellert, A. Heunisch, A. Roosen**
The origin of anisotropic shrinkage in tape cast green tapes
Int. J. Appl. Ceram. Technol. 8 (2011) 1312–1319 DOI: 10.1111/j.1744-7402.2011.02665.x

04/11 **N. Douard, R. Detsch, R. Chotard-Ghodsnia, C. Damia, U. Deisinger, E. Champion**
Processing, physico-chemical characterisation and *in vitro* evaluation of silicon containing β-tricalcium phosphate ceramics
Mat. Sc. Eng.: C 31 (2011) 531–539 DOI: 10.1016/j.msec.2010.11.008

05/11 **G. Gao, S. Reibstein, M. Peng, L. Wondaraczek**
Tunable dual-mode photoluminescence from nanocrystalline Eu-doped Li_2ZnSiO_4 glass ceramic phosphors
Journal of Materials Chemistry, 21 (2011) 3156–3161 DOI: 10.1039/c0jm03273e

06/11 **G. Gao, R. Meszaros, M. Peng, L. Wondraczek**
Broadband UV-to-green photoconversion in V-doped lithium zinc silicate glasses and glass ceramics
OPTICS EXPRESS 19 (2011) 312–318 DOI: 10.1364/OE.19.00A312

07/11 **G. Gao, S. Reibstein, M. Peng, L. Wondraczek**

Dual-mode photoluminescence from nanocrystalline Mn^{2+}-doped Li, Zn-aluminosilicate glass ceramics

Phys. Chem. Glasses: Eur. J. Glass Sci. Technol. Part B 52 (2011) 1–4

08/11 **C. Gommes, N. Travitzky, W. Acchar, H. Birolis, D. Hotza**

Laminated object manufacturing of LZSA glass-ceramics

Rapid Prototyping Journal 17/6 (2011) 424–428

DOI: 10.1108/13552541111184152

09/11 **N. Granzow, S.P. Stark, M. A. Schmidt, A. S. Tverjanovich, L. Wondraczek**

Supercontinuum generation in chalcogenidesilica step-index fibers

OPTICS EXPRESS 19 (2011) 21003–21010 DOI: 10.1364/OE.19.021003

10/11 **S. Gruber, R. N. Klupp Taylor, H. Scheel, P. Greil, C. Zollfrank**

Cellulose-biotemplated silica nanowires coated with a dense gold nanoparticle layer

Materials Chemistry and Physics 129 (2011) 19–22

DOI: 10.1016/j.matchemphys.2011.04.027

11/11 **K. Gutbrod, P. Greil, C. Zollfrank**

Carbon auto-doping improves photocatalytic properties of biotemplated ceramics

Applied Catalysis B: Environmental 103 (2011) 240–245

DOI: 10.1016/j.apcatb.2011.01.034

12/11 **B. Gutbrod, D. Haas, N. Travitzky, P. Greil**

Preceramic paper derived alumina/zirconia ceramics

Adv. Eng. Mat. 13 (2011) 494–501 DOI: 10.1002/adem.201100017

13/11 **E. Hahn, J. Hum, J. Will, K. Zuo, D. Jiang, P. Greil**

Influence of Aggregated Powder Structures on Sintering Bahaviour of Multilayer Hydroxyapatite Laminates

J. Ceram. Sci. Tech. 02 (2011) 61–68 DOI: 10.4416/JCST2010-00034

14/11 **E. Hahn, T. Fey, K. Zuo, D.-L.Jiang, P. Greil**

Residual Stress Strengthening in Layered Tricalcium Phosphate (TCP) Bioceramics

J. Ceram.Sci. Tech., 02 (2011) 133–138 DOI: 10.4416/JCST2011-00005

15/11 **V. Ischenko, Y.-S. Jang, M. Kormann, P. Greil, N. Popovska, C. Zollfrank, J. Woltersdorf**

The effect of SiC substrate microstructure and impurities on the phase formation in carbide-derived carbon

Carbon 49 (2011) 1189–1198, DOI: 10.1016/j.carbon.2010.11.035

16/11 **E. Kamseu, B. Ceron, H. Tobias, E. Leonelli, M.C. Bignozzi, A. Muscio, A. Libbra**

Insulating behavior of metakaolin-based geopolymer materials assess with heat flux meter and laser flash techniques

Journal of Thermal Analysis and Calorimetry (2011) 1–11 in Press

DOI: 10.1007/s10973-011-1798-9

17/11 **C. Knieke, P. Vozdecky, A. Roosen, W. Peukert**

Verfahrenstechnische Fortschritte für die Herstellung neuer Materialien: Foliengießen aus Nanopartikeln

Chemie Ingenieur Technik 83 (2011) 1–11, DOI: 10.1002/cite.201000138

18/11 **G. Lakshminarayana, L. Wondraczek**

Photoluminescence and energy transfer in Tb^{3+}/Mn^{2+} co-doped $ZnAl_2O_4$ glass ceramics

Journal of Solid State Chemistry 184 (2011) 1931–1938 DOI: 10.1016/j.jssc.2011.05.059

19/11 **K. Lorenz, S. Bauer, K. Gutbrod, J.P. Guggenbichler, C. Zollfrank**

Anodic TiO_2 nanotube layers electrochemically filled with MoO_3 and their antimicrobial properties

Biointerphases 6 (2011) 1–6, DOI: 10.1116/1.3566544

20/11 **A.-K. Maier, L. Dezmirean, J. Will, P. Greil**

Three-dimensional printing of flash-setting calcium aluminate cement

J. Mater Sci 46 (2011):2947–2954, DOI 10.1007/s10853-010-5170-4

21/11 **R. Melcher, N. Travitzky, C. Zollfrank, P. Greil**

3D printing of Al_2O_3/Cu–O interpenetrating phase composite

Mater Sci 46 (2011) 1203–1210 DOI: 10.1007/s10853-010-4896-3

22/11 **R. Mezaros, R. Zhao, N. Travitzky, T. Fey, P. Greil, L. Wondraczek**

Three-dimensional printing of a bioactive glass

Glass Technol.: Eur. J. Glass Sci. Technol. 52 (2011) 111–116

23/11 **R. Meszaros, M. Wild, B. Merle, L. Wondraczek**
Flexural strength of PVD-coated float glass for architectural applications
Glass Technol.: Eur. J. Glass Sci. Technol. A 52 (2011) 190–196

24/11 **D. Opdenbosch, G.F. Popovski, O. Paris, C. Zollfrank**
Silica replication of the hierarchical structure of wood with nanometer precision
J. Mater. Res. 26 (2011) 1193–1201 DOI: 10.1557/jmr.2011.98

25/11 **J. Pedimonte, N. Travitzky, M. Korn, S. Kriegelstein, P. Greil**
Surface Modification of an Alumina-Based Bioceramic for Cement Application
Advanced Engineering Materials 13 (2011) DOI: 10.1002/adem.201180004

26/11 **M. Peng, G. Dong, L. Wondraczek, L. Zhang, J. Qiu**
Discussion on the origin of NIR emission from Bi-doped materials
Journal of Non-Crystalline Solids 357 (2011) 2241–2245
DOI: 10.1016/j.jnoncrysol.2010.11.086

27/11 **M. Peng, N. Zhang. L. Wondraczek, J. Qiu, Z. Yang, Q. Zhang**
Ultrabroad NIR luminescence and energy transfer in Bi and Er/Bi co-doped germanate glasses
OPTICS EXPRESS 19 (2011) 20799–20807 DOI: 10.1364/OE.19.020799

28/11 **S. Reibstein, L. Wondraczek, D. de Ligny, S. Krolikowski, S. Sirotkin, J.-P. Simon, V. Martinez, B. Champagnon**
Structural heterogeneity and pressure-relaxtion in compressed borosilicate glasses by in situ small angel X-ray scattering
Journal of Chemical Physics 134 (2011) 204502-6 DOI: 10.1063/1.3593399

29/11 **L. Schlier, M. Steinau, N. Travitzky, P. Greil**
Ferrosiliochromium-Filled Polymer-Derived Ceramics
Int. J. Appl. Ceram. Technol. 8 (2011)1–8 DOI: 10.1111/j.1744-7402.2011.02616.x

30/11 **L. Schlier, W. Zhang, N.Travitzky, P. Greil, J. Cypris, M. Weclas**
Macro-Cellular Silicon carbide Reactors for Nonstationary Combustion Under Piston Engine-Like Conditions
Int. J. of App. Cer. Tec. 8 (2011) 1237–1245 DOI: 10.1111/j.1744-7402.2010.02591.x

31/11 **M. Schmidt, L. Wondraczek, H.W. Lee, N. Granzow, N. Da, P.S.J. Russell**
Complex Faraday Rotation in Microstructured Magneto-optical Fiber Waveguides
Advanced Materials 23 (2011) 2681–2688, DOI: 10.1002/adma.201100364

32/11 **M. Schmirler, T. Knorr, T. Fey, A. Lynen, P. Greil, B.J.M. Etzold**
Fast production of monolithic carbide-derived carbons with secondary porosity produced by chlorination of carbides containing a free metal phase
Carbon 49 (2011) 4359–4367 DOI: 10.1016/j.carbon.2011.06.013

33/11 **N. Straue, S. Prado, S. Polster, A. Roosen**
Profile rod technique: Continuous manufacture of ceramic green tapes and coatings with submicron thickness demonstrated for nano particulate ZnO powders
J. Amer. Ceram. Soc. 94 (2011) 1698–1705 DOI: 10.1111/j.1551-2916.2010.04302.x

34/11 **P. Vozdecky, A. Roosen, Q. Ma, F. Tietz, H.P. Buchkremer**
Properties of Tape-Cast Y-substituted Strontium Titanate for Planar Anode Substrates in SOFC Applications
J. Mater. Sci. 46 (2011) 3493–3499 DOI: 10.1007/s10853-011-5255-8

35/11 **F. Wolff, L. Zirkel, S. Betzold, M. Jakob, V. Maier, F. Nachtrab, B. Ceron Nicolat, T. Fey**
Using Supercritical Carbon Dioxide for Physical Foaming of Advanced Polymer Materials
Intern. Polymer Processing XXVI (2011) 437–443 DOI: 10.3139/217.2469

36/11 **L. Wondraczek, J.C. Mauro, J. Eckert, U. Kühn, J. Horbach, J. Deubener, T. Rouxel**
Towards Ultrastrong Glasses
Adv. Mater. 23 (2011) 4578–4586 DOI: 10.1002/adma.201102795

37/11 **A. Wonisch, P. Polfer, T. Kraft, A. Dellert, A. Heunisch, A. Roosen**
A Comprehensive Simulation Scheme for Tape Casting: From Flow Behavior to Anisotropy Development
J. Amer. Ceram. Soc. 94 (2011) 2053–2060 DOI: 10.1111/j.1551-2916.2010.04358.x

38/11 **Q. Yan, Y. Liu, G. Chen, N. Da, L. Wondraczek**
Photoluminescence of Mn^{2+} Centers in Chalcohalide Glasses
J. Am. Ceram. Soc. 94 (2011) 660–662 DOI: 10.1111/j.1551-2916.2010.04356.x

39/11 **D.C. Yu, S. Ye, M.Y. Peng, Q.Y.Zhang, J. Wang, L. Wondraczek**
Efficient near-infrared downconversion in $GdVO_4$:Dy^{3+} phosphors for enhancing the photo-responanse of solar cells
Solar Energy Materials & Solar Cells 95 (2011) 1590-1593
DOI: 10.1016/j.solmat.2011.01.004

40/11 D.C. Yu, X.Y.Huang, S. Ye, M. Y. Peng, Q. Y. Zhang, L. Wondraczek

Three-photon near infrared quantum splitting in β-$NaYF_4$:Ho^{3+}

Applied Physics Letters 99 (2011) 161904-1–161904-3 DOI: 10.1063/1.3652916

Interfacial reactions between tellurite melts and silica during the production of microstructured optical devices

Contents lists available at ScienceDirect

Journal of Non-Crystalline Solids

journal homepage: www.elsevier.com/locate/jnoncrysol

Interfacial reactions between tellurite melts and silica during the production of microstructured optical devices

N. Da [a], A.A. Enany [a], N. Granzow [b], M.A. Schmidt [b], P.St.J. Russell [b], L. Wondraczek [a,*]

[a] Department of Materials Science, University of Erlangen-Nuremberg, Erlangen 91058, Germany
[b] Max-Planck-Institute for the Science of Light, Erlangen 91058, Germany

ARTICLE INFO

Article history:
Received 12 August 2010
Received in revised form 20 December 2010
Available online 21 January 2011

Keywords:
Tellurite
Silica
Interface
Rheology

ABSTRACT

Interfacial reactions between silica glass and tellurite melts were studied under confined conditions in the temperature regime of 400–700 °C, applying two different sampling techniques: isothermal heat-treatment of a several micrometer thick tellurite film, confined in a silica/tellurite/silica sandwich, and capillary filling of tellurite melts into silica microcapillaries. The sandwich technique provides detailed *ex situ* insights on the interface chemistry, microstructure and diffusion after given treatment times and temperatures. Data on dynamic viscosity, surface tension, wetting behaviour and eventual scaling effects was obtained from the capillary filling technique. For temperatures > 500 °C, silica is completely wet by the considered tellurite melts. At $T = 600$ °C and for a treatment time of 20 min or longer, cationic diffusion of Na^+ and Te^{4+} into the silica substrate occurs to a depth of several micrometers. At the same time, the tellurite melt attacks the silica surface, leading to the formation of a stationary silica–tellurite reaction layer and silica dissolution. Dissolved silica was observed to re-precipitate from the tellurite melt by liquid–liquid phase separation. In the early reaction stages, as a result of alkali diffusion into the silica substrate, β-quartz crystallizes at the interface (what can be avoided by using alkali-free filling glasses). Obtained data set the boundary conditions for the generation of tellurite–silica all-solid fiber waveguides by melt infiltration of silica photonic crystal fibers or microcapillaries.

1. Introduction

Recently, we proposed a novel technique for the fabrication of all-solid glass–glass photonic crystal fibers (PCFs) and capillary waveguides by pressure-assisted melt infiltration of silica PCFs or microcapillaries, respectively [1,2]. The approach was shown to enable combination of glasses which are, usually, considered incompatible because of significant differences in their thermomechanical and rheologic properties [2]. Exemplarily, photonic band-gap guidance has been demonstrated in a so-prepared silica–tellurite PCF [1], and various potential applications, ranging from super-continuum generation to optical filters and polarizers, have been discussed for silica–chalcogenide as well as silica–tellurite waveguides [1,2]. Optical performance of such a waveguide, however, is strongly dependent on the lateral and transversal homogeneity that can be achieved during the filling process. Depending on whether low optical loss is desired in the silica structure, in the filled sections of the fiber, or in both, several aspects must be taken into account. That is, particularly interfacial reactions that occur at the filling temperature between the filling medium and the silica matrix must be controlled. For the case of tellurite filling, such reactions may involve diffusion of tellurite species into the silica matrix, dissolution of silica in the tellurite melt, interfacial crystallization and phase separation. Secondly, process-induced volume reactions may occur such as increasing fictive pressure [3,4], the generation of structural anisotropy as a result of shear flow [5,6], isotropic changes in network topology as a result of the applied body forces [7], solution and re-boiling of gases [8,9], or pressure and confinement-dependent crystallization or phase separation processes [10]. In a first consideration, especially the interfacial reactions would lead to the occurrence of scattering centers inside the waveguide and, hence, to very high optical loss. While such reactions are less critical for chalcogenide melts (which typically do not wet silica), they are of significant importance for the fabrication of tellurite–silica hybride devices [1]. In the present paper, we are therefore focusing on the description and quantification of reactions that occur in the relevant temperature regime between exemplary tellurite melts (alkali-free and alkali-containing, respectively) and silica substrates, under confined conditions. This is done on the basis of an analysis of the effect of silica impurities on tellurite melts and the wetting behaviour, rheology, interdiffusion and crystallization at tellurite–silica contacts.

2. Experimental

As exemplary tellurite compounds, we have chosen (mol%) 75 TeO_2–10 ZnO–15 Na_2O (TZN) and 77 TeO_2–20.5 ZnO–2.5 La_2O_3 (TZL). In

* Corresponding author. Tel.: +49 9131 852 7553.
E-mail address: lothar.wondraczek@glas-keramik.uni-erlangen.de (L. Wondraczek).

0022-3093/$ – see front matter © 2011 Elsevier B.V. All rights reserved.
doi:10.1016/j.jnoncrysol.2010.12.051

Journal of Non-Crystalline Solids 357 (2011) 3202–3206

Contents lists available at ScienceDirect

Journal of Non-Crystalline Solids

journal homepage: www.elsevier.com/locate/jnoncrysol

Rapid Communication

Formation and structure of ionic (Na, Zn) sulfophosphate glasses

Ning Da [a], Oliver Grassmé [a,1], Karsten H. Nielsen [a], Gerhard Peters [b], Lothar Wondraczek [a,*]

[a] Chair of Glass and Ceramics, Department of Materials Science, University of Erlangen-Nuremberg, Erlangen 91058, Germany
[b] Institute of Inorganic Chemistry, University of Kiel, Kiel 24118, Germany

ARTICLE INFO

Article history:
Received 7 December 2010
Received in revised form 14 February 2011
Available online 10 March 2011

Keywords:
glass formation
sulfophosphate
pyrophosphate
structure

ABSTRACT

Supercooled ortho- and pyrophosphate melts of the type P_2O_5–EO–A_2O (E = $(Zn^{2+}, Ca^{2+}, Sr^{2+}, Ba^{2+}, Mg^{2+}, Mn^{2+})$; A = (Li^+, Na^+, K^+)) exhibit unusually high sulfate solubility. This enables facile fabrication of low-melting sulfophosphate glasses with SO_3 content of up to 25 mol%. Sulfur is incorporated into those glasses practically exclusively in the form of isolated SO_4^{2-} groups. The Q_i-group distribution of phosphate species is dominated by Q^1 and Q^0 groups, whereby replacing P_2O_5 with SO_3 results in increasing depolymerization. In this way, the glass forming region can readily be extended to compounds with an average number of bridging oxygen per phosphate anion of less than 0.5. In ionic (Na, Zn) sulfophosphate glasses, cations Zn^{2+} and Na^+ appear to cluster distinctively around PO_4^{3-} and SO_4^{2-} groups, respectively.

1. Introduction

Exploration and development of low melting inorganic glasses – glasses with a glass transition temperature T_g well below 400 °C and a softening temperature well below 500 °C – are receiving continuous attention from academic as well as industrial perspectives. At present, this is motivated by potential applications in organic/inorganic co-forming processes [1,2], the possibility of injection moulding (e.g. [3]), low-temperature sealing and melt-infiltration of rigid preforms for biomedical or optical applications [4–6]. Glass forming systems which are typically considered in this respect range from phosphates [7], particularly zinc [8,9] and tin [10] phosphates, to bismuthates, tellurites and chalcogenides (e.g. [11]). Many of these systems, however, are limited by one or more drawbacks such as the presence of toxic or rare components, weak chemical durability and high reactivity with water, strong devitrification tendency and/or the need of severe synthesis conditions. From the simple standpoint of T_g and viscosity–temperature-dependence, we have shown recently that sulfophosphate glasses might offer an alternative to overcome some of these problems [12].

Although for historical reasons, nomenclature is somewhat ambiguous [13,14], with sulfophosphate, we refer to systems which contain oxides of sulfur, phosphor and at least one other component in mol% quantities, and where $(SO_4^{2-}) \approx (PO_4^{3-})$. In a first consideration, these could be understood as pyrophosphate (invert) glasses within which phosphate groups are partly substituted by sulfate groups. Surprisingly, this class of glasses has been essentially disregarded by the broader scientific community and is therefore practically not understood today. This stands in sharp contrast to their expected properties and, particularly, their non-intuitive ease of fabrication.

To our best knowledge, sulfophosphate glasses in the present sense have first been described by Arkhipov, Mamoshin et al. in the early 1980s [15–21]. At that time, the material appears to have been studied primarily with respect to vitrification of sulfate-rich ashes. More recently, a rigorous overview, specifically on sulfur-containing iron phosphate glasses for immobilization of nuclear waste, was given by Bingham and Hand [22]. Simultaneous extrusion or moulding of polymer–sulfophosphate blends was suggested by Beall et al. [23,24] and later by Greiner et al. [25,26]. Some further applications were considered by, e.g., Fechner et al. [27,28]. Only recently, sulfophosphate glass ceramics have been introduced [29]. Whereas during the discovery of sulfophosphate glasses, initially, sulfate solubility appears to have been the major subject of interest, already shortly after Mamoshin et al.'s first reports, low T_g and softening temperature became primary targets. In this context, glass formation has now been studied in, e.g., Na_2SO_4–$ZnSO_4$–$NaPO_3$ [15], Na_2O–SiO_2–(P_2O_5)–SO_3 [17], M_2O_3–P_2O_5–SO_3–R_2O–RO [18], $ZnSO_4$–KPO_3–$NaPO_3$, Li_2SO_4–Na_2SO_4–K_2SO_4 [16], xS:(1-x)$AgPO_3$ [30], Na_2SO_4–P_2O_5–H_2O [19], $SrSO_4$–KPO_3–$Na_2B_4O_7$ [20] and Li_2O–Li_2SO_4–P_2O_5 [31,32]. In various cases, it has been shown that homogeneous glasses with T_g < 330 °C can be prepared at melting temperatures of <800 °C without the necessity of specifically high cooling rates [11]. T_g was reported to generally decrease with increasing sulfate content whereas at least in Na_2O–ZnO–P_2O_5–SO_3, at the same time, kinetic fragility decreases (on a high level) and empirical glass stability appears to increase. It has also been noted that in an almost archetypical way, rheologic properties of sulfophosphate melts appear related to topology and topological heterogeneity. In contrast, however, except for some preliminary spectroscopic analyses [17], only little has been reported on their and the corresponding glasses' structure.

* Corresponding author. Tel.: +49 9131 852 7553.
E-mail address: lothar.wondraczek@ww.uni-erlangen.de (L. Wondraczek).
[1] Now with: Siemens AG, Erlangen 91058, Germany.

0022-3093/$ – see front matter © 2011 Elsevier B.V. All rights reserved.
doi:10.1016/j.jnoncrysol.2011.02.037

Int. J. Appl. Ceram. Technol., 8 [6] 1312–1319 (2011)
DOI: 10.1111/j.1744-7402.2011.02665.x

International Journal of
Applied Ceramic TECHNOLOGY
Ceramic Product Development and Commercialization

The Origin of Anisotropic Shrinkage in Tape-Cast Green Tapes

Armin Dellert, Andreas Heunisch, and Andreas Roosen*

Department of Materials Science, Glass and Ceramics, University of Erlangen-Nuremberg, 91058 Erlangen, Germany

Cast green tapes exhibit an undesired shrinkage anisotropy attributed to particle alignment. In contrast, a high degree of particle alignment is desired for templated grain growth techniques. This paper investigates pure alumina and low temperature co-fired ceramic (LTCC) tapes, which were cast from powders of different morphology. It describes how the particle shape controls particle orientation and therefore anisotropic shrinkage. Special emphasis is given to the time dependent rotation behavior of the particles in the shear gradient during casting and to the casting parameters which influence the flow profile. This understanding is the key factor for the interpretation of particle orientation and anisotropic shrinkage.

Introduction

Ceramic green tapes can be further processed via punching, metallization, and lamination to build up complex multilayer devices, for example, capacitors, inductors, highly integrated circuits, actuators, and gas sensors.[1,2] These large volume productions are based on the established low cost tape casting process.[3,4] The trend in microelectronic industry toward further miniaturization demands denser packaging and higher integration of circuits, for example, in LTCC-based devices. This already leads to punched and printed structures having < 100 μm feature size. During firing, the exact position of all the features in the different layers must be maintained relative to each other. Therefore, a small deviation in the specified shrinkage, which is typically between 15 and 20%, can lead to device failure. The control of the exact position becomes even more complicated because of the anisotropic shrinkage of tape-cast sheets. Anisotropic shrinkage of ceramic green tapes has been reported in several studies using different materials.[5–7] It can be ascribed to an anisotropic microstructure of the green tapes,[8–12] which is

*[author's email address]

Materials Science and Engineering C 31 (2011) 537–550

Contents lists available at ScienceDirect

Materials Science and Engineering C

journal homepage: www.elsevier.com/locate/msec

Processing, physico-chemical characterisation and *in vitro* evaluation of silicon containing β-tricalcium phosphate ceramics

N. Douard [a], R. Detsch [b], R. Chotard-Ghodsnia [a], C. Damia [a], U. Deisinger [c], E. Champion [a,*]

[a] Université de Limoges, CNRS, ENSCI, SPCTS, UMR 6638, 123 Avenue Albert Thomas, 87060 Limoges Cedex, France
[b] Biocer Forschungs-GmbH, Ludwig-Thoma-Straße 36c, 95447 Bayreuth, Germany
[c] Friedrich-Baur-Research Institute for Biomaterials, University of Bayreuth, Universitätsstr. 30, 95440 Bayreuth, Germany

ARTICLE INFO

Article history:
Received 17 June 2010
Received in revised form 9 August 2010
Accepted 12 November 2010
Available online 18 November 2010

Keywords:
Tricalcium phosphate
Silicon
Powder synthesis
Sintering
In vitro evaluation

ABSTRACT

For bone grafting applications, the elaboration of silicon containing beta-tricalcium phosphate (β-TCP) was studied. The synthesis was performed using a wet precipitation method according to the hypothetical theoretical formula $Ca_{3-x}(PO_4)_{2-x}(SiO_4)_x$. Two silicon loaded materials (0.46 wt.% and 0.95 wt.%) were investigated and compared to a pure β-TCP. The maturation time of the synthesis required in order to obtain β-TCP decreased with the amount of silicon. Only restrictive synthesis conditions allow preparing silicon containing β-TCP with controlled composition. To obtain dense ceramics, the sintering behaviour of the powders was evaluated. The addition of silicon slowed the densification process and decreased the grain size of the dense ceramics. Rietveld refinement may indicate a partial incorporation of silicon in the β-TCP lattice. X-ray photoelectron spectroscopy and transmission electron microscopy analyses revealed that the remaining silicon formed amorphous clusters of silicon rich phase. The *in vitro* biological behaviour was investigated with MC3T3-E1 osteoblast-like cells. After the addition of silicon, the ceramics remained cytocompatible, highlighting the high potential of silicon containing β-TCP as optimised bone graft material.

1. Introduction

Bone mineral is a biological calcium phosphate material which contains various ionic substitutions [1]. Therefore, calcium phosphate materials are widely used for bone replacement in surgery due to their chemical compositions close to the bone mineral. These bioceramics favour bone reconstruction, thanks to high properties of resorbability for β-tricalcium phosphate (β-TCP – $Ca_3(PO_4)_2$) and good osteoconductivity for hydroxyapatite (HA – $Ca_{10}(PO_4)_6(OH)_2$) [2]. The bone remodelling process involves the coupled action of osteoblasts (bone-forming cells) and osteoclasts (bone-resorbing cells) [3] and silicon (Si) seems to play a role during this process. Indeed, Carlisle suggested that Si is implied in the first stage of mineralisation [4]. Xynos et al. stated that ionic products of bioactive glass dissolution, rich in Si element, increased the proliferation of osteoblast cells, up to 155% of the control [5]. Thus, the doping of calcium phosphates with Si would be a potential method to improve their bioactivity. The synthesis and characterisation of pure Si-substituted hydroxyapatite (Si-HA), where silicate substitutes for phosphate, was well investigated and conducted to the formula $Ca_{10}(PO_4)_{6-x}(SiO_4)_x(OH)_{2-x}$ [6,7]. *In vivo* [8] and *in vitro* [9] studies revealed an enhancement of the biological behaviour of HA after the silicon doping. In order to prepare calcium phosphate bioceramics with both higher resorption rates than HA and increased bioactivity, the study of silicon doped β-tricalcium phosphate appears of interest. Ghaith et al. prepared a silica containing β-TCP material through laser irradiation of a silica sol spin coated at the surface of dense β-TCP pellets [10]. Droplets of an amorphous phase containing silica remained embedded in the β-TCP. Bandyopadhyay et al. also reported the preparation, *via* a solid state method, of a nontoxic β-TCP with silica as dopant [11]. Wei et al. investigated the (Si, Zn) co-doping of TCP which led to β-TCP or α-TCP or a mixture of the two phases depending on the amount of dopants [12,13]. Except these studies, mainly the doping of α-TCP with silicon has been investigated [14–16]. On this basis, the aim of the present work was to investigate the possible incorporation of silicon into the β-TCP lattice. The study is focused on the powder synthesis *via* a wet precipitation method and further sintering. Particular attention was given to the determination of the chemical composition of ceramics (nature and location of the chemical phases within the ceramic material). Then, the influence of silicon on the *in vitro* cytocompatibility of the materials was investigated using a murine pre-osteoblastic cell line.

* Corresponding author. Tel.: +33 555457460; fax: +33 555457588.
E-mail address: eric.champion@unilim.fr (E. Champion).

0928-4931/$ – see front matter
doi:10.1016/j.msec.2010.11.009

Journal of Materials Chemistry

Dynamic Article Links

Cite this: J. Mater. Chem., 2011, 21, 3156

www.rsc.org/materials

PAPER

Tunable dual-mode photoluminescence from nanocrystalline Eu-doped Li_2ZnSiO_4 glass ceramic phosphors

Guojun Gao, Sindy Reibstein, Mingying Peng† and Lothar Wondraczek*

Received 29th September 2010, Accepted 9th December 2010
DOI: 10.1039/c0jm03273e

We report on tunable photoluminescence from mixed-valence Eu-doped nanocrystalline Li_2ZnSiO_4 glass ceramics. After preparation of the precursor glass in air, gradual reduction of Eu^{3+} to Eu^{2+} occurs intrinsically during thermal annealing and precipitation of crystalline Li_2ZnSiO_4. Dual-mode photoemission can be generated for exciting at a wavelength of about 360 nm. The resulting colour of luminescence, ranging from orange/red to blue, can be controlled by adjusting the annealing temperature and, hence, the degree of crystallization: with increasing annealing temperature, the ratio of luminescence intensities related to Eu^{3+} and Eu^{2+} species, respectively, varies as a result of increasing degree of Eu^{3+}-reduction as well as distinct changes in the optical scattering behaviour of the obtained glass ceramic. At the same time, the bandwidth of Eu^{2+}-related photoemission increases from 87 to 154 nm. The underlying mechanisms of photoemission and energy transfer from Eu^{2+} to Eu^{3+} are discussed on the basis of dynamic emission spectroscopy and structural considerations, and a description of the internal reduction process is given.

Introduction

Inorganic phosphor materials based on lanthanide-doped oxides and mixed-anion species are receiving great attention for potential applications in solid state lighting, display technology and various other areas.[1–4] Among the various dopant species, europium in divalent or trivalent oxidation state is traditionally occupying a dominant role. The electronic configuration of Eu is $[Xe]4f^7 5d^1 6s^2$. Photoluminescence from Eu^{3+}-doped matrices is characterized by a series of sharp emission bands which are located in the red spectral region. They can be assigned to the electronic transitions $^5D_0 \rightarrow {}^7F_J$ ($J = 0, 1, 2, 3, 4$) and, hence, their position is practically independent on ligand field strength whereas their intensity ratio is partly related to ligand symmetry.[5] For Eu^{2+}, photoemission occurs as a result of $4f^6 5d^1(T_{2g}) \rightarrow 4f^7(^8S_{7/2})$. In this case, the active electronic level is not shielded against the surrounding ligands and position and width of the emission band are strongly dependent on the host lattice.[6–9]

In oxide matrices, particularly when employing Eu_2O_3 as raw material, europium is usually incorporated in its trivalent form. In order to obtain Eu^{2+}-doped materials, one of four general reduction strategies can typically be applied: (i) to prepare the material in a strongly reducing atmosphere, *e.g.* H_2 or CO (*e.g.* ref. 10), (ii) to extrinsically reduce the polyvalent species in an as-prepared material, *e.g.* by high-energy photoreduction or thermal treatment in a reducing atmosphere (*e.g.* ref. 11–13), (iii) to provide a sufficiently acidic environment in which the reduced species can be obtained even for synthesis in air,[14,15] or (iv) to promote an intrinsic reduction process, *e.g.* by initiating a structural rearrangement in a frozen-in system.[12,13] For environmental, technological and cost-related reasons, the latter two methods are the most attractive, but can be applied only to a limited number of chemical systems.

Compared to conventional solid-state reaction, the glass ceramic route (preparation of a precursor glass and recrystallization of this glass to a dense and homogeneous polycrystalline material[24]) provides various technological and property-related advantages (*e.g.* ref. 25–28). Specific to the present case, it enables an attractive strategy to generate Eu^{2+} and mixed-valence Eu-doped materials *via* path (iv).[25] Nanocrystalline Eu-doped Li_2ZnSiO_4 glass ceramics are therefore introduced as such a material. Based on structural considerations as well as dynamic and static spectroscopic data, it is shown in the present report how the ratio between divalent and trivalent europium dopants and, hence, the colour of photoluminescence can be finely tuned from blue to orange and red by controlling the annealing and crystallization process, and how dual-band photoemission can be achieved.

Experimental

Zinc silicate glasses represent a classical candidate for the precipitation of nanocrystals after annealing. In particular, on the zinc-rich side, nanocrystalline β-willemite (Zn_2SiO_4) glass ceramics can readily be obtained.[29] If crystalline Li_2ZnSiO_4 is

Department of Materials Science, University of Erlangen-Nuremberg, Erlangen, 91058, Germany. E-mail: lothar.wondraczek@ww.uni-erlangen.de; Fax: +49 (0)913] 2853[; Tel: +49 (0)913] 85 27553
† Present address: Institute of Optical Communication Materials, South China University of Technology, Guangzhou, 510641, China.

Broadband UV-to-green photoconversion in V-doped lithium zinc silicate glasses and glass ceramics

Guojun Gao,[1] Robert Meszaros,[1] Mingying Peng,[1,2] and Lothar Wondraczek[1,*]

[1]*Department of Materials Science, University of Erlangen-Nuremberg, 91058 Erlangen, Germany*
[2]*Institute of Optical Communication Materials, South China University of Technology, Guangzhou 510641, China*
[*]*lothar.wondraczek@uni-erlangen.de*

Abstract: We report on photoluminescence of vanadium-doped lithium zinc silicate glasses and corresponding nanocrystalline Li_2ZnSiO_4 glass ceramics as broadband UV-to-VIS photoconverters. Depending on dopant concentration and synthesis conditions, VIS photoemission from $[VO_4]^{3-}$ is centered at 550-590 nm and occurs over a bandwidth (FWHM) of ~250 nm. The corresponding excitation band covers the complete UV-B to UV-A spectral region. In as-melted glasses, the emission lifetime is about 34 µs up to a nominal dopant concentration of 0.5 mol%. In the glass ceramic, it increases to about 45 µs. For higher dopant concentration, a sharp drop in emission lifetime was observed, what is interpreted as a result of concentration quenching. Self-quenching is further promoted by energy transfer to V^{4+} centers ($^2\Gamma_{12} \rightarrow {}^2\Gamma_{13}$). Partitioning of vanadium into V^{5+} and V^{4+} was examined by electron paramagnetic resonance and X-ray photoelectron spectroscopy. Suppression of V^{5+}-reduction requires careful adjustment of the optical basicity of the host glass and/or synthesis conditions.

OCIS codes: (160.4670) Optical materials; (140.3380) Laser materials; (160.2540) Fluorescent and luminescent materials; (140.4480) Optical amplifiers.

References and links

1. Y. Fujimoto, F. Tajiro, K. Izumi, S. Yoshida, S. Miyazaki, M. Sarai, K. Tanaka, Y. Kawabe, and E. Hanamura, "Vanadium-doped $MgAl_2O_4$ crystals as white light source," J. Lumin. **128**(3), 282–286 (2008).
2. J. El Ghoul, C. Barthou, M. Sradoun, and L. El Mir, "Optical characterization of SiO_2/Zn_2SiO_4:V nanocomposite obtained after the incorporation of ZnO:V nanoparticles in silica host matrix," J. Phys. Chem. Solids **71**(3), 194–198 (2010).
3. M. Anpo, I. Tanahashi, and Y. Kubokawa, "Photoluminescence and photoreduction of V_2O_5 supported on porous vycor glass," J. Phys. Chem. **84**(25), 3440–3443 (1980).
4. S. Dzwigaj, M. Matsuoka, M. Anpo, and M. Che, "Evidence of three kinds of tetrahedral vanadium (V) species in VSiB zeolite by diffuse reflectance UV-Visible and photoluminescence spectroscopies," J. Phys. Chem. B **104**(25), 6012–6020 (2000).
5. M. Morita, S. Kajiyama, T. Kai, D. Ravi, and T. Sakurai, "Physicochemical control of valence in luminescence of Cr(III) and V (III, IV) complexes embedded in (sol-gel) SiO_2 glasses," J. Lumin. **94–95**, 91–95 (2001).
6. S. Dzwigaj, J. Kraft, M. Che, S. Lim, and G. L. Haller, "Photoluminescence study of the introduction of V in Si-MSM-41: role of surface defects and their associated SiO˙ and SiOH groups," J. Phys. Chem. B **107**(16), 3856–3861 (2003).
7. ure D. C. Yu, S. Ye, M. Y. Peng, Q. Y. Zhang, J. R. Qiu, J. Wang, and L. Wondraczek, "Efficient near-infrared downconversion in $GdVO_4$:Dy^{3+} phosphors for enhancing the photo response of solar cells," Sol. Ener. Mat. Sol. Cell (2011), doi:10.1016/j.solmat.2011.01.004.
8. W. Höland and G. H. Beall, *Glass Ceramic Technology* (American Ceramic Society, 2002).
9. G. Gao, N. Da, S. Reibstein, and L. Wondraczek, "Enhanced photoluminescence from mixed-valency Eu-doped nanocrystalline silicate glass ceramics," Opt. Express **18**(S4 Suppl 4), A575–A583 (2010).
10. G. Gao, S. Reibstein, M. Peng, and L. Wondraczek, "Tunable dual-mode photoluminescence from nanocrystalline Eu-doped Li_2ZnSiO_4 glass ceramics phosphors," J. Mater. Chem. **21**(9), 3156–3161 (2011).

0142474 - $15.00 USD Received 11 Feb 2011; revised 5 Apr 2011; accepted 14 Apr 2011; published 18 Apr 2011

Phys. Chem. Glasses: Eur. J. Glass Sci. Technol. B April 2011 52 (2) 59–63

Dual-mode photoluminescence from nanocrystalline Mn^{2+}-doped Li,Zn-aluminosilicate glass ceramics

*Guojun Gao, Sindy Reibstein, Mingying Peng[1] & Lothar Wondraczek**

Department of Materials Science, University of Erlangen-Nuremberg, Martensstrasse 5, 91058 Erlangen, Germany

Manuscript received 9 November 2010
Revised version received 23 December 2010
Accepted 23 December 2010

We report on the photoluminescence (PL) of Mn^{2+}-doped (Li^+, Zn^{2+}) aluminosilicate glasses and glass ceramics. Glass ceramics are fabricated by controlled crystallization of as-melted precursor glasses. X-ray diffraction (XRD), electron spin resonance (ESR) and PL analyses indicate precipitation of $Li_{2-2y-x}Zn_yMn_xSiO_4$ with relatively low x and y values during the earlier phase of crystallization and $x \rightarrow 1$ in the later phase. During the crystallization process, Mn^{2+} ions, octahedrally coordinated in the precursor glass, partially precipitate on tetrahedral Zn^{2+} sites. This gives rise to the simultaneous occurrence of green and red luminescence, respectively, due to spin-allowed $^4T_1(G) \rightarrow {}^6A_1(S)$ and spin-forbidden $^4T_1(G) \rightarrow {}^6A_1(S)$ in $^{[IV]}Mn^{2+}$ and $^{[VI]}Mn^{2+}$. Accordingly, the amount of $^{[IV]}Mn^{2+}$ species, the ratio of $^{[VI]}Mn^{2+}/^{[IV]}Mn^{2+}$ and, hence, the ratio between green and red photoemission bands can be controlled by the temperature at which the glass ceramics are produced. FWHM of the resulting emission spectrum can be increased from about 100000 to about 50000 cm^{-1}. In parallel, as a result of multiple scattering, emission intensity appears to generally increase with increasing degree of crystallization.

Introduction

As for most *d–d* transitions in transition metal ions,[1] photoluminescence from Mn^{2+}-centres ([Xe]$3d^5$) is strongly dependent on ligand field strength and may occur over the spectral range from deep green to far red.[2–8] The corresponding excitation scheme spans the spectral range of about 300 to 500 nm. Distinct excitation bands are typically located at ~350, ~360, ~410, ~420 and ~500 nm, corresponding to the transitions of $^6A_1(S) \rightarrow {}^4E(D)$, $^6A_1(S) \rightarrow {}^4T_2(D)$, $^6A_1(S) \rightarrow {}^4A_1(G)$, $^4E(G)$, $^6A_1(S) \rightarrow {}^4T_2(G)$ and $^6A_1(S) \rightarrow {}^4T_1(G)$, respectively. Hence, Mn^{2+}-doped phosphors have a long tradition in various types of luminescent light sources, e.g. ultraviolet (UV)-blue LED-based systems, fluorescent tubes or compact fluorescent lamps (CFLs). Although photoemission spectra are usually characterized by one broad peak which can be, to a large extent, shifted towards either blue or red, two principal cases may generally be distinguished: if Mn^{2+} ions are incorporated on tetrahedral lattice sites ($^{[IV]}Mn^{2+}$) photoemission typically occurs in the green spectral range; when their coordination environment is octahedral ($^{[VI]}Mn^{2+}$), photoemission lies in the orange or red spectral regime. Consequently, for matrices within which Mn^{2+} can precipitate simultaneously on both types of lattice sites, dual-mode luminescence[9] can be generated and the resulting emission spectrum spans the spectral range from about 500–700 nm. If, in this case, the ratio of $[^{[IV]}Mn^{2+}]/[^{[VI]}Mn^{2+}]$ can be adjusted in a controlled way, the emission colour can be tuned to generate, e.g. warm white or yellow light of high colour quality. This would offer an interesting alternative to rare-earth doped materials (e.g. Refs 9, 10).

While over several decades, the optoelectronic properties of Mn^{2+} species have been studied for numerous glassy and (poly)crystalline matrix materials, related knowledge on Mn^{2+}-doped glass ceramics in which both $[^{[IV]}Mn^{2+}]$ and $[^{[VI]}Mn^{2+}]$ can be generated simultaneously is still limited.[9] In comparison to conventional polycrystalline phosphors, such glass ceramics, *per se*, offer several technological advantages. In particular, they enable facile production of luminescent microbeads by conventional melt processing.[11] When the colour of photoemission is not controlled by distinct combinations of multiple optically active dopant species but by the process of crystallization, they further enable straightforward recycling by simple remelting.

In the present paper, it is shown how such dual-mode luminescence can be obtained and controlled in Mn^{2+}-doped Li_2ZnSiO_4 glass ceramics. Optoelectronic properties will be discussed in relation to microstructure.

Experimental procedures

Samples with nominal composition $48SiO_2$·$24Li_2O$·$15{\cdot}8ZnO$·$8Al_2O_3$·$3K_2O$·$1P_2O_5$·$0{\cdot}2MnO$ (SLZAKP[10,12]) (mol%) were prepared by conventional melting and quenching from a 100 g batch of analytical grade reagents SiO_2, Li_2CO_3, ZnO, Al_2O_3, K_2CO_3, $NH_4H_2PO_4$ and $MnCO_3$. Melting was performed in alumina crucibles at 1550°C for 2 h. Subsequently, melts were poured into preheated graphite moulds and annealed for 2 h at 450°C. From the obtained glass slabs, individual

* Corresponding author. Email: lothar.wondraczek@ww.uni-erlangen.de
[1] Now with South China University of Technology, Guangzhou, China

Laminated object manufacturing of LZSA glass-ceramics

Cynthia Gomes
BAM Bundesanstalt für Material Forschung und prüfung, Berlin, Germany

Nahum Travitzky and Peter Greil
Department of Materials Science, Glass and Ceramics, University of Erlangen-Nuremberg, Erlangen, Germany

Wilson Acchar
Department of Physics, Federal University of Rio Grande do Norte, Natal, Brazil

Hansu Birol
Centro de Inovações CSEM Brasil, Belo Horizonte, Brazil, and

Antonio Pedro Novaes de Oliveira and Dachamir Hotza
Department of Mechanical Engineering, Ceramic and Glass Materials, Federal University of Santa Catarina, Florianópolis, Brazil

Abstract

Purpose – This paper seeks to detail the fabrication of a glass-ceramic substrate, based on the Li_2O-ZrO_2-SiO_2-Al_2O_3 (LZSA) system, by laminated object manufacturing (LOM) using water-based cast tapes.

Design/methodology/approach – Small amounts of $ZrSiO_4$ were added to control the thermal expansion coefficient (TEC) of the original glass-ceramic (LZSA5Zr: LZSA + 5 wt% $ZrSiO_4$). In order to verify the influence of the amount and nature of crystalline phases on the thermal and dielectric behavior of the material, LZSA and LZSA5Zr laminates were sintered at 700°C for 30 min and crystallized at either 800 or 850°C for 30 min.

Findings – LZSA laminates (sintered and crystallized at 700 and 800°C, respectively) exhibited a relative density of ~ 90 percent, a dielectric constant of 8.39, a dielectric loss tangent of 0.031 and TEC of $5.5 \times 10^{-6} K^{-1}$ (25-550°C). The addition of 5 wt% $ZrSiO_4$ to original LZSA glass-ceramics led to a nearly constant TEC value of $6 \times 10^{-6} K^{-1}$ throughout the whole temperature interval (25-800°C). Dielectric properties of LZSA5Zr did not show any remarkable change when compared to original LZSA.

Originality/value – The thermal, mechanical and electrical properties of LZSA glass-ceramic laminates fabricated by LOM makes them potential candidates for substrate applications.

Keywords Ceramics and glass, Thermal expansion, Dielectric properties, Laminated object manufacturing

Paper type Research paper

I. Introduction

Among other applications, glass-ceramic substrates may be employed for microelectronic packages, using the so-called low-temperature co-fired ceramic (LTCC) approach (Pannhorst, 1995; Moulson and Herbert, 2003; Birol *et al.*, 2006). The substrates used in microelectronic packages must fulfill several requirements such as: low dielectric constant for optimized transmission of signals, high dielectric strength, compatible thermal expansion coefficient (TEC) with the printed components, high mechanical strength, smooth surfaces free of distortion and of visual defects, and low cost high production (Prudenziati, 1994; Shimada *et al.*, 1983).

The majority of the ceramic substrates used in microelectronics are based on alumina, beryllia, magnesia, zirconia, and glass-ceramics (Prudenziati, 1994; Shimada *et al.*, 1983). The selection of the substrate is related to the application area of interest. It requires a careful evaluation of the chemical, mechanical, thermal, and electrical properties of the potential candidate. LTCC substrates based on glass-ceramic fulfill most of these conditions, whilst providing other benefits such as flexibility of design and fabrication in addition to reduced sintering temperatures. However, the production of these components demand fundamental and advanced ceramics processing techniques like powder preparation (Reed, 1995; Lange, 1989), colloidal processing (Lewis, 2000; Horn, 1990), and tape casting (Mistler, 1998; Hellebrand, 1996).

Sintering of the Li_2O-ZrO_2-SiO_2-Al_2O_3 (LZSA) glass-ceramic system occurs by viscous flow (Montedo *et al.*, 2008). The effect of ZrO_2 substitution by Al_2O_3 in the Li_2O-ZrO_2-SiO_2 (LZS) system (de Oliveira *et al.*, 2000) resulted in decrease of the glass transition temperature (T_g) and consequently increase of the material sinterability.

The current issue and full text archive of this journal is available at www.emeraldinsight.com/1355-2546.htm

Rapid Prototyping Journal
15/6 [2011] 424–429
© Emerald Group Publishing Limited [ISSN 1355-2546]
[DOI 10.1108/13552541111184152]

The authors are grateful to the Brazilian Foundation for the Coordination of Higher Education Graduate Training (CAPES) and to the German Academic Exchange Agency (DAAD) for supporting this work.

Supercontinuum generation in chalcogenide-silica step-index fibers

N. Granzow,[1,*] S. P. Stark,[1] M. A. Schmidt,[1] A. S. Tverjanovich,[2] L. Wondraczek,[4] and P. St.J. Russell[1,3]

[1]*Max Planck Institute for the Science of Light, Guenther-Scharowsky Str. 1, 91058 Erlangen, Germany*
[2]*Department of Chemistry, St. Petersburg State University, Universitetskii pr. 26, Petrodvorets, St. Petersburg, 198504 Russia*
[3]*Department of Physics, University of Erlangen-Nuremberg, Staudtstr. 7, 91058 Erlangen, Germany*
[4]*Institute of Glass and Ceramics, Department of Materials Science and Engineering, University of Erlangen-Nuremberg, Martensstr. 5, 91058 Erlangen, Germany*
*nic.olaf.granzow@mpl.mpg.de
www.pcfiber.com*

Abstract: We explore the use of a highly nonlinear chalcogenide-silica waveguide for supercontinuum generation in the near infrared. The structure was fabricated by a pressure-assisted melt-filling of a silica capillary fiber (1.6 μm bore diameter) with $Ga_4Ge_{21}Sb_{10}S_{65}$ glass. It was designed to have zero group velocity dispersion (for HE_{11} core mode) at 1550 nm. Pumping a 1 cm length with 60 fs pulses from an erbium-doped fiber laser results in the generation of octave-spanning supercontinuum light for pulse energies of only 60 pJ. Good agreement is obtained between the experimental results and theoretical predictions based on numerical solutions of the generalized nonlinear Schrödinger equation. The pressure-assisted melt-filling approach makes it possible to realize highly nonlinear devices with unusual combinations of materials. For example, we show numerically that a 1 cm long As_2S_3:silica step-index fiber with a core diameter of 1 μm, pumped by 60 fs pulses at 1550 nm, would generate a broadband supercontinuum out to 4 μm.

OCIS codes: (060.2280) Fiber design and fabrication; (060.2390) Fiber optics, infrared; (060.4370) Nonlinear optics, fibers; (060.7140) Ultrafast processes in fibers; (320.6629) Supercontinuum generation.

References and links

1. B. H. Chapman, J. C. Travers, S. V. Popov, A. Mussot, and A. Kudlinski, "Long wavelength extension of CW-pumped supercontinuum through soliton-dispersive wave interactions," Opt. Express **18**(24), 24729–24734 (2010).
2. W. J. Wadsworth, N. Joly, J. C. Knight, T. A. Birks, F. Biancalana, and P. St. J. Russell, "Supercontinuum and four-wave mixing with Q-switched pulses in endlessly single-mode photonic crystal fibres," Opt. Express **12**(2), 299–309 (2004).
3. A. Rulkov, M. Vyatkin, S. Popov, J. Taylor, and V. Gapontsev, "High brightness picosecond all-fiber generation in 525-1800nm range with picosecond Yb pumping," Opt. Express **13**(2), 377–381 (2005).
4. J. K. Ranka, R. S. Windeler, and A. J. Stentz, "Visible continuum generation in air-silica microstructure optical fibers with anomalous dispersion at 800 nm," Opt. Lett. **25**(1), 25–27 (2000).
5. M. Foster and A. Gaeta, "Ultra-low threshold supercontinuum generation in sub-wavelength waveguides," Opt. Express **12**(14), 3137–3143 (2004).
6. P. St. J. Russell, "Photonic-crystal fibers," J. Lightwave Technol. **24**(12), 4729–4749 (2006).
7. J. M. Dudley, G. Genty, and S. Coen, "Supercontinuum generation in photonic crystal fiber," Rev. Mod. Phys. **78**(4), 1135–1184 (2006).
8. J. C. Travers, "Blue extension of optical fibre supercontinuum generation," J. Opt. **12**(11), 113001 (2010).
9. F. G. Omenetto, N. A. Wolchover, M. R. Wehner, M. Ross, A. Efimov, A. J. Taylor, V. V. R. K. Kumar, A. K. George, J. C. Knight, N. Y. Joly, and P. St. J. Russell, "Spectrally smooth supercontinuum from 350 nm to 3 μm in sub-centimeter lengths of soft-glass photonic crystal fibers," Opt. Express **14**(11), 4928–4934 (2006).

(153522 - $15.00 USD Received 20 Aug 2011; revised 26 Sep 2011; accepted 27 Sep 2011; published 6 Oct 2011

Applied Catalysis B: Environmental 103 (2011) 240–245

Contents lists available at ScienceDirect

Applied Catalysis B: Environmental

journal homepage: www.elsevier.com/locate/apcatb

Carbon auto-doping improves photocatalytic properties of biotemplated ceramics

Kai Gutbrod, Peter Greil, Cordt Zollfrank*

Department of Materials Science and Engineering - Glass and Ceramics, University of Erlangen-Nuremberg, Martensstr. 5, D-91058 Erlangen, Germany

ARTICLE INFO

Article history:
Received 3 December 2010
Received in revised form 17 January 2011
Accepted 21 January 2011
Available online 27 January 2011

Keywords:
Photocatalysis
Carbon auto-doping
Titanium dioxide
Biotemplating

ABSTRACT

Biotemplated porous ceramics based on titania are promising candidates for the photo induced degradation of organic compounds in polluted streaming media, such as water or gas vapors. Reactors in various shapes can easily be produced by stringing a natural tissue template. Porous biotemplated ceramics were processed by vacuum infiltration of a titanium(IV)-isopropoxide-based sol into freeze dried stems of soft rush (*Juncus effusus*) and subsequent calcination between 400 and 800 °C. The solution of carbon in titania during calcination drastically improved the surface dependent photocatalytic activity, which was evaluated in comparison to commercially available titania powders. The biotemplated ceramics calcined below 600 °C showed the anatase phase, whereas calcination at higher temperatures leads to a mixture of anatase and rutile. The carbon content as measured by energy dispersive X-ray spectroscopy was reduced from 31.0 mol% after calcination at 400 °C–1.6 mol% after calcination at 800 °C. The auto-formation of Ti–OC/Ti–OCO bonds due to the temperature induced substitution of oxygen atoms by carbon atoms from the biotemplate and the formation of interstitial carbon was verified by X-ray Photoelectron Spectroscopy measurements. The lowest band edge energy, calculated from UV/vis-spectrometry measurements was found at 419 nm (2.96 eV) for the biotemplated samples calcined at 800 °C. The specific surface varied between 0.5 m^2/g and 45 m^2/g.

1. Introduction

Several studies in recent years demonstrated the high efficiency of titanium dioxide (TiO_2) for the photocatalytic degradation of organic compounds in various applications such as antibacterial agents [1,2], self-cleaning surfaces and in water and air purification [3]. The photocatalytic efficiency of TiO_2 refers to the absorption of a photon with a higher energy than the band gap (anatase: 3.23 eV, rutile: 3.10 eV) and the subsequent generation of an electron-hole pair under illumination with ultraviolet light. On the surface, the formation of OH radicals by trapped holes and of HO_2 radicals by trapped electrons may occur, if the charge-carriers are not recombined in the bulk TiO_2. The high oxidation power of these radicals causes degradation of adsorbed organic compounds [4]. Due to the small fraction of ultraviolet (UV) part in sun light (app. 5%) [12], numerous studies were performed to enhance the photocatalytic activity of titania by shifting the band gap to a lower energy level and thus into the area of visible light (VIS). One of the most promising ideas to solve this problem is a modification of the titania structure by doping with metals, such as strontium [5], palladium [6], tin [7], silver [8], rare earth metals, such as cerium, samarium, gadolinium, europium [9] or non-metallic elements, such as nitrogen [10–14], sulfur [14] and carbon [14–19]. Usually, the photocatalytic behavior of these materials was investigated on powders.

In fluid water and air purification, the use of powders for the degradation of organic compounds is of limited benefit, due to the necessity of the removal of the powder particles from the fluid medium after the purification process. Three-dimensional porous structures, such as honeycomb [20,21] and biological structures [22], may serve as catalyst carriers. A high surface area and permeability are required to achieve an effective photocatalytic reduction rate. The cellular structure of natural plants was demonstrated to offer a high potential to fulfill these requirements. The aerenchyma cellular structure in stems of the soft rush (*J. effusus*) was selected for our experiments. The effect of auto-doping of carbon during the sample preparation on the photocatalytic activity was evaluated by a comparison of the biotemplated samples with several reference powders and correlated to the specific surface of each sample. The results of catalytic efficiency (degradation of methylene blue (MB)) were correlated to the band edge energy of each material.

* Corresponding author. Tel.: +49 9131 85 27560; fax: +49 9131 85 28311.
E-mail address: cordt.zollfrank@ww.uni-erlangen.de (C. Zollfrank).

0926-3373/$ – see front matter © 2011 Elsevier B.V. All rights reserved.
doi:10.1016/j.apcatb.2011.01.034

CARBON 49 (2011) 3189–3198

available at www.sciencedirect.com

ScienceDirect

journal homepage: www.elsevier.com/locate/carbon

The effect of SiC substrate microstructure and impurities on the phase formation in carbide-derived carbon

Vladislav Ischenko [a], *Yeon-Suk Jang* [b], *Martina Kormann* [c], *Peter Greil* [b], *Nadejda Popovska* [c], *Cordt Zollfrank* [b,*], *Jörg Woltersdorf* [a,1]

[a] *Max-Planck-Institute for Microstructure Physics, Weinberg 2, D-06120 Halle, Germany*
[b] *University of Erlangen-Nuremberg, Department of Materials Science and Engineering, Glass and Ceramics, Martensstr. 5, D-91058 Erlangen, Germany*
[c] *University of Erlangen-Nuremberg, Department of Chemical- and Bioengineering, Chemical Reaction Engineering, Egerlandstraße 3, D-91058 Erlangen, Germany*

ARTICLE INFO

Article history
Received 27 July 2010
Accepted 19 November 2010
Available online 25 November 2010

ABSTRACT

Carbon layers were obtained by etching of different silicon carbides with Cl_2/H_2 gas mixtures at high temperatures (carbide-derived carbon). The resulting layers were studied by analytical and high resolution transmission electron microscopy. It was found, that etching of high purity single crystal SiC wafers exclusively yields amorphous carbon. The development of graphite-like and nanodiamond inclusions was observed using commercially available sintered SiC and polymer-derived SiC, which both contained boron- and carbon-rich phases. The presence of turbostratic graphite regions and isolated diamond particles in the bulk of non-chlorinated sample was revealed in the commercial polycrystalline SiC substrate. This fact points to the possible nucleation and growth of diamond phases during sintering of the commercial SiC substrate. Chlorination of boron-implanted single crystal SiC wafer showed that the presence of boron-rich dopants in the SiC alone does not trigger the nucleation of diamond phases. An initial surplus of carbon in the SiC substrates appeared to be required as could be shown for boron doped polycarbosilane derived SiC. Thermodynamic considerations assisted by quantum chemical calculations showed the low effect of hydrogen in the Cl_2/H_2 gas mixtures during SiC chlorination for the nucleation of diamond phases.

1. Introduction

A number of methods are available in the literature describing the formation of carbon layers on the surface of metal carbides by selective elimination of the metal atoms from the substrate [1–8]. One of the most promising approaches, which allows minimization of contamination of the carbon layer and enables the formation of uniform carbon layers on the carbide surfaces even with complex geometry, is the etching of metal carbide with chlorine [9–12]. The carbide-derived carbon (CDC) is essentially formed as an amorphous carbon containing both sp^2- and sp^3-hybridized carbon species. Depending on the ratio of sp^2- to sp^3-species, the ordering of carbon into sp^2-rich graphite-like or sp^3-rich diamond phases in the CDC matrix can be observed. In particular, it has been reported [13] that adding hydrogen to the etching gas mixture, to saturate the dangling bonds at the carbon atoms, can stabilize the diamond nuclei. Contrary, diamond

* Corresponding author: Fax: +49 9131 8528311.
E-mail address: cordt.zollfrank@ww.uni-erlangen.de (C. Zollfrank).
[1] In memoriam Prof. Dr. Jörg Woltersdorf.
0008-6223/$ – see front matter © 2010 Elsevier Ltd. All rights reserved.
doi:10.1016/j.carbon.2010.11.035

J Therm Anal Calorim
DOI 10.1007/s10973-011-1798-9

Insulating behavior of metakaolin-based geopolymer materials assess with heat flux meter and laser flash techniques

E. Kamseu · B. Ceron · H. Tobias · E. Leonelli · M. C. Bignozzi · A. Muscio · A. Libbra

Received: 8 April 2011 / Accepted: 8 July 2011

Abstract Thermo physical behavior of metakaolin-based geopolymer materials was investigated. Five compositions of geopolymers were prepared with Si/Al from 1.23 to 2.42 using mix of sodium and potassium hydroxide (~ 7.5 M) as well as sodium silicate as activator. The products obtained were characterized after complete curing to constant weight at room temperature. The thermal diffusivity (2.5–4.5 × $(10^{-7}m^2/s)$ and thermal conductivity (0.30–0.59 W/m K) were compared to that of existing insulating structural materials. The correlation between the thermal conductivity and parameters as porosity, pore size distribution, matrix strengthening, and microstructure was complex to define. However, the structure of the geopolymer matrix, typical porous amorphous network force conduction heat flux to travel through very tortuous routes consisting of a multiple of neighboring polysialate particles.

Keywords Geopolymer · Insulation · Porous matrix · Thermal diffusivity · Thermal conductivity

Introduction

Insulating materials are using to slow heat transfer. In the modern times, as mankind became more sophisticated, a wide range of largely synthetic materials are developed which proves to be far superior insulators. However, with each step away from the natural substances, mankind not only saw incremental improvements in the ability to insulate, but also huge increases in the environmental and health problems caused by various synthetic insulation materials.

More sustainable insulating matrices have been developed from alumina (Al_2O_3) and silica (SiO_2) or combination of both. Two oxides with thermal conductivity of 6–10 and 18–30 W/m K, respectively for SiO_2 and Al_2O_3 in crystalline form. The transformation of the crystalline structure to amorphous creates a high level disorder in the special arrangement of atoms and decreases the thermal conductivity to ~ 1.5 W/m K. Additional voids and pores will enable the amorphous structure to be filled in air and insulating gas with consequence in further decrease of heat transfer ability through the amorphous matrix.

The gas-filled pores have a small role to play, the solid matter structures a decisive one. The structure includes the bulk matter and the voids (pores). The chemical composition of the material will determine the thermal conductivity while the pores content will affect the effective value. Thus, the insulating behavior of a material is governed by parameter such as porosity, gas- and liquid-filled pores, mineral content, and grain size distribution [1–5]. Hence, insulating materials can be produced by various combinations of

E. Kamseu (✉) · E. Leonelli
Department of Materials and Environmental Engineering, University of Modena and Reggio Emilia, Via Vignolese 905/A, 41125 Modena, Italy
e-mail: kamseuelie2001@yahoo.fr; elie.kamseu@unimore.it

B. Ceron · H. Tobias
Department Werkstoffwissenschaften Lehrstuhl für Glas Und Keramik, Universtat Erlangen-Nürnberg, Martensstr. 5, 91058 Erlangen, Germany

M. C. Bignozzi
Department of Civil, Environmental and Materials Engineering, University of Bologna, Via Terracini 28, 40131 Bologna, Italy

A. Muscio · A. Libbra
Department of Mechanical and Civil Engineering, University of Modena and Reggio Emilia, Via Vignolese 905/B, 41125 Modena, Italy

Published online: 05 August 2011

Chemie Ingenieur Technik

Forschungsarbeit

Verfahrenstechnische Fortschritte für die Herstellung neuer Materialien – Foliengießen aus Nanopartikeln

Catharina Knieke[1], Pavel Vozdecky[2], Andreas Roosen[2] und Wolfgang Peukert[3,*]

DOI: 10.1002/cite.201000118

Am Beispiel der Herstellung keramischer Folien wird gezeigt, wie verfahrenstechnische Fortschritte zu verbesserten Werkstoffeigenschaften führen. Ein wesentlicher verfahrenstechnischer Fortschritt ist die Möglichkeit, Nanopartikel durch Echtzerkleinerung in Rührwerkskugelmühlen in hoher Ausbeute herzustellen. Die nanoskaligen Suspensionen können direkt zu keramischen Folien verarbeitet werden. Die Verarbeitung der Nanopartikel erfordert eine Anpassung der bestehenden Prozessbedingungen und führt zu deutlichen Eigenschaftsverbesserungen der daraus hergestellten Werkstoffe hinsichtlich Gefügestruktur, Oberflächenrauhigkeit, Festigkeit und optischer Transparenz.

Schlagwörter: Keramische Folien, Nanomahlung, Rührwerkskugelmühle

Eingegangen: 29. Juli 2010; *revidiert:* 21. Dezember 2010, *akzeptiert:* 21. Januar 2011

Advanced Processes for Better Materials – Tape Casting from Nanoparticles

It is shown by the example of a ceramic tape casting process, how advances in the field of process engineering lead to improved material properties. One great advance is the possibility of producing nanoparticles in stirred media mills. The nanosized particle suspensions can be directly processed to ceramic tapes. The processing of nanoparticles requires specifically adjusted process conditions, but leads to a drastic improvement of the final product properties. Hence, dense and crack-free ceramic tapes with a higher mechanical strength, a lower surface roughness and a translucent character compared to tapes from micro-sized powders can be obtained.

Keywords: Ceramic tapes, Nano-milling, Stirred media mill

1 Einleitung

Die Werkstoffwissenschaften und die Verfahrenstechnik wurden und werden in Deutschland bisher als Wissenschaftsrichtungen mit relativ wenigen Berührungspunkten wahrgenommen. Während die Werkstoffwissenschaften traditionell das Endprodukt im Blick hatten, war die Verfahrenstechnik in der Vergangenheit überwiegend auf die Unit Operations fokussiert. Die Herstellung und Verarbeitung keramischer, metallischer oder polymerer Werkstoffe für Funktions- oder Strukturmaterialien war und ist die Domäne der Werkstoffwissenschaftler, während die Verfahrenstechnik systematische Untersuchungen zur Filtration, zum Trocknen oder zum Zerkleinern vorantrieb. In den letzten Jahren haben sich allerdings tiefgehende Veränderungen ergeben: mit wachsender Komplexität der Produkte nahm in den Werkstoffwissenschaften die Bedeutung der Prozesstechnologie zu, während in der Verfahrenstechnik die Wende hin zu den Produkteigenschaften und zum Product Engineering vollzogen wurde.

Eine Vorreiterrolle spielt hier sicher die Partikeltechnologie, die sich ausgehend von einer mechanischen Verfahrenstechnik strategisch weiter entwickelt hat zur Wissenschaft und Technologie von dispersen Systemen. Die Stoffwandlung an Partikelsystemen erfolgt nicht mehr nur mit mechanischen, sondern auch mit biologischen, chemi-

[1] Dipl.-Ing. Catharina Knieke, New Jersey Institute of Technology, Otto H. York Department of Chemical, Biological and Pharmaceutical Engineering, Newark, NJ, USA. [2] Pavel Vozdecky, Prof. Dr. Andreas Roosen, Universität Erlangen-Nürnberg, Lehrstuhl für Glas und Keramik, Martensstraße 5, 91058 Erlangen, Germany. [3] Prof. Dr.-Ing. Wolfgang Peukert (wpeukert@lfg.uni-erlangen.de), Universität Erlangen-Nürnberg, Lehrstuhl für Feststoff- und Grenzflächenverfahrenstechnik, Cauerstraße 4, 91058 Erlangen, Germany.

Journal of Solid State Chemistry 184 (2011) 1931–1938

Contents lists available at ScienceDirect

Journal of Solid State Chemistry

journal homepage: www.elsevier.com/locate/jssc

Photoluminescence and energy transfer in Tb^{3+}/Mn^{2+} co-doped $ZnAl_2O_4$ glass ceramics

Gandham Lakshminarayana, Lothar Wondraczek *

Department of Materials Science, University of Erlangen-Nuremberg, Erlangen 91058, Germany

ARTICLE INFO

Article history:
Received 24 January 2011
Received in revised form
13 April 2011
Accepted 29 May 2011
Available online 6 June 2011

Keywords:
Phosphor
Glass ceramic
Rare earth
Transition metal
Energy transfer
Lighting

ABSTRACT

We report on Tb^{3+} as efficient sensitizer for red photoemission from Mn^{2+}-centers in ZnO–B_2O_3–Al_2O_3–Si_2O–Na_2O–SrO glasses and corresponding gahnite glass ceramics. In comparison to singly or co-doped glasses, the glass ceramics exhibit significantly increased emission intensity. Structural considerations, ESR, and dynamic luminescence spectroscopy indicate partial incorporation of Mn^{2+} as well as Tb^{3+} into the crystalline phase, the former on octahedral Zn^{2+}-sites. Interionic distance and charge transfer probability between both species depend on crystallization conditions. This enables control of the energy transfer process and, hence, tunability of the color of photoemission by simultaneous emission from Tb^{3+} and Mn^{2+} centers. Concentration quenching in Mn^{2+}-singly doped materials was found at a critical dopant concentration of about 1.0 mol%. The energy transfer process was studied in detail by dynamic as well as static luminescence spectroscopy. Spectroscopic results suggest the application of the studied materials as single or dual-mode emitting phosphor for luminescent lighting.

1. Introduction

Zinc aluminate ($ZnAl_2O_4$) is a wide-band gap semiconductor ($E_g = 3.8$ eV), which occurs naturally as the mineral gahnite and is a member of the spinel family. Spinels represent an important class of chemically and thermally stable crystalline materials. The interaction between ZnO and Al_2O_3 to form $ZnAl_2O_4$ spinel [cubic, space group $Fd3m$, $a = 8.088$ Å] follows diffusion of Zn and O and an effective unilateral transfer of ZnO [1] as shown in Fig. 1. Of the contributing cations, Zn^{2+} is tetrahedrally coordinated and Al^{3+} occupies octahedral sites [2]. Occupation (or substitution) of these two sites is decided by various factors, such as ionic size, cationic charge, electron distribution and electronic state [3], and gahnite and other spinels provide a suitable host lattice for various dopant species, e.g., luminescence properties of rare-earth doped zinc spinels have been reported recently [4–6]. By precipitating gahnite crystals from a transition metal (TM) or rare earth (RE) doped glass melt and partitioning the dopant species into the crystal phase, their optical activity can typically be enhanced significantly [7–18].

The ground state of the Mn^{2+} ion is $^6A_{1g}$ (spherically non-degenerated, octahedral symmetry). As all of the excited states are quartets or doublets, the optical absorption spectra of Mn^{2+} ions exhibit only spin forbidden transitions [19]. Excitation bands lie in the UV–Vis spectral region, and photoluminescence typically results from the $^4T_{1g}(G) \rightarrow {}^6A_{1g}(S)$ transition [20]. This transition becomes partially allowed as a result of spin–orbit interactions. Typically, d–d transitions are strongly dependent on the field strength of the surrounding ligands because the d-shell is only weakly shielded from its environment. In Mn^{2+}, its spectral position can vary from green to deep red color, depending on coordination and ligand field strength. Usually, tetrahedral coordination ($^{IV}Mn^{2+}$, weak crystal field) results in green emission whereas octahedral coordination ($^{VI}Mn^{2+}$, stronger crystal field) results in orange to red emission [19]. Over decades, this property has made Mn^{2+}-doped materials one of the most important types of phosphors in lighting and display applications [21]. On the other hand, Tb^{3+} exhibits a relatively simple energy level structure with the ground state $^7F_6$, and several other low-lying excited states (i.e., $^5D_{4,\,3,\,2,\,1,\,0}$, $^5L_{10}$, $^5G_6$, $^5L_6$, etc.). Typically, Tb^{3+}-doped materials show intense photoluminescence in the green spectral region [22]. In a co-doped material, energy transfer from one ion (sensitizer) to another ion (activator) may occur, in principle, in whole or partly by non-radiative and/or radiative processes [23–25]. Such energy transfer processes have recently received significant attention, involving ion pairs such as Eu^{2+}/Mn^{2+} [26,27], Sm^{3+}/Tb^{3+} [28], Ce^{3+}/Tb^{3+} [29], Tb^{3+}/Eu^{3+} [30], and Ce^{3+}/Eu^{2+} [31,32]. Due to the forbidden $^4T_1 \rightarrow {}^6A_1$ transition of Mn^{2+}, the fluorescence intensity of Mn^{2+} singly doped materials is low under UV excitation. An efficient sensitizer would significantly enhance red photoemission from Mn^{2+} also under UV

* Corresponding author. Fax: +49 9131 28311.
E-mail address: lothar.wondraczek@ww.uni-erlangen.de (L. Wondraczek).

0022-4596/$ - see front matter © 2011 Elsevier Inc. All rights reserved.
doi:10.1016/j.jssc.2011.05.059

Anodic TiO_2 nanotube layers electrochemically filled with MoO_3 and their antimicrobial properties

Kathrin Lorenz
Department of Materials Science and Engineering, Glass and Ceramics, Friedrich-Alexander-University of Erlangen-Nuremberg, D-91058 Erlangen, Germany and Department of Materials Science and Engineering, Surface Science and Corrosion, Friedrich-Alexander-University of Erlangen-Nuremberg, D-91058 Erlangen, Germany

Sebastian Bauer
Department of Materials Science and Engineering, Surface Science and Corrosion, Friedrich-Alexander-University of Erlangen-Nuremberg, D-91058 Erlangen, Germany

Kai Gutbrod
Department of Materials Science and Engineering, Glass and Ceramics, Friedrich-Alexander-University of Erlangen-Nuremberg, D-91058 Erlangen, Germany

Josef Peter Guggenbichler
Laboratory for the Development of Healthcare Products, A-6345 Kössen, Austria

Patrik Schmuki[a)]
Department of Materials Science and Engineering, Surface Science and Corrosion, Friedrich-Alexander-University of Erlangen-Nuremberg, D-91058 Erlangen, Germany

Cordt Zollfrank
Department of Materials Science and Engineering, Glass and Ceramics, Friedrich-Alexander-University of Erlangen-Nuremberg, D-91058 Erlangen, Germany

(Received 18 January 2011; accepted 24 February 2011; published 17 March 2011)

In the present work, the authors produce a Ti surface with a TiO_2 nanotube coating and investigate the electrochemical filling of these layers with MoO_3. The authors demonstrate that using a potential cycling technique, a homogenous MoO_3 coating can be generated. Controllable and variable coating thicknesses are achieved by a variation of the number of cycles. Thicknesses from a few nanometers to complete filling of the nanotube layers can be obtained. A thermal treatment is used to convert the as-deposited amorphous MoO_3 phases into MoO_3. These MoO_3 loaded nanotube layers were then investigated regarding their antimicrobial properties using strains of *Staphylococcus aureus*, *Escherichia coli*, and *Pseudomonas aeruginosa*. The authors found that the combination of crystalline MoO_3 on TiO_2 nanotubes shows excellent antimicrobial properties. © *2011 American Vacuum Society*. [DOI: 10.1116/1.3566544]

I. INTRODUCTION

Health care associated infections [nosocomial infections (NIs)] are the fourth leading cause of disease in industrialized countries and the most common complication affecting hospitalized patients.[1] Reports from the U.S. indicate that NIs account for 2×10^6 infections and 90 000 preventable deaths per year.[2] However, it has been described that the surfaces of the inanimate environment such as instruments, cables, switches, accessories, doorknobs, bed gear, blankets, and last but not the least sanitary installations can act as a reservoir for multiresistant pathogens.[3] Effective strategies to reduce the number of NIs by infection transmission through genuine bacteria free inanimate surfaces will increase the state of health in society. Therefore, reducing microbial contamination and biofilm growth on inanimate surfaces in health care units and also in public environments has become an area of increased scientific and economic interest.[4] Current approaches to decrease microbial contamination on inanimate surfaces are either preventive or biocidal.[4] The first category aims at preventing adhesion of the infectious agents on the surface through an antiadhesive coating. These include poly(ethylene glycol),[5] diamondlike carbon,[6] self-cleaning surfaces (Lotus effect),[7,8] and amphiphilic polymer coatings.[9] Since the infectious agents are not eliminated, their presence might be still a risk for patients. A more reliable approach is the use of biocidal coatings on material surfaces.[10] Successfully applied technologies employ organic antibiotics such as Triclosan[11] or inorganic antimicrobials such as silver ions,[12–14] copper ions,[15] and photocatalytic agents (TiO_2).[16] Some existing antimicrobial modified surfaces suffer from a number of limitations, including the rapid release of the adsorbed antibiotic in the first hours after application,[2] development of resistance against agents, or general cytotoxicity as, for example, reported for silver ions on mammalian cells.[17]

It was recently found that some transition metal oxides such as molybdenum oxides (MoO_x, $2 < x < 3$) are exceptionally effective agents against severe nosocomial pathogens such as *S. aureus*, *E. coli*, and *P. aeruginosa*.[18–20] The

a)Electronic mail: schmuki@www.uni-erlangen.de

J Mater Sci (2011) 46:2947–2954
DOI 10.1007/s10853-010-5170-4

Three-dimensional printing of flash-setting calcium aluminate cement

Anne-Kathrin Maier · Laura Dezmirean · Julia Will · Peter Greil

Received: 4 August 2010 / Accepted: 7 December 2010 / Published online: 22 December 2010

Abstract Three-dimensional indirect printing of flash-setting calcium aluminate cement (CAC) was investigated. Upon water injection into a biphasic mixture of tricalcium aluminate ($3CaO \cdot Al_2O_3$) and dodecacalcium heptaaluminate ($12CaO \cdot 7Al_2O_3$) (phase ratio 0.56/0.44) initially a gel formed acting as a bonding phase which stabilizes the printed object geometry. Post-exposure in water finally resulted in the formation of $2CaO \cdot Al_2O_3 \cdot 8H_2O$ and $4CaO \cdot Al_2O_3 \cdot 19H_2O$ reaction phases as confirmed by SEM, X-ray diffraction, and FTIR analyses. Reduction of porosity by volume expansion upon hydrolysis reaction from 50% after printing to 20% after post-treatment gave rise for an increase of compressive strength from 5 to 20 MPa, respectively. A bone regenerating scaffold for a microvascular loop model was fabricated by 3D printing and hydraulic reaction bonding to demonstrate the potential of using flash-setting calcium aluminate cement powder for biomedical ceramic applications.

Introduction

Three-dimensional printing (3DP) is an additive manufacturing technology used in ceramic prototype manufacturing [1–3]. Typically, 3D printing of ceramic powder systems involves a local solidification reaction of a binder with the injected printing solution. Post-processing of the porous printed parts requires removal of the binder and a subsequent sintering process at high temperatures to consolidate the printed object. Anisotropic packing structure of the bonded powder granules in the printed component may cause a non-uniform densification. Furthermore, a high linear shrinking of typically 15–25% may give rise for reduced dimensional accuracy upon conversion of the printed object into the sintered object.

The flexibility of shaping, however, makes 3DP interesting for the formation of biomedical implants from synthetic materials that are individually tailored to the tissue defect [4]. Thus, for example, biocompatible bone substitutes were manufactured by 3D printing from a variety of materials including tetracalciumphosphate, tricalciumphosphate, hydroxyapatite, etc [5–7]. In order to reduce high sintering temperatures for consolidation of printed shapes reaction bonding at ambient temperature was applied. For example, tricalcium phosphate (TCP) powder was reaction bonded applying diluted phosphoric acid as printing solution, which triggered local formation of dicalcium phosphate dihydrate under acidic conditions [8, 9].

Hydraulic cement systems may undergo hydrolysis setting reactions and can serve as a bonding system for stabilizing printed shapes during 3DP. A pronounced volume increase upon hydrolysis reaction offers a high potential for reducing the porosity and hence improving the mechanical properties [10]. Calcium aluminate cements (CACs; standard cement chemistry nomenclature: C = CaO, A = Al_2O_3, H = H_2O) are hydraulic setting systems which are widely used for chemical and abrasion resistant devices, high temperature refractories (alumina-rich CACs), and for dental applications [11]. Furthermore, CACs were found to be host cements to produce macro defect-free (MDF) cements [12]. The MDF cement consists of the cement phase, a polymer phase, and an interphase which is formed through the reactions of the polymers and the hydration products. MDF cements have received large attention since

A.-K. Maier (✉) · L. Dezmirean · J. Will · P. Greil
Department of Materials Science (Glass and Ceramics), University of Erlangen-Nürnberg, Martensstr. 5, 91058 Erlangen, Germany
e-mail: Anne-Kathrin.Maier@ww.uni-erlangen.de

J Mater Sci (2011) 46:1203–1210
DOI 10.1007/s10853-010-4896-3

3D printing of Al_2O_3/Cu–O interpenetrating phase composite

Reinhold Melcher · Nahum Travitzky · Cordt Zollfrank · Peter Greil

Received: 15 March 2010 / Accepted: 3 September 2010 / Published online: 15 September 2010

Abstract Porous alumina preforms were fabricated by indirect 3D printing using a blend of alumina and dextrin as a precursor material. The bimodal granulate powder distribution with a bed density of 0.8 g/cm^3 was increased to 1.4 g/cm^3 by overprinting. The porosity of the sintered bodies was controlled by adjusting the printing liquid to precursor powder ratio in the range of 33–44 vol%. The green bodies exhibited bending strengths between 4 and 55 MPa. An isotropic linear shrinkage of ~17% was obtained due to dextrin decomposition and Al_2O_3 sintering at 1600 °C. Post-pressureless infiltration of the sintered preforms with a Cu–O alloy at 1300 °C for 1.5 h led to the formation of a dense Al_2O_3/Cu–O interpenetrating phase composite (IPC). X-ray analysis of the fabricated composites showed the presence of α-Al_2O_3, Cu and Cu_2O. $CuAl_2O_4$ spinel was not observed at the grain boundaries during HRTEM examination. The Al_2O_3/Cu–O interpenetrating phase composite revealed a fracture toughness of 5.5 ± 0.3 MPam$^{1/2}$ and a bending strength of 236 ± 32 MPa. In order to demonstrate technological capability of this approach, complex-shaped bodies were fabricated.

R. Melcher · N. Travitzky (✉) · C. Zollfrank · P. Greil
Department of Materials Science and Engineering, Glass and Ceramics, University of Erlangen-Nuremberg, Martensstr. 5, 91058 Erlangen, Germany
e-mail: nahum.travitzky@ww.uni-erlangen.de

N. Travitzky · P. Greil
Centre for Advanced Materials and Processes (ZMP), Dr. Mack-Str. 81, 90762 Fuerth, Germany

Introduction

Owing to the inability of current technology related methods to produce complex-shaped ceramic parts with the desired microstructures and properties, novel additive processing techniques, such as stereolithography (SLA), selective laser sintering (SLS), fused deposition modelling (FDM), laminated object manufacturing (LOM) and three-dimensional printing (3D printing), have been emerged in last two decades, resulting in the fabrication of ceramic bodies with complex geometry [1–3].

3D printing (3DP™) is based on the principle of ink-jet printing. Two different approaches are usually discerned: direct and indirect 3D printing. In case of direct 3D printing, a dilute suspension of ceramic powder in a volatile liquid is used as ink and printed on an absorbent substrate. Repeated overprinting results in 3D green parts. In case of indirect 3D printing [4], a binder solution is locally applied on a powder layer by an ink-jet print head, causing the powder particles to bind to one another and to the printed cross-section one level below. This process is repeated until the entire part is completed. The main advantage of indirect printing is the use low viscous liquids such as water. The powder bed, however, must contain a water-soluble binder such as dextrin [5]. Indirect 3D printing was used to fabricate complex shaped ceramic structures of $TiAl_3/Al_2O_3$ [6], TiC/Ti–Cu [7], Ti_3SiC_2 [8, 9], Si–SiC [10, 11], WC/Co and TiC [12], Al_2O_3/SiO_2 [13] amongst others.

Successful use of the 3D printing, however, requires granulated powder with enhanced free-flow properties to achieve a homogeneous spreading of powder bed layers [14]. Various approaches such as application of spherical particles, bimodal particle size distribution, granulation of fine powders as well as optimisation of volume share of temporary organic compounds were used in order to

Glass Technol.: Eur. J. Glass Sci. Technol. A, August 2011, 52 (4), 111–116

Three-dimensional printing of a bioactive glass

Robert Meszaros, Rong Zhao, Nahum Travitzky, Tobias Fey, Peter Greil & Lothar Wondraczek

Chair of Glass and Ceramics, Department of Materials Science and Engineering, University of Erlangen-Nuremberg, 91058 Erlangen, Germany

Manuscript received 28 February 2011
Revision received 6 April 2011
Manuscript accepted 7 April 2011

We report on three-dimensional printing and subsequent sintering of 13-93 bioactive glass as a powerful method for the fabrication of patient-specific inlays and substitutes for unloaded implants. In a multi-method study, an assessment of thermal sintering, isotropic and anisotropic shrinkage, crystallisation and microstructural evolution was performed as a prerequisite for the development of a suitable 3D-printing and sintering process. Concave and convex model geometries were then produced, and their consolidation behaviour was examined with respect to process parameters such as adequate preparation of precursor glass powders, particle size used, glass viscosity, green body preparation and sintering conditions. Almost complete densification could be achieved for sintering temperatures of 742–795 °C. Crystallisation was observed to involve subsequent precipitation of diopside (~750 °C), pseudowollastonite (~850 °C) and calcium phosphate (~900 °C). A process window of 712–745 °C reducing to 712–730 °C, if crystallisation must be avoided, is suggested for sintering of 3D printed bioactive glass type 13–93.

1. Introduction

Bioactive glasses offer a wide variety of properties which make them attractive for the use in tissue engineering. These include high surface reactivity, *in vivo* resorption, and bonding to hard and soft tissue.[1,2] Depending on composition, bioactive glasses may exhibit osteoinduction, osteostimulation or osteoconduction, and may support growth and proliferation of various cell types.[3–5] A variety of processing techniques such as conventional melt casting, replica methods, sintering, direct foaming, tape casting, gel casting, or sol-gel processes are currently employed to fabricate bioactive glass bodies of various geometries and degrees of porosity.[6–11] Drawbacks of these methods often include limited control over pore size, geometry and interconnectivity, overall porosity, limited reproducibility and insufficient mechanical performance. As an intriguing alternative, additive manufacturing (AM) techniques have been investigated by a number of research groups for manufacture of complex scaffolds and implants from bioactive ceramics,[12–14] polymers,[15–17] metals,[18] cements[19] or composites.[20,21] However, for the fabrication of bioactive glass bodies, only fused deposition modeling has been considered for AM, so far.[22] As a processing technique, AM provides the unique opportunity to generate functional prototypes of complex designs from geometric models constructed on CAD/CAM systems.[23–25] This enables enhancement and direction of bone in-growth and vascularisation of the scaffold. Generally, AM techniques are divided into direct and indirect methods. In the former, a specimen is fabricated directly from the material of choice, for example by fused deposition modeling[21] or 3D-printing.[19,20] Indirect techniques typically start from a negative mould which is fabricated by AM (e.g. stereolithography,[20] wax printing) and subsequently transferred into a bioactive scaffold. Using direct and indirect AM techniques, implant materials can be individually adapted for each patient, which is of great benefit in clinical practice.

The present report focuses on the demonstration of three-dimensional AM and subsequent sintering of a bioactive glass for the production of patient-specific bioactive glass or glass ceramic inlays and substitutes for unloaded implants. The bioactive glass type 13-93 was chosen for its ability to support cell growth[3–5,26] and its high *in vitro* bioactivity.[27–31] As prerequisite, basic glass properties, process conditions and sintering behaviour are assessed. In comparison to Bioglass 4555, 13-93 is thought to exhibit a favourable viscosity–temperature dependence and a higher crystallization stability so that viscous sintering may be achieved without the occurrence of devitrification.[32–36]

2. Experimental

2.1. Preparation of bioactive glass powders

To demonstrate additive 3D-manufacture of bioactive glass bodies, in the present study, a glass of nominal composition (in wt%) $6Na_2O$, $12K_2O$, $5MgO$, $20CaO$, $4P_2O_5$ and $53SiO_2$ was chosen. This composition corresponds to that of bioactive glass type 13-93.[27] The precursor glass was prepared by conventional melting of a 2.5 kg batch of Na_2CO_3, K_2CO_3, MgO, $CaCO_3$, $Ca_3(PO_4)_2$, and SiO_2 (analytical grade) in a platinum crucible at 1400 °C for 1 h, using an electric

*Corresponding author: Email: lothar.wondraczek@glass.uni-erlangen.de

Glass Technol.: Eur. J. Glass Sci. Technol. A, December 2011, 52 (6), 190–196

Flexural strength of PVD coated float glass for architectural applications

Robert Meszaros,[1] Michael Wild,[2] Benoit Merle[3] & Lothar Wondraczek[3,4,]*

[1] *Institute of Glass and Ceramics, Department of Materials Science, University of Erlangen-Nuremberg, 91058 Erlangen, Germany*
[2] *Interpane Glasgesellschaft mbH, 94447 Plattling, Germany*
[3] *Institute of General Materials Properties, Department of Materials Science, University of Erlangen-Nuremberg, 91058 Erlangen, Germany*
[4] *Energie Campus Nürnberg, 90403 Nuremberg, Germany*

Manuscript received 24 May 2011
Revision received 30 June 2011
Manuscript accepted 30 June 2011

The effect of PVD coatings on the ring-on-ring flexural strength of soda lime silica float glass was studied. A 70% increase from 280±8 to 478±10 MPa was observed on the air-side of the glass after applying a multilayer low emissivity coating of 100 nm total thickness. A similar but less pronounced effect could be obtained with a TiO_2 single layer of 50 nm. At the same time, for both coatings, the Weibull modulus was found to approximately double. Results are interpreted on the basis of two assumptions: initial defects on the glass surface are covered by the coating, and their growth is prevented due to the protective function of the coating, especially as a humidity barrier. Both assumptions were confirmed by atomic force microscopy and micromechanical analyses. This barrier function leads to significantly improved resistance to long term fatigue and stress corrosion, respectively.

1. Introduction

While glasses count among the intrinsically strongest synthetic materials,[1] their practical strength is largely determined by the presence of surface flaws.[2–4] Such flaws may occur on various length scales, from macroscopic scratches to, ultimately, topological heterogeneity which may be pertinent to the glass itself.[5] They may originate from numerous sources such as forming and handling processes, corrosion and subcritical growth of smaller flaws, especially in the presence of water.[6–9] Since avoiding the typical sources of flaws is largely impossible, much effort is presently being put into strategies to improve the defect resistance and/or toughness of glasses for large-scale applications. Such strategies may comprise thermal and chemical tempering (toughening),[10–13] (thermal) polishing and etching[14–16] or the deposition of permanent coatings or glazes.[17–20] The latter are usually based on sol-gel processes, chemical vapour deposition and epoxy or colloidal systems. The actual mechanism which underlies the increase in mechanical strength after coating deposition is often not unambiguously clear because it typically comprises a convolution of effects, from defect coverage, crack tip blunting, corrosion protection and alteration of surface hardness to the creation of residual stresses.

In reality, the applicability of coating procedures to improve the mechanical performance of glasses is largely limited by cost. This limit can most effectively be overcome if coatings which are already applied to glass for a given application can be designed to additionally provide toughening functions. In this respect, the present study is focussed on the effects of physical vapour deposited (PVD) coatings on the mechanical properties of glasses for architectural applications, where PVD coatings are deposited on soda–lime–silica (SLS) float glass on a large scale. The primary purpose of such coatings is to generate specific spectral reflectivity. Typical applications are low emissivity (low-E) and solar protection as shown for example in Figure 1. Both types of coatings are

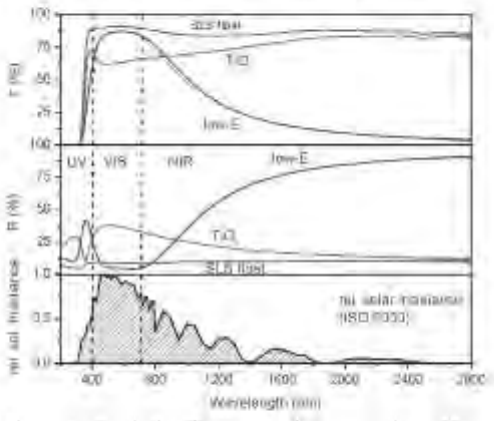

Figure 1. Spectral reflectance and transmission of low-E, TiO_2 and uncoated SLS float glass. The relative solar spectral irradiance according to ISO 9050 is shown for comparison.

* Corresponding author. Email: lothar.wondraczek@ww.uni-erlangen.de

ARTICLES

Silica replication of the hierarchical structure of wood with nanometer precision

Daniel Van Opdenbosch
Department for Materials Science and Engineering—Glass and Ceramics, University of Erlangen-Nuremberg, D-91058 Erlangen, Germany

Gerhard Fritz-Popovski and Oskar Paris
Institute of Physics, Montanuniversitaet Leoben, A-8700 Leoben, Austria

Cordt Zollfrank[a)]
Department for Materials Science and Engineering—Glass and Ceramics, University of Erlangen-Nuremberg, D-91058 Erlangen, Germany

(Received 3 January 2011; accepted 21 March 2011)

The structural features of wood were replicated in silica on all levels of hierarchy from the macroscopic to the nanoscopic level of the cellulose elementary fibrils. This was achieved by a series of processing steps on spruce wood templates. Sodium chlorite was used to partially remove the lignin matrix from the wood cell walls, exposing the cellulose fibrils. These were optionally functionalized with maleic acid anhydride to stabilize the fibrillar structure and reduce the shrinkage of the template. Repeated infiltration with tetraethyl orthosilicate in ethanol deposited silica on the fibrils. Calcination at 500 °C removed the rest of the organic template by oxidation and resulted in the fusion of the deposited material into a positive silica replica. Small-angle x-ray scattering evidenced fibrillar structures parallel to the original cellulose fibrils at length scales in the order of 10 nm, suggesting the successful nanoscopic replication of the cellulose fibrils and their orientation.

I. INTRODUCTION

Biomimetic mineralization is the replication of a biological template into an inorganic structural or functional material and provides a powerful tool to create complex material structures.[1–3] These can include detailed structural features, such as undercuts, gradients, or continuous networks, which can only be elaborately produced with conventional top–down fabrication methods.[4,5] Natural functional materials are interesting templates for converting them into inorganic materials for a wide range of materials for various applications.[3,5–10]

Wood is such a natural structural and functional material comprising several levels of hierarchy.[11] Tracheids with diameters of 10–20 μm (latewood) or 30–40 μm (earlywood) are the dominating structural features of the xylems of softwoods such as spruce (*Picea abies*) or pine (*Pinus silvestris*).[12] The wood xylem cell walls are composed of helically oriented cellulose fibril arrays embedded in a biopolymer matrix of lignin and hemicelluloses, which function as a connective intermediate.[13,14] Several models have been proposed for the spatial arrangement of the biopolymer components in the wood cell wall.[15–17] In native spruce wood, the fibril arrays have diameters of roughly 10–20 nm[14] and are composed of elementary cellulose fibrils of about 2.5 nm in diameter,[18] embedded in a hemicellulose and lignin matrix. In the dominatingly thick S2 cell wall layer of normal spruce early-sapwood, the cellulose fibrils are arranged parallel and their angle with respect to the cell axis is between 3° and 5°.[19,20] They, therefore, form a group of helices wound around the cell lumen.

The replication of wood and its structural features on the hierarchical level of the cells has been successfully demonstrated in a wide range of materials,[21,22] prominently carbon,[23,24] silicon carbide,[25] silicon/silicon carbide,[26,27] or silica.[28] However, the replication of the wood structure on all levels of hierarchy down to the fibril level could so far only be successfully achieved in very few investigations. Some of the authors of this study have recently been able to synthesize for the first time a ceria/zirconia ceramic replica with nanometer precision this way.[29] Other workers were able to produce silica replicates of wood, but they were either rather vague on the actual nature of the samples produced, suggesting that no monolithic samples were produced[30] or did claim, but not conclusively show the replication of the fibril structure of the templates used.[31] Nanometer-scale replication is, however, thought to be the key to novel functional properties based on hierarchical structuring, such as for instance actuators[10] or optical devices.[32]

a)Address all correspondence to this author.
e-mail: cordt.zollfrank@ww.uni-erlangen.de
DOI: 10.1557/jmr.2011.98

RESEARCH ARTICLE

ADVANCED BIOMATERIALS

DOI: 10.1002/adem.201180004

Surface Modification of an Alumina-Based Bioceramic for Cement Application**

By J. Pedimonte,* N. Travitzky, M. Korn, S. Kriegelstein and P. Greil

Biograde zirconia toughened alumina (ZTA) has found wide application in load bearing endoprosthetic implants due to high strength, fracture toughness, and wear resistance. In order to enhance bonding to acrylic bone cement (BC) for implants, fixation modification of ZTA with a thin layer of porous anodic alumina (PAA) was investigated. An Al-layer of approximately 500 nm was sputtered on the ZTA substrate which subsequently was electrochemically oxidized by anodic polarization in $H_2C_2O_4$ or H_3PO_4 solution. PAA layers with a total porosity ranging from 11 to 30%, mean pore spacing of 90–200 nm and pore diameters of 30–110 nm were prepared. Compared to unmodified ZTA/BC interface (≈ 30 MPa), the PAA modified specimens (ZTA/PAA/BC) achieved a significantly higher interface bonding strength (≈ 60 MPa) measured by four point bending on composite beam specimens. While crack propagation in the unmodified ZTA/BC specimen was found to proceed along the interface, fracture analysis on the ZTA/PAA/BC specimens showed a mixed mode fracture with part of the fracture propagation localized along the PAA/BC interface and part through BC. Thus, pore structure controlled mechanical interlocking is expected to offer a high potential for applying PAA surface modification to improve biomaterial to BC bonding.

Advanced ceramics have become of particular interest for biomedical implant applications due to their biocompatibility, chemical inertness, high strength, and excellent creep and fatigue resistance in physiological environment. Biograde alumina-based ceramics have been major components in a growing number of orthopedic arthoplasties including total hip replacement, knee replacement, and other joint replacement surgeries including shoulder, finger, metacarpus, foot finger, jaw, and spine.[1] Zirconia-toughened alumina composites were demonstrated to achieve superior crack growth resistance compared to monophase alumina and an excellent bending strength, hardness and fracture toughness with values exceeding 1 GPa, 15 GPa and 6 MPa·m$^{1/2}$, respectively.[2,3] Compared to Al_2O_3 bioceramics which suffer from an inferior toughness,[4] the zirconia toughened alumina (ZTA) offers a high resistance to crack propagation which may offer the option to improve lifetime and reliability of ceramic joint prostheses.[5] Furthermore stabilized ZrO_2 ceramics exhibit a pronounced sensitivity to hydrolytic degradation[6] which was not observed in ZTA where ZrO_2 is embedded in the Al_2O_3 matrix.[7]

Long-term stability of prosthetic component fixation in bone can be achieved with either biological or cemented anchorage. Positive response of the host tissue and high biocompatibility of ZTA ceramics were reported, which promotes ongrowth or ingrowth of bone and forms an intimate contact of the tissue to the implant surface.[8,9] Cemented anchorage achieves fixation with the help of a form-fitting cement that fills the gaps between the implant and the inner surface of the trabecular bone. In both situations, however, improvement of interface bonding strength is required in order to enhance load-bearing capability and reduce failure rates of load bearing implant components fixed to living bone. In the case of cementless fixation, a variety of chemical surface treatments including hydroxylation,[10] phosphate coupling,[11] and hydroxyapatite coating were

[*] J. Pedimonte, Dr. N. Travitzky, Prof. P. Greil
Department of Materials Science, Glass and Ceramics Martensstr. 5, 91058 Erlangen, (Germany)
E-mail: joana.pedimonte@ww.uni-erlangen.de
M. Korn
Department of Materials Science, General Materials Properties Martensstr. 5, 91058 Erlangen, (Germany)
Dr. S. Kriegelstein
University Hospital, Clinics for Trauma Surgery Krankenhausstr. 12, 91054 Erlangen, (Germany)

[**] Financial support from Bavarian Research Foundation (BFS) is gratefully acknowledged. The authors are thankful to experimental support from the Cluster of Excellence EAM and from the Chair of Electron Devices, University of Erlangen.

journal of Non-Crystalline Solids 357 (2011) 2241–2245

Contents lists available at ScienceDirect

Journal of Non-Crystalline Solids

journal homepage: www.elsevier.com/locate/jnoncrysol

Discussion on the origin of NIR emission from Bi-doped materials

Mingying Peng [a,*], Guoping Dong [a], Lothar Wondraczek [b], Liaolin Zhang [a], Na Zhang [a], Jianrong Qiu [a,*]

[a] Institute of Optical Communication Materials, School of Materials Science and Engineering, South China University of Technology, Guangzhou 510640, China
[b] Department of Materials Science, University of Erlangen-Nuremberg, Erlangen 91058, Germany

ARTICLE INFO

Article history:
Received 9 July 2010
Received in revised form 30 September 2010
Accepted 2 November 2010
Available online 18 December 2010

Keywords:
Laser glass;
Bi-doped materials;
Luminescence;
Broadband fiber amplifier

ABSTRACT

Ever since the discovery of ultra-broadband near-infrared (NIR) photoluminescence (PL) from Bi-doped silicate glass, this class of materials and corresponding devices have experienced rapid progress. This is mainly driven by the suggested use in broadband optical amplifiers and novel lasers for future telecommunication networks. Currently, it appears that the optical bandwidth which is provided by Bi-doped glasses and crystals cannot be achieved by any rare-earth (RE) based amplifier, or by the combination of multiple RE-doped devices. However, the nature of the optically active NIR emission centers remains highly debated. The present paper critically reviews the various arguments and models which have been proposed in this context over the last decade. From the overall conclusions, the major open questions are identified.

1. Introduction

In 1999, Murata et al. found a bismuth-doped silica glass exhibiting fluorescence at 1132 nm with a full width at half maximum (FWHM) of 150 nm and a lifetime of 650 μs [1]. When excited at a wavelength of 500 nm, a quantum yield of 66% was observed. Based on theoretical calculations, it was shown that generation of optical pulses with a duration as short as 13 fs is possible and, hence, the material is of significant interest for use in laser amplification [1]. The experimental demonstration was provided in 2003 by Fujimoto and Nakatsuka showing optical amplification at 1.3 μm from Bi-doped silica glass when pumped with 810 nm [2]. In 2004, Peng et al. extended the group of known near-infrared (NIR) emitting Bi-doped glasses to germanates and demonstrated that the FWHM could be as broad as 300 nm [3]. A further breakthrough followed in 2005 with the realization of continuous wave lasing in the spectral region from 1150 to 1300 nm by Dianov et al. [4]. Since then, research on Bi-doped NIR-emitting glasses, crystals and optical devices has experienced rapid growth and is now conducted in laboratories on almost every continent. NIR emission from bismuth-based centers has successively been reported for silicate [1,2,5–16], germanate [3,7,17–21], aluminoborate [22], aluminophosphate [23,24], chalcogenide [25–28], germanosilicate [29,30], aluminosilicate [6,9,31] and borosilicate glasses [31,32] as well as for polycrystalline SrB_4O_7 [8], single crystals of $RbPb_2Cl_5$ [33], BaF_2 [34], α-BaB_2O_4 [35] and various other materials. Also on the area of device fabrication, progress has been very rapid. That is, within only two years, efficient all-fiber optical amplifiers and fiber lasers have emerged from the first demonstration of lasing. Only recently, a quantum efficiency of up to 1.0 ± 0.05 has been reported for a bismuth-doped fiber [36]. For a bismuth-doped chalcogenide glass, NIR luminescence was reported to peak at 1300 nm with an extraordinary FWHM of up to 600 nm at room temperature. The FWHM can be further increased to 850 nm when the temperature is lowered to 5 K. Hence, it covers the entire spectral range of optical telecommunication [22]. Similar spectral properties have not been observed from any rare-earth (RE)-doped optical material, or even combinations of materials.

Surprisingly, the nature of this NIR photoluminescence is still unknown, although many hypotheses have been formulated, attributing emission to Bi^{3+} [37–40], Bi-clusters [17], Bi^+ [22,23,25,26,28,34,35], BiO [8,31,41], dimer ions Bi_2, Bi_2^+ and Bi_2^{3+} [11,12,24,42], Bi^0 [43,44], molecular orbital models [40,45,46] or even point defects [21]. In the present paper, all these attempts to clarify the origin of NIR emission will be critically evaluated with the goal to condense the accumulated information into a potential resolution of the problem, and to identify directions for future research.

The various hypotheses appeared in the chronological order: (1) Bi^{3+} (Fujimoto and Nakatsuka [37]), (2) bismuth in lower valency (Peng et al. [3]), (3) Bi^+ (Meng et al. [22,23]), (4) Bi-clusters (Peng et al. [17]), (5) BiO (Ren et al. [41]), (6) Bi_2/Bi_2^+ (Khonthon et al. [11]), (7) Bi_2^+/Bi_2^{3+} (Sokolov et al. [42]), (8) point defects (Sharonov et al. [21]), (9) Bi^0 (Peng et al. [43]), (10) intramolecular charge transfer in $Bi^{3+}O_n^{2-}$ molecules (Kustov et al. [45,46]), and (11) radiative recombination of e–h pairs in $Bi^{3+}O_n^{2-}$ molecules (Razdobreev et al. [40]). We categorize these into three groups: (A) bismuth in higher valency, i.e. Bi^{3+} and related molecules; (B) bismuth in lower valency, i.e. BiO, Bi^+, Bi^0, cluster ions; and (C) point defects. Emphasis will be on the first two groups.

Missing from the above list are Bi^{5+} and Bi^{2+} species. Materials doped with either of these two typically absorb and emit in the ultraviolet (UV) and/or visible (VIS) spectral range. Emission lifetimes

* Corresponding authors. Tel.: +86 20 22236910; fax: +86 20 87114804.
E-mail addresses: pengmingying@scut.edu.cn (M. Peng), qiurong@scut.edu.cn (J. Qiu).

0022-3093/$ - see front matter © 2010 Elsevier B.V. All rights reserved.
doi:10.1016/j.jnoncrysol.2010.11.016

Ultrabroad NIR luminescence and energy transfer in Bi and Er/Bi co-doped germanate glasses

Mingying Peng,[1,*] Na Zhang,[1] Lothar Wondraczek,[2] Jianrong Qiu,[1,3] Zhongmin Yang,[1] and Qinyuan Zhang[1]

[1]*Institute of Optical Communication Materials and State Key Laboratory of Luminescent Materials and Devices, South China University of Technology, Guangzhou 510640, China*

[2]*Department of Materials Science, University of Erlangen-Nuremberg, Erlangen 91058, Germany*

[3]*jgr@scut.edu.cn*

[*]*pengmingying@scut.edu.cn*

Abstract: The effects of temperature, pump power and excitation wavelength on near-infrared photoluminescence from Bi-doped multi-component germanate glasses are presented. Compared to conventional silica/silicate matrices, the examined material exhibits superior resistance to thermal quenching and less pronounced excited state absorption for pumping at 808 nm. It is shown that by selecting the optimal excitation wavelength, photoemission can be initiated from multiple active centers in parallel, resulting in an emission bandwidth (full width at half maximum) of more than 370 nm. Er^{3+}/Bi co-doping is presented as an effective means to significantly enhance emission intensity around 1.5 μm by suppressing the typical Er^{3+}-related red-to-green upconversion. Besides its relevance for Bi-doped materials, this also indicates a new route towards improving the performance of Er-based optical devices. The mechanism of $Er^{3+}\rightarrow$Bi energy transfer is examined in detail. Adjusting the molar ratio between both species provides an effective tool for tuning the emission scheme and further increasing emission bandwidth.

OCIS codes: (160.2750) Glass and other amorphous materials; (160.2540) Fluorescent and luminescent materials; (140.4480) Optical amplifiers; (060.4510) Optical communications.

References and links

1. M. Hilbert and P. Lopez, "The world's technological capacity to store, communicate, and compute information," Science **332**(6025), 60–65 (2011).
2. M. Hughes, T. Suzuki, and Y. Ohishi, "Advanced bismuth-doped lead-germanate glass for broadband optical gain devices," J. Opt. Soc. Am. B **25**(8), 1380–1386 (2008).
3. M. Peng, J. Qiu, D. Chen, X. Meng, J. Yang, X. Jiang, and C. Zhu, "Bismuth- and aluminum-codoped germanium oxide glasses for super-broadband optical amplification," Opt. Lett. **29**(17), 1998–2000 (2004).
4. S. Zhou, H. Dong, G. Feng, B. Wu, H. Zeng, and J. Qiu, "Broadband optical amplification in silicate glass-ceramic containing beta-Ga_2O_3:Ni^{2+} nanocrystals," Opt. Express **15**(9), 5477–5481 (2007).
5. M. A. Hughes, T. Akada, T. Suzuki, Y. Ohishi, and D. W. Hewak, "Ultrabroad emission from a bismuth doped chalcogenide glass," Opt. Express **17**(22), 19345–19355 (2009).
6. I. Bufetov and E. Dianov, "Bi-doped fiber lasers," Laser Phys. Lett. **6**(7), 487–504 (2009).
7. E. Dianov, V. Dvoyrin, V. Mashinsky, A. Umnikov, M. Yashkov, and A. Guryanov, "CW bismuth fibre laser," Quantum Electron. **35**(12), 1083–1084 (2005).
8. V. Dvoyrin, V. Mashinsky, and E. Dianov, "Efficient Bismuth-Doped Fiber Lasers," IEEE J. Quantum Electron. **44**(9), 834–840 (2008).
9. S. Zhou, H. Dong, H. Zeng, G. Feng, H. Yang, B. Zhu, and J. Qiu, "Broadband optical amplification in Bi-doped germanium silicate glass," Appl. Phys. Lett. **91**(6), 061919 (2007).
10. V. V. Dvoyrin, V. M. Mashinsky, L. I. Bulatov, I. A. Bufetov, A. V. Shubin, M. A. Melkumov, E. F. Kustov, E. M. Dianov, A. A. Umnikov, V. F. Khopin, M. V. Yashkov, and A. N. Guryanov, "Bismuth-doped-glass optical fibers–a new active medium for lasers and amplifiers," Opt. Lett. **31**(20), 2966–2968 (2006).

#151373 - $15.00 USD Received 19 Jul 2011; accepted 23 Aug 2011; published 4 Oct 2011

10 October 2011 / Vol. 19, No. 21 / OPTICS EXPRESS 20799

THE JOURNAL OF CHEMICAL PHYSICS 134, 204502 (2011)

Structural heterogeneity and pressure-relaxation in compressed borosilicate glasses by *in situ* small angle X-ray scattering

S. Reibstein,[1] L. Wondraczek,[1,a)] D. de Ligny,[2] Sebastian Krolikowski,[1] S. Sirotkin,[2] J.-P. Simon,[3] V. Martinez,[2] and B. Champagnon[2]
[1]*Department of Material Science, Glass and Ceramics–WW3, University of Erlangen-Nuremberg, Martensstraße 5, 91058 Erlangen, Germany*
[2]*Laboratoire de Physico-Chimie des Matériaux Luminescents, Université Claude Bernard Lyon 1, UMR 5620 CNRS, 69622 Villeurbanne, France*
[3]*Laboratoire de Science et Ingénierie des Matériaux et Procédés, Université Joseph Fourier, UMR 5266 CNRS, 38402 St. Martin d'Hères, France*

(Received 4 March 2011; accepted 3 May 2011; published online 24 May 2011)

We report on Brillouin and *in situ* small angle X-ray scattering (SAXS) analyses of topological heterogeneity in compressed sodium borosilicate glasses. SAXS intensity extrapolated to very low angular regimes, $I(q = 0)$, is related to compressibility. From Brillouin scattering and analyses of the elastic properties of the glass, the Landau-Placzek ratio is determined and taken as a direct reflection of the amplitude of frozen-in density fluctuations. It is demonstrated that with increasing fictive pressure, topological (mid- and long-range) homogeneity of the glass increases significantly. Heating and cooling as well as isothermal scans were performed to follow the evolution of density fluctuations upon pressure recovery. For a sample with a fictive pressure p_f of 470 MPa, complete recovery to $p_f = 0.1$ MPa was observed to occur close to the glass transition temperature. The values of fictive and apparent fictive temperature, respectively, as obtained via the intersection method from plots of $I(q = 0)$ vs. temperature were found in good agreement with previous calorimetric analyses. Isothermal scans suggest that mid- and long-range recovery govern macroscopic density relaxation. © *2011 American Institute of Physics*. [doi:10.1063/1.3585390]

I. INTRODUCTION

A complete description of the glass transition requires consideration of both the time-temperature (t,T) and time-pressure (t,p) planes.[1] A glass which is obtained from a super-cooled liquid by varying p and/or T may then be described according to its fictive pressure p_f (Ref. 1) and fictive temperature T_f.[2–4] P_f and T_f represent the configurational state, which was imposed on the glass during freezing. Their values stand for the last point on the real p,T-plane at which, for a given observation time, the system was in a fully relaxed (equilibrium) state. Together, they describe the "distance from equilibrium"[5] of the considered glass[6] and, hence, its potential energy at real p and T. In a pragmatic consideration, they can be used to assess the system's thermomechanical history and resulting physical properties (e.g. molar volume, homogeneity, network topology,[7–8] and coordination[9–10]), respectively, which were generated during freezing. Depending on the observation time, endothermal relaxation, and exothermal recovery,[11] respectively, occur towards real T and p. Thereby, p_f and T_f appear to relax simultaneously. The relaxation timescale appears to equal the timescale of shear relaxation[12] and, thus, is primarily governed by viscosity η. Since viscosity depends on network topology, it must be considered as a non-equilibrium property, too.[13] While on the t, T-plane, viscosity always relaxes antiparallel to T_f, the problem is more complex on the t, p-plane, where $d\eta/dp$ can be either positive or negative.[14,15] Depending on the examined glass, non-equilibrium viscosity (pertinent to the frozen-in structural configuration) can be observed either at $p < p_f$ or at $p > p_f$.[3,7,10] The thermodynamic implications are not restricted to the entropy term but will also affect the compressibility. Hence, also the compressibility comprises a configurational part. The state which is frozen-in during the glass transition can then be observed by enthalpy measurements as well as by compressibility measurements to assess residual and dynamic density and concentration fluctuations. In the present work, to investigate the compressibility variation with fictive pressure for a representative sodium borosilicate glass,[9,10] we are employing two experimental methods: Synchrotron small angle X-ray scattering (SAXS) and evaluation of the Landau-Placzek ratio (LPR). SAXS intensity extrapolated to very low angular regimes ($q = 0$) is directly related to compressibility.[17,18] LPR, the ratio between Rayleigh scattering, originating from elastic fluctuations and Brillouin scattering, based on acoustic interactions, reflects directly the amplitude of frozen-in density fluctuations.[19] Beyond previous calorimetric and structural analyses of pressure effects on short-range order, this approach will enable to assess and correlate heterogeneity as a function of p_f and T_f on the mid- to long-range scale.

a)Electronic mail: lothar.wondraczek@ww.uni-erlangen.de. Tel.: +49(0)9131 85 27553. Fax: +49(0)9131 28311.

Int. J. Appl. Ceram. Technol., 8 [6] 1509–1516 (2011)
DOI: 10.1111/j.1744-7402.2011.02616.x

International Journal of
Applied Ceramic TECHNOLOGY
Ceramic Product Development and Commercialization

Ferrosilicochromium-Filled Polymer-Derived Ceramics

Lorenz Schlier, Martin Steinau, and Nahum Travitzky†

Department of Materials Science, Glass and Ceramics, Friedrich Alexander University Erlangen-Nuremberg, 5, 91058 Erlangen, Germany

Juergen Gegner

Department of Material Physics, SKF GmbH, 97421 Schweinfurt, Germany
Institute of Material Science, University of Siegen, 57068 Siegen, Germany

Peter Greil

Department of Materials Science, Glass and Ceramics, Friedrich Alexander University Erlangen-Nuremberg, 5, 91058 Erlangen, Germany

Rectangular green bodies fabricated from a granulated mixture of polymethylsilesquioxane (PMS), ferrosilicochromium ($FeSiCr_2$), and SiC were cross-linked in a warm press at 240°C under a pressure of 9 MPa. The samples were then pyrolyzed at 950°C and subsequently heat treated at 1270°C in N_2 atmosphere at pressures up to 5 MPa. For the composites with 25 vol% $FeSiCr_2$ a total linear shrinkage of < 7% was measured while the residual porosity decreased to 3%. A bending strength of ~ 285 MPa, fracture toughness of ~ 3.7 MPa $m^{0.5}$, hardness of ~ 9.5 GPa, and elastic modulus of ~ 180 GPa were evaluated.

Introduction

Ceramics for engineering applications are commonly manufactured using powder-based shaping techniques and subsequent heat treatments at temperatures exceeding

This work was financially supported by the SKF GmbH.

Int. J. Appl. Ceram. Technol., 8 [5] 1237–1245 (2011)
DOI: 10.1111/j.1744-7402.2010.02591.x

International Journal of
Applied Ceramic TECHNOLOGY
Ceramic Product Development and Commercialization

Macro-Cellular Silicon carbide Reactors for Nonstationary Combustion Under Piston Engine-Like Conditions

Lorenz Schlier, Wei Zhang, Nahum Travitzky,* and Peter Greil

Department of Materials Science (Glass and Ceramics), University of Erlangen-Nuremberg, D- 91058 Erlangen, Germany

Jochen Cypris and Miroslaw Weclas

Department of Mechanical Engineering, University of Applied Sciences Nuremberg, D-90489 Nuremberg, Germany

Strut lattice structures of reaction-bonded silicon infiltrated silicon carbide ceramics (RB-SiSiC) for air–fuel mixture formation and for nonstationary lean-burn under pressure applications were fabricated. The lattice design with a high porosity >80% was shaped by indirect three-dimensional printing. It was shown that pre-ignition processes in the porous reactor are much faster than in a free combustion, especially at lower temperatures. Interaction of high velocity diesel jets with cylindrical strut ligaments of the SiSiC lattice structure offers a new possibility for quick and efficient fuel distribution (multi-jet splitting) in space.

Introduction

Porous burners are an advanced combustion technology whereby a premixed fuel/air mixture burns within the cavities of a solid porous matrix. Burner performance is characterized by an ultra-low exhaust

The Cluster of Excellence "Engineering of Advanced Materials" funded by DFG is gratefully acknowledged for financial support. M. Weclas thanks the Federal Ministry of Education and Research (BMBF) and German Federation of Industrial Research Associations (AiF) for financial support of the presented investigation (Project No. 1 N220C).
*silicon.materials@ww.uni-erlangen.de

Materials Views
www.MaterialsViews.com

ADVANCED MATERIALS
www.advmat.de

RESEARCH NEWS

Complex Faraday Rotation in Microstructured Magneto-optical Fiber Waveguides

Markus A. Schmidt, Lothar Wondraczek, Ho W. Lee, Nicolai Granzow, Ning Da, and Philip St. J. Russell*

Magneto-optical glasses are of considerable current interest, primarily for applications in fiber circuitry, optical isolation, all-optical diodes, optical switching and modulation. While the benchmark materials are still crystalline, glasses offer a variety of unique advantages, such as very high rare-earth and heavy-metal solubility and, in principle, the possibility of being produced in fiber form. In comparison to conventional fiber-drawing processes, pressure-assisted melt-filling of microcapillaries or photonic crystal fibers with magneto-optical glasses offers an alternative route to creating complex waveguide architectures from unusual combinations of glasses. For instance, strongly diamagnetic tellurite or chalcogenide glasses with high refractive index can be combined with silica in an all-solid, microstructured waveguide. This promises the implementation of as-yet-unsuitable but strongly active glass candidates as fiber waveguides, for example in photonic crystal fibers.

1. Introduction

Magneto-optical (MO) materials have found application in many areas of photonics, especially in the realization of optical isolators or diodes.[1] In such devices, optical isolation is achieved by altering the propagation of light by application of an external magnetic field. The magnetic field changes the optical response of the medium by inducing circular birefringence via the Faraday effect, resulting in a rotation of the plane of polarization of an incoming linearly polarized light beam.[2] The magnitude of the Faraday effect is governed by the Verdet constant, V_D, which is a characteristic property of the material. The macroscopic response is governed by the interaction of the magnetic field with microscopic magnetic moments that are inherent to the electronic structure of the material. Depending on the configuration of the electronic orbitals, MO materials can exhibit diamagnetic as well as paramagnetic responses, with the resulting Verdet constant often being larger or smaller than the sum of the individual contributions.[3]

Dr. M. A. Schmidt, H. W. Lee, N. Granzow, Prof. P. St. J. Russell
Max Planck Institute for the Science of Light
Guenther-Scharowsky Strasse 1, 91058 Erlangen, Germany
Prof. L. Wondraczek, N. Da
Department of Materials Science
University of Erlangen-Nuremberg
91058 Erlangen, Germany
E-mail: lothar.wondraczek@uni-erlangen.de

DOI: 10.1002/adma.201100364

Most current applications rely on MO crystals to provide large Verdet constants at acceptable levels of optical attenuation.[3] Today's benchmark material is yttrium-iron-garnet ($Y_3Fe_5O_{12}$) (YIG).[3–7] It has high optical transparency throughout the visible and IR regions, provides a relatively large Verdet constant and can be processed using planar-etching and implantation techniques. On the other hand, planar optical isolators, per se, are limited to a relatively small number of applications due to geometric restrictions. However, although a fiber optic approach is strongly desirable, it is difficult to implement because it relies on the availability of an MO glass[8] that is suitable for drawing into fiber.[9] As of now, MO glasses remain handicapped by a comparatively small Verdet constant,[10–12] although there has been significant progress in the design of novel magnetoactive glasses in recent years. Since the degree of Faraday rotation depends on the product of the Verdet constant and the optical path-length, materials with a smaller Verdet constant offer an attractive alternative to crystalline materials if the path-length can be increased and an MO glass can be identified, which is suitable for fiber, rod, or tube fabrication and stable against phase separation and crystallization, and produced in relatively large volumes of high purity and high homogeneity, also, ideally, being nontoxic. To fabricate an MO step-index fiber, the core material must have a refractive index that is higher than the cladding glass. Another approach is to use photonic crystal fibers (PCFs), which consist of an array of hollow channels parallel to the fiber axis.[13,14] As recently shown in fused silica PCF, these channels can be pressure-filled from the melt with many materials such as metals, semiconductors and low melting point glasses.[15–21]

The first step towards achieving a relatively large Verdet constant in a fiber was recently taken by drawing a step index fiber from a heavily terbium-doped silica preform.[22–24] Such fiber drawing processes, however, are limited to very specific combinations of core and cladding materials because their rheological and thermomechanical properties must be compatible. The PCF approach is an interesting alternative, offering more versatility in control of the guidance properties.

Here, we provide a review of recent progress in the development of MO glasses for waveguide applications. We present the first example of a hybrid MO waveguide, fabricated by pressure-assisted melt-filling of a fiber capillary. This points

CARBON 49 (2011) 4359–4367

available at www.sciencedirect.com

ScienceDirect

journal homepage: www.elsevier.com/locate/carbon

Fast production of monolithic carbide-derived carbons with secondary porosity produced by chlorination of carbides containing a free metal phase

Martina Schmirler [a], *Tilman Knorr* [a], *Tobias Fey* [b], *Arthur Lynen* [c], *Peter Greil* [b], *Bastian J.M. Etzold* [a,*]

[a] Universität Erlangen-Nürnberg, Lehrstuhl für Chemische Reaktionstechnik, Egerlandstr. 3, 91058 Erlangen, Germany
[b] Universität Erlangen-Nürnberg, Lehrstuhl Glas und Keramik, Martensstr. 5, 91058 Erlangen, Germany
[c] Schunk Ingenieurkeramik GmbH, Hans-Martin-Schleyer Straße 5, 47877 Willich-Münchheide, Germany

ARTICLE INFO

Article history:
Received 24 March 2011
Accepted 5 June 2011
Available online 12 June 2011

ABSTRACT

Hierarchical structured carbide-derived carbons (CDC) are produced by high temperature chlorination of silicon carbides containing free silicon (Si/SiC). The influence of free silicon in the precursor carbide on the resulting pore and carbon structure and production rate is studied. The two phases – free silicon and silicon carbide – of Si/SiC gives the possibility to synthesize a monolithic carbon with the typical microporous character and narrow pore size distribution combined with larger voids in the micrometer range, while the carbon structure itself stays unchanged. The study revealed that using Si/SiC material increases the production rate for carbide-derived carbons dramatically, due to higher reactive surface area and lower mass transfer limitations, which allows for the time effective production of larger monoliths.

1. Introduction

Due to the potential applications in gas storage, catalysis or as electrode material in supercapacitors, the synthesis of porous carbons is intensively studied. Activated carbons are by far the most common porous carbons studied, known and used [1,2]. Nevertheless, a special interest for defined and controlled carbon pore structure similarly known for oxide materials represented by zeolites and ordered mesoporous oxides has developed [3]. One method to synthesize ordered carbon pore structures is templating, where a hard or soft template is used as a spacer during the pyrolysis of carbon precursors. Ryoo et al. were the first to present the synthesis of ordered mesoporous carbons by hard templating with ordered mesoporous oxides [4,5]. Thereby the hard template needs to show a connected pore system like SBA-15 to prevent a collapse of the carbon structure during template removal. Kyotani et al. could show that zeolites can act as a hard template if a two-step process of wet impregnation and pyrolysis of furfuryl alcohol and subsequent carbon deposition via chemical gas deposition is performed [6,7]. A different approach towards carbons with controlled pore structure is the use of carbides as carbon precursor and selective extraction of the non-carbon element [8–11]. These so called carbide-derived carbons (CDC), with tunable and narrow pore size distribution in the micropore and lower mesopore region, are foundation of this study. Common synthesis of CDC is the extraction of the non-carbon element (M) from a carbide(MC) by chlorination according the following equation [8–11]:

$$MC + \frac{x}{2}Cl_{2(g)} \xrightarrow{400-1200^{\circ}C} MCl_x + C_{(s)} \qquad (1)$$

* Corresponding author.
E-mail address: bastian.etzold@crt.cbi.uni-erlangen.de (B.J.M. Etzold).
0008-6223/$ – see front matter
doi:10.1016/j.carbon.2011.06.013

journal

J. Am. Ceram. Soc., 94 [6] 1698–1705 (2011)
DOI: 10.1111/j.1551-2916.2010.04302.x

Profile Rod Technique: Continuous Manufacture of Submicrometer-Thick Ceramic Green Tapes and Coatings Demonstrated for Nanoparticulate Zinc Oxide Powders

Nadja Straue,[†] Stephanie Prado,[‡] Sebastian Polster,[‡] and Andreas Roosen[†,‡]

[†]Department of Materials Science and Engineering, Glass and Ceramics, University of Erlangen-Nuremberg, 91058 Erlangen, Germany

[‡]Department of Electrical, Electronic and Communication Engineering, Electron Devices, University of Erlangen-Nuremberg, 91058 Erlangen, Germany

There is a fast-growing market for printable electronics, which requires new techniques for micro- and nanofabrication suitable for mass production of functional electronic products. This makes the evaluation and comparison of different printing techniques highly important. In this work, a coating process, referred to as "profile rod technique," is presented as an alternative to the spin-coating process for the production of nanoparticulate zinc oxide (ZnO) layers with thicknesses of several hundred nanometers. Such layers could be used, e.g., as semiconducting layers for printed thin film transistors. The profile rod technique, in contrast to spin-coating, is a continuous process, which allows for easier mass production and reduction in manufacturing costs. To compare the spin-coating and the profile rod process, submicrometer-thick layers of ZnO nanoparticle dispersions in ethanol were prepared. Different dispersion techniques were studied concerning their applicability for the manufacture of nanosized particle dispersions because well-dispersed suspensions are the basic requirement for the manufacture of submicrometer-thick layers with high morphological quality. The quality of the deposited layers was evaluated concerning their microstructure. Moreover, the profile rod technique could be successfully used for the manufacture of submicrometer ceramic green tapes.

I. Introduction

There is a lack of methods to manufacture thin layers from particulate systems continuously with thicknesses in the submicrometer range. Using doctor blading techniques, the difficulty to accurately adjust the casting head relative to the moving carrier tape and the casting head design limit the production of tapes with thicknesses below 3 μm.[1,2] On the other hand, techniques like spin-coating are noncontinuous. The availability of continuous processes is important, e.g., for the further development of printed electronics.[3] This report looks for new processes, which are suitable for the deposition of thin layers at a large scale and low cost. This is done at the example of zinc oxide (ZnO) powders, which is a promising material for the manufacture of printed semiconductors.[4–6]

ZnO is a semiconductor with a wide bandgap of 3.4 eV at room temperature, a large excitation binding energy of 60 meV, and high mechanical and thermal stability compared with other semiconductors. Furthermore, it is the subject of ongoing research in the field of *p*-type conductivity, diluted ferromagnetic properties, and nanostructure fabrication and is thus an interesting semiconducting compound.[4,7] Thin ZnO layers are conventionally fabricated by sputtering, chemical vapor deposition, and pulsed laser deposition, which are rather expensive processes because either laser or vacuum technology is needed.[5,10]

In this report, an ethanol ink based on commercially available ZnO nanoparticles synthesized via gas phase synthesis was developed and further processed via the spin-coating and the profile rod technique. For the development of the ink, steric stabilization by applying carboxylic acid is described as an effective technique for the creation of stable nanosized dispersions.[11–14]

Spin-coating is used for comparison in this work, because it is very easy to prepare thin nanoparticulate layers with a high morphological quality using this technique. A major drawback of the spin-coating process is its incapacity for scale-up or large area coating. Also the well-known Langmuir–Blodgett technique or several innovative processes recently reported in the literature like sacrificial layer electrophoretic deposition[15] or generation of self-assembled monolayers at fluid interfaces[16] are rather limited in their potential for large volume manufacturing.

The profile rod technique, which was used in this work, represents an advancement of the wire baring technique used by Kitano *et al.*[17] to fabricate thin carbon layers. For the wire baring technique, a steel wire is wrapped around a shaft, the device is placed on a flexible substrate, and the dispersion is pressed through the gaps between the wires during coating. Little has been published about the possibilities and limitations of this process. Therefore, in this paper, the technique was intensively studied with regard to the deposition of dispersions and for the creation of submicrometer ceramic green tapes.

II. Experimental Procedure

(1) Powder Characterization and Preparation of Dispersions

For the preparation of stable ZnO dispersions, a nanosized powder (VP ZnO 20, Evonik Degussa GmbH, Hanau, Germany) was used. The density of the powder was determined by helium pycnometry to be 5.3 g/cm^3 (Accupyc 1330, Micromeritics Instrument Corp., Norcross, GA). The specific surface area of the powder was determined by Brunauer–Emmett–Teller (BET) to be 20.04 m^2/g (ASAP 2000, Micromeritics Instrument Corp.) and thus corresponds to a Sauter diameter x_s of 54 nm of the primary particles. The particles are very irregularly shaped, rods, flakes, and spheres are present.

Because the preparation of completely deagglomerated dispersions is of utmost importance for the manufacture of thin layers,[18] different dispersion techniques were investigated and evaluated. In order to prepare stable dispersions of the particles

R. Moreno—contributing editor

Manuscript No. 28251. Received June 25, 2010; approved November 4, 2010.
This work was financially supported by the German Research Foundation (DFG) (Graduiertenkolleg 1161/2) and the Evonik Degussa GmbH (Marl, Germany).
†Author to whom correspondence should be addressed. e-mail: nadja.straue@ww.uni-erlangen.de

J Mater Sci (2011) 46:3493–3499
DOI 10.1007/s10853-011-5253-8

Properties of tape-cast Y-substituted strontium titanate for planar anode substrates in SOFC applications

Pavel Vozdecky · Andreas Roosen · Qianli Ma · Frank Tietz · Hans Peter Buchkremer

Received: 15 October 2010 / Accepted: 6 January 2011 / Published online: 15 January 2011

Abstract This work evaluates the use of fine-grained yttrium-substituted strontium titanate powders for the preparation of planar anode supported solid oxide fuel cells. Starting from a submicron-sized powder of Y-substituted strontium titanate $Sr_{0.895}Y_{0.07}TiO_3$ (SYT), which was synthesised via spray pyrolysis followed by a grinding process, suspensions of high solid concentration were prepared by steric stabilisation. From these suspensions, tape casting slurries of up to 25 vol% were produced and further processed to ceramic green tapes using the doctor blade technique. The theological behaviour of the slurries was investigated in dependence on the content of solids and organic additives. Furthermore, the binder burnout and sintering behaviour of the green sheets were characterised. After firing, crack-free substrates of high planarity were obtained. The achieved properties of the sintered tapes such as density, porosity, warping, mechanical strength, and electrical conductivity were determined in dependence on sintering temperature.

Introduction

Tape casting is a well-known process for the manufacture of thin and flat ceramic substrates. This process allows the manufacture of ceramic green tapes with constant thickness on a large scale at low costs. These ceramic green sheets are the basic product for the manufacture of substrates or ceramic multilayer devices, e.g., capacitors, inductors, high integrated circuits, actuators, and gas sensors [1]. In the field of high temperature fuel cells, tape casting is a favoured technique for the manufacture of planar solid oxide fuel cells (SOFCs) [2]. The tape casting process is well described in the literature [3–5]. Typically ceramic powders with an average particle size between 1 and 3 μm, but also submicron and recently nano-sized powders are used for tape casting [6]. Their use also allows the reduction of sintering temperatures [7–9].

Strontium titanate-based powders have promising advantages for SOFCs applications, e.g., a thermal expansion behaviour matching that of the solid electrolyte [10–12], high electrical conductivity after high temperature reduction [11–14] and a low chemical expansion or shrinkage during changes of the gas composition in the case of $Sr_{1-x}Y_xTiO_3$ materials [11, 15]. Especially the latter property is important to guarantee a safe and reliable operation after incidental oxidation of the anode. This has been demonstrated with button cells using $Sr_{0.8}La_{0.2}TiO_3$ [16] and very recently with cells of realistic cell size applying SYT as anode substrate [17]. The SYT-based cells withstand 100 redox cycles without mechanical damage and, depending on the redox cycling conditions, a stable performance.

In addition to the properties listed in [11], a ceramic anode substrate should exhibit a thickness of 0.2–0.8 mm, a porosity of 20–40%, a mean pore diameter of approx. 1 μm and a mechanical strength of about 80–100 MPa comparable with conventional cermet anode substrates [18].

This work describes the preparation of SYT sheets by tape casting for application as SOFC anode substrate. To achieve deagglomerated, stable SYT suspensions of high

P. Vozdecky · A. Roosen (✉)
Department of Materials Science, Glass and Ceramics, University of Erlangen-Nuremberg, 91058 Erlangen, Germany
e-mail: andreas.roosen@ww.uni-erlangen.de

Q. Ma · F. Tietz · H. P. Buchkremer
Forschungszentrum Jülich GmbH, Institute of Energy and Climate Research (IEK-1), 52425 Jülich, Germany

COMMUNICATION

ADVANCED ENGINEERING MATERIALS

DOI: 10.1002/adem.201000267

How Degradation of Calcium Phosphate Bone Substitute Materials is influenced by Phase Composition and Porosity**

By S. Schaefer*, R. Detsch*, F. Uhl, U. Deisinger and G. Ziegler

The chemical composition of calcium phosphate (CaP) materials for the regenerative therapy of large bone defects is similar to that of bone. Additionally, calcium phosphates show an excellent biocompatibility. Besides the support of defect healing calcium phosphate implants should be completely degraded within an adequate time period to be replaced by newly formed bone. Although degradation of CaP-implants occurs mainly by dissolution of the material, it is important to characterize the osteoclastic resorption as well, which is involved in native bone remodeling. The degradation of bone substitutes made of calcium phosphate ceramics is influenced by various parameters, such as defect size and localization, the general health situation, and age of the patient, but also material properties are important. Especially, the calcium phosphate composition is crucial for the degradation behavior of a calcium phosphate material. Additionally, at the cellular level the micro- and macroporosity, including interconnecting pores, influences both, the dissolution and the osteoclastic resorption. In our study, three different calcium phosphate materials (hydroxyapatite, tricalcium phosphate, and a biphasic calcium phosphate) and two different geometries (dense 2D samples and porous 3D scaffolds) are compared regarding their dissolution and resorption behavior. The results show, that the dissolution of CaP-ceramics, as examined by the incubation in a degradation solution, depends mainly on the calcium phosphate phase but also on the porosity of the implant. Regarding the resorption, cell proliferation and differentiation of a monocytic cell line as well as the formation of resorption lacunas are analyzed. Cell proliferation is comparable on all phase compositions. Cell differentiation and resorption, however, are influenced by the calcium phosphate phase composition and by the implant porosity as well. By understanding these two mechanisms of degradation, bone substitute materials and, as a result, the bone regeneration of large bone defects using CaP-ceramics can be improved.

The replacement of lost or severely damaged bone is one of the important aspects in the field of regenerative medicine. An alternative to the substitution by autologous or allogenic materials is the use of synthetic calcium phosphates. Calcium phosphate ceramics, mainly hydroxyapatite (HA) and β-tricalcium phosphate (TCP) are bone substitute materials, which have been used for more than four decades.[1,2] These materials show an excellent biocompatibility, because their chemical composition is similar to the inorganic part of the human bone.[3] However, synthetic bone substitute materials should not only replace the missing bone, but they should be integrated in bone repair and the physiological remodeling process.

The degradation occurring in this process is regulated by two mechanisms: (1) the dissolution due to the solubility of the calcium phosphate phase in physiological solution, and (2) the cellular degradation by osteoclasts, also called resorption. Besides patient related factors (defect localization, defect size, age, gender, and health situation), degradation is mainly influenced by the phase composition of the material and the geometry of the implant, meaning the implant size, but also its micro- and macroporosity. Although degradation of CaP-implants depends amongst others on the dissolution of the material, the osteoclastic resorption as an essential

[*] S. Schaefer, Dr. Ing. U. Deisinger
Friedrich-Baur-Research Institute for Biomaterials, University of Bayreuth, 95440 Bayreuth, (Germany)
E-mail: susanne.schaefer@fbi-biomaterialien.de
[*] Dr.-Ing. R. Detsch, F. Uhl, Prof. Dr.-Ing. G. Ziegler
BioCer Entwicklungs-GmbH, Ludwig-Thoma-Str. 36 c, 95447 Bayreuth, (Germany)
E-mail: rainer.detsch@uw.uni-erlangen.de
[**] This study was funded by Federal Ministry of Education and Research (BMBF), Germany (no. 03I5019).

REGULAR CONTRIBUTED ARTICLES

F. Wolff[1], L. Zirkel[1], S. Betzold[1], M. Jakob[1], V. Maier[2], F. Nachtrab[3], B. Ceron Nicolat[4], T. Fey[4], H. Münstedt[1]*

[1] Institute of Polymer Materials, Friedrich-Alexander-University Erlangen-Nürnberg, Germany
[2] Institute of General Materials Properties, Friedrich-Alexander-University Erlangen-Nürnberg, Germany
[3] Development Center X-Ray Technology (EZRT), Fraunhofer Gesellschaft, Fürth, Germany
[4] Institute of Glass and Ceramics, Friedrich-Alexander-University Erlangen-Nürnberg, Germany

Using Supercritical Carbon Dioxide for Physical Foaming of Advanced Polymer Materials

Foams from high performance polymers find more and more interest. The processes to generate them can be difficult, however. It is shown how physical foaming with CO_2 can be used as a first step to assess the potentials of such materials. For investigations of such kind an autoclave on a laboratory scale which allows pressure variations up to 300 bars and temperatures up to 300° C was set up. The samples are saturated with supercritical carbon dioxide (s.c. CO_2) which acts as a foaming agent. Depending on the process and material parameters different foam characteristics and cell morphologies were obtained and characterised. The potential of this method is demonstrated for two different classes of advanced polymer materials, thermoplastic fluoropolymers (FEP), and a silicone resin. In the case of the fluoropolymer, previously prepared films were foamed and the effects of various process parameters on the foam characteristics were investigated. Besides the general potential of foams from fluoropolymers, they are candidates for polymeric piezoelectric materials with a relatively high temperature stability. Silicone polymers possess some properties superior to common organic polymers. First results on the foaming behaviour of a silicone resin are presented.

1 Introduction

The foaming of polymers is a widely used method to widen the spectrum of their properties. Moreover, foams of advanced polymers offer even higher application potentials compared to those of standard polymers. The industrially applied physical foaming processes are economic and environmentally friendly (e.g. Jacobs et al., 2008). However, their developments need expensive equipments. Tests on a laboratory scale are a good possibility to get a first insight into the foaming behaviour of materials not widely investigated before.

A versatile way to obtain basic results on the manufacturing of cellular polymers is the foaming with supercritical fluids in an autoclave process. Several investigations dealt with the foaming of polymers by means of supercritical carbon dioxide (s.c. CO_2). Most of them focused on amorphous polymers examining the influence of different process parameters on the foaming behaviour (e.g. Arora et al., 1998; Goel and Beckmann, 1994a, 1994b; Reverchon and Cardea, 2007; Liao et al., 2010). Besides a few systematic investigations on semi-crystalline polymers (e.g. Baldwin et al., 1996a, 1996b; Xu et al., 2007) this technique has also been applied to biodegradable polymers (Tsivintzelis et al., 2007a, 2007b), thermoplastic elastomers (Ito et al., 2007; Zhai et al., 2010; Dai et al., 2005), nano composites (Zhu et al., 2010), and blends (Jin et al., 2001; Krause et al., 2002; Wang et al., 2003). Only little is known about the foaming of advanced polymer materials such as high temperature thermoplastics (Behrendt et al., 2006, Krause et al., 2001, 2002; Sun et al., 2002; Wang et al., 2009; Zirkel et al., 2009) or preceramic polymers (Kim et al., 2002; Kim and Park, 2003).

The aim of this paper is to point out the potential of this foaming method using two very different advanced polymer materials and to get an idea of their properties. The first example is a fluorinated ethylene propylene copolymer (FEP) which is a semi-crystalline high temperature thermoplast. The foaming is carried out below its melting point (T_m − 260 °C), i.e. in a partially molten state. In case of the FEP, thin films were foamed because of their promising application as ferroelectrets with high thermal and temporal charge stability, e.g. as membranes for audio systems (cf. Wirges et al., 2007). Due to a charging process of the cells in an electric field, this nonpolar cellular polymer is able to exhibit piezoelectric properties. The performance of these ferroelectrets is affected by the structure and the properties of the foams.

The second material presented is a silicone resin. It is an amorphous polymer and was foamed above its glass transition temperature as T_g is lowered to values below room temperature due to the CO_2 dissolved under pressure. This material can be used as precursors for ceramics, since it can be crosslinked and subsequently pyrolysed (e.g. Greil, 1995, 2000). Therefore, this method is an interesting way to manufacture preceramic foams.

* Mail address: Helmut Münstedt, Institute of Polymer Materials, Friedrich-Alexander-University Erlangen-Nürnberg, Martensstr. 7, D-91058 Erlangen, Germany
E-mail: helmut.muenstedt@www.uni-erlangen.de

RESEARCH NEWS

ADVANCED MATERIALS
www.advmat.de

Materials Views
www.MaterialsViews.com

Towards Ultrastrong Glasses

Lothar Wondraczek, John C. Mauro, Jürgen Eckert, Uta Kühn, Jürgen Horbach, Joachim Deubener, and Tanguy Rouxel*

The development of new glassy materials is key for addressing major global challenges in energy, medicine, and advanced communications systems. For example, thin, flexible, and large-area glass substrates will play an enabling role in the development of flexible displays, roll-to-roll processing of solar cells, next-generation touch-screen devices, and encapsulation of organic semiconductors. The main drawback of glass and its limitation for these applications is its brittle fracture behavior, especially in the presence of surface flaws, which can significantly reduce the practical strength of a glass product. Hence, the design of new ultrastrong glassy materials and strengthening techniques is of crucial importance. The main issues regarding glass strength are discussed, with an emphasis on the underlying microscopic mechanisms that are responsible for mechanical properties. The relationship among elastic properties and fracture behavior is also addressed, focusing on both oxide and metallic glasses. From a theoretical perspective, atomistic modeling of mechanical properties of glassy materials is considered. The topological origin of these properties is also discussed, including its relation to structural and chemical heterogeneities. Finally, comments are given on several toughening strategies for increasing the damage resistance of glass products.

1. Introduction

Glassy materials have a unique history of continuous use spanning more than thirty thousand years. Their enabling role in numerous society-changing applications has often been taken for granted, and the brittleness of glass has been perceived as its gravest handicap. Over the centuries, accepting this handicap and benefiting from optical properties and universal processability, glasses have found their role in applications with low levels of tensile stress. In recent years, however, new and very high demand has arisen for novel approaches towards stronger or, more precisely, more damage resistant glasses.[1] Strength, toughness, and elastic properties of glass are now a major bottleneck for further development of short-haul high-capacity telecommunication and fiber-to-the-home technologies; flexible substrates and roll-to-roll processing of displays, solar modules, and planar lighting devices; large-scale and high-altitude architectural glazing; lightweight packaging; ultrastiff composites; and numerous other applications. Increasing the strength and toughness of glass would not only enable exciting new applications, but also lead to a significant reduction of material investment for existing applications. In this respect, both oxide and metallic glasses have come to a crossroads: a significant leap in practical toughness will be possible only if a new level of conceptual understanding can be attained and applied.

While the understanding that the experimental strength of glass is primarily determined by macro- and microstructural defects (Figure 1) became well accepted in the early 20th century,[2,3] more recently it has been recognized that glass constitutes the intrinsically strongest man-made material that can be produced on a large scale (e.g., a tensile strength of up to 26 GPa was demonstrated for vitreous silica[4]). However, these high intrinsic strengths are compromised by the material's low resistance to surface damage. At the same time, wholly new classes of glassy materials have entered the scene, and the interplay between brittleness, plasticity, and elasticity of disordered solids must now be put into a much broader context. For example, it now appears as if, on a laboratory scale, the physical limits of strength and toughness are in close reach, at least for certain metallic glass compositions.[5,6] Identification of determinant parameters and their engineering towards ultrahigh toughness is the major challenge in the field.[5,7]

Prof. L. Wondraczek
Department of Materials Science
University of Erlangen-Nuremberg
Erlangen 91058, Germany
E-mail: lothar.wondraczek@ww.uni-erlangen.de
Dr. J. C. Mauro
Corning Incorporated
Corning, NY 14831 USA
Prof. J. Eckert, Dr. U. Kühn
Institute for Complex Materials
IFW Dresden
Dresden 01171, Germany
Prof. J. Eckert
Institute of Materials Science
TU Dresden, Dresden 01062, Germany
Prof. J. Horbach
Institute of Theoretical Physics II
University of Düsseldorf
Düsseldorf 40225, Germany
Prof. J. Deubener
Institute of Non-Metallic Materials
Clausthal University of Technology
Clausthal-Zellerfeld 38678, Germany
Prof. T. Rouxel
LARMAUR
Université Rennes I
Rennes 35042, France

DOI: 10.1002/adma.201102795

journal

J. Am. Ceram. Soc., 94 [7] 2053–2060 (2011)
DOI: 10.1111/j.1551-2916.2010.04358.x

A Comprehensive Simulation Scheme for Tape Casting: From Flow Behavior to Anisotropy Development

Andreas Wonisch,† Pit Polfer, and Torsten Kraft

Fraunhofer Institute for Mechanics of Materials IWM, D-79108 Freiburg, Germany

Armin Dellert, Andreas Heunisch, and Andreas Roosen*

Friedrich-Alexander-University of Erlangen-Nuremberg, Department of Materials Science III (Glass and Ceramics), D-91058 Erlangen, Germany

A new simulation scheme for tape casting is presented and applied. The model allows considering both the macroscopic flow behavior and the orientation of individual particles inside the ceramic slurry. It is based on the smoothed particle hydrodynamics method, a particle-based computational fluid dynamics solver, and Jeffery's equations of particle motion, which describe the rotation of rigid, ellipsoidal particles in a fluid. It is shown how different process parameters and the rheological behavior of the slurry influence its flow behavior, which in turn affects the orientation of nonspherical particles inside the slurry. The simulations predict that a preferred, anisotropic particle orientation develops in the green tapes, whose extent depends mainly on the powder properties. All simulations are performed with real tape-casting data concerning geometry of casting unit, casting parameters, slurry rheology, and powder properties. The anisotropy results are confirmed by experimental analysis of cross sections of tape-cast films made from different powders.

I. Introduction

In the ceramic industry, tape casting[1–4] is widely used as a manufacturing process for numerous devices, like e.g. substrates for thick- and thin-film circuitry, capacitors, piezoelectric actuators, gas sensors, etc., where high material qualities and tight geometrical tolerances are required.[5–7] Because the fluid mechanical conditions inside the casting chamber and below the doctor blade strongly influence the quality of the final green tapes,[8,9] detailed knowledge of the flow behavior is important to guarantee a high degree of reproducibility.

Although it is possible to determine the flow field experimentally by using laser Doppler velocimetry,[8] it is costly and restricted to translucent model fluids. Modeling the process is a very flexible and less expensive alternative that slowly gained attention during the last several years. Previous research can be differentiated in theoretical models and numerical simulation schemes. One of the earliest mathematical models of tape casting was based on Newtonian fluids and a two-dimensional (2D) geometry, which allowed making basic predictions about the velocity distribution below the blade and about tape thickness.[10] More detailed models were developed subsequently, incorporating the complex rheological behavior of the slurry by using different power-law models for non-Newtonian flow,[11–13] the Bingham constitutive equation,[14,15] or more complex models like the Herschel–Bulkley model for viscoplastic behavior.[16] One recent study also investigated the flow behavior of the slurry after it has passed the blade.[17] However, such models are limited to simple geometries and cannot predict the flow field in the whole casting unit. Computational fluid dynamics (CFD) methods, on the other hand, numerically solve the differential equations governing the flow, which makes them a prime tool for analyzing it. Nonetheless, only few CFD studies considered tape casting so far and those which did have been restricted to two dimensions.[18,19]

One reason why CFD-based simulations are not widely used to simulate tape casting—despite their obvious benefits—might be due to their complex nature, requiring extensive know-how and special software. An alternative to traditional, grid-based methods is smoothed particle hydrodynamics (SPH), a particle-based, meshless CFD scheme. It was originally invented for astronomical purposes,[20] but since then rapidly developed further and was applied to a wide range of different applications in fluid mechanics.[21,22] In this method, the continuum is discretized by individual particles that move with the flow. The main advantages of SPH over grid-based CFD approaches are its ability to easily handle free surfaces and its lower complexity.

While CFD-based macroscopic models allow calculating the flow properties, they cannot directly predict the resulting particle structure inside the slurry after it has left the casting unit. However, during tape casting usually an anisotropic microstructure develops, which leads to an anisotropic sintering response.[23–25] The alignment of nonspherical particles, resulting in particle contact and pore shape anisotropy, is mentioned most frequently as the driving force for the anisotropic sintering shrinkage.[9,26] Despite its importance for product quality, few simulation studies so far considered particle structure of green tapes. Greil *et al.*[27] used the discrete element method (DEM) for microscopic simulations of the slurry. However, such simulations are computational demanding—the before mentioned DEM study was restricted to 2D representative volume cells and spherical particles. Computational time to simulate the whole slurry would be prohibitive.

An alternative approach for obtaining information about particle orientation is possible by solving Jeffery's equations of motion.[28] These equations describe the rotation and alignment of rigid, ellipsoidal particles in a general flow field at low Reynolds number, which results from hydrodynamic shear and extensional forces. They can only be solved analytically for simple flows.[28,29] However, numerical techniques can be used to calculate the orientation of an ellipsoidal shaped particle in a general flow field.[30–32] Information about average particle orientation can then be obtained by solving the equations for a specific flow field for a large number of initially randomly oriented particles, assuming that the particles' spacing is wide enough that hydrodynamic and body–force interactions can be neglected.[29,30] This

E. Suvaci—contributing editor

Manuscript No. 28661. Received September 21, 2010; approved November 24, 2010.
This work was supported by the Deutsche Forschungsgemeinschaft under contract No. Kr 1729/9-1 and Ro 1512/3-1.
*Member, The American Ceramic Society.
†Author to whom correspondence should be addressed. e-mail: andreas.wonisch@iwm.fraunhofer.de

journal

J. Am. Ceram. Soc., 94 [3] 601–602 (2011)
DOI: 10.1111/j.1551-2916.2010.04136.x
© 2011 The American Ceramic Society

Photoluminescence of Mn^{2+} Centers in Chalcohalide Glasses

Qiqi Yan, Yinyao Liu, and Guorong Chen†

Key Laboratory for Ultrafine Materials of Ministry of Education, School of Materials Science and Engineering, East China University of Science and Technology, Shanghai 200237, China

Ning Da and Lothar Wondraczek‡

Department of Materials Science, University of Erlangen/Nuremberg, Erlangen 91058, Germany

We report on photoluminescence from Mn^{2+}-doped chalcohalide glasses of the GeS_2–Ga_2S_3–CsCl system. Upon blue excitation at 447 nm, a broad emission band occurs in the green spectral range from 500 to 600 nm, indicating the presence of tetrahedrally coordinated Mn^{2+} species. When the Mn^{2+}-concentration is increased up to 2 mol%, an increasingly intense secondary emission band evolves at about 610–660 nm. Meanwhile, the intensity of the green band decreases gradually and shifts toward the red, resulting a very flatten luminescence from 500 to 750 nm, which provides a promising white light emitting source. As for the origin of this unique luminescence behavior of Mn^{2+}, it is proposed that the ligand coordination number of Mn^{2+} in the present chalcohalide glasses experiences a partial change from tetrahedral to octahedral coordination.

I. Introduction

As an alternative to rare-earth ions (RE^{3+}), transition metal ions (TM^{n+}) and, in particular, due to high color purity and luminescence efficiency, divalent manganese ions have over decades been of large interest as optically active emission center in luminescent light sources.[1,2] Exhibiting a $3d^5$ electronic configuration, photoemission typically occurs via $^4G \rightarrow {}^6S$ transitions. The energy gap of this transition is strongly dependent on ligand field strength, and hence, luminescence may occur over a very broad spectral range.[3–5] For example, if Mn^{2+} exists in tetrahedral coordination such as in Zn_2SiO_4, the crystal field is relatively weak and luminescence typically occurs in the green spectral range.[1] On the other hand, orange or red photoluminescence may be observed from materials where Mn^{2+} ions are present in octahedral coordination, such as in phosphate or even sulfophosphate glasses and glass ceramics.[6,7] From this perspective, Mn^{2+} has been intensively studied over the last decades. However, knowledge on its properties in nonoxide chalcogenide matrices is still rather limited although such systems might be of considerable interest in, e.g., thin-film spectral converters. Usually, due to their narrow band gap, chalcogenide glasses exhibit a lower absorption edge in the infrared or red spectral region. Hence, they are not transparent in the visible region. The band gap can be broaden by incorporating halides such as KBr or CsCl into the glass, pushing the absorption edge toward the near ultraviolet (UV), while at the same time, maintaining the low maximum phonon energy of chalcogenide glasses.[10,11] Considering the complex ionic structure of chalcohalide glasses, distinct spectral properties may be expected for potential Mn^{2+} dopants.

In the present paper, we have therefore studied the optical properties of Mn^{2+}-doped GeS_2–Ga_2S_3–CsCl chalcohalide glasses by means of absorption and photoluminescence spectroscopy.

II. Experimental Procedure

Bulk glasses of nominal composition (mol%) 37.5 GeS_2–22.5 Ga_2S_3–(40−2x) CsCl–x $MnCl_2$ (x = 0.5, 0.75, 1.0, 1.5, and 2.0) were synthesized by the conventional melt-quenching method, using high-purity raw materials (Ge, Ga, and S, 5N, and CsCl and $MnCl_2$, 3N, respectively). Individual batches of 4 g were melted under vacuum in sealed silica ampoules in a rocking furnace at 900°C for 12 h. Subsequently, they were quenched in water at ambient temperature. Glass samples obtained were annealed at 300°C for 2 h in order to remove internal stresses. Specimens were cut into discs of $\varnothing$ 10 × 2 mm^3 and polished with the superfine Al_2O_3 powders for the following spectroscopic analyses. Absorption spectra were recorded on a Jasco V-570 spectrophotometer (Jasco International Co. Ltd., Tokyo, Japan). Optical excitation and emission spectra were collected with a high-resolution spectrofluorometer (Fluorolog-3, Horiba Jobin Yvon Inc., Edison, NJ) using a 450 W Xe-lamp as an excitation source. Electron paramagnetic resonance (EPR) spectra of samples were recorded on an EMX-8/2.7 EPR spectrometer (Bruker, Karlsruhe, Germany), operating in the X-band frequency (9.861 GHz). All measurements were carried out at room temperature.

III. Results and Discussion

Figure 1 depicts the typical EPR fingerprint of Mn^{2+}-centers doped into the studied glass matrices (whereby no resonance was observed in undoped glasses). As a characteristic of Mn^{2+} ions ($3d^5$, $S = I = 5/2$), the spectra exhibit a sextet of hyperfine lines centered at $g \approx 2.0$. For increasing concentration of Mn^{2+} ions, as a result of increasing degree of hyperfine interaction of Mn^{2+}–Mn^{2+} pairs and increasingly ionic character of the ligands,[9,12,13] the hyperfine structure becomes increasingly smooth and finally disappears when the Mn^{2+} concentration reaches 2.0 mol%. At this stage, only a single broad resonance can be observed. Noteworthy, in the present case, the hyperfine splitting is smaller than usually reported for oxide glasses with similar dopant concentration. Because smaller splitting typically results from a more covalent bonding character of the anion,[14] this reflects the fact that chalcohalide glasses can provide a

† Author to whom correspondence should be addressed. e-mail: gchen@ecust.edu.cn

Manuscript No. 25889. Received September 10, 2010; approved November 13, 2010.
This work was financially supported by the Shanghai Pujiang Academic Discipline Project (Project No. B502) and National Natural Science Foundation of China, No. 50872032, as well as from the German Excellence Initiative (within the cluster "Engineering of Advanced Materials – Hierarchical Structure Formation for Functional Devices") and gratefully acknowledged.

‡ Author to whom correspondence should be addressed. e-mail: lothar.wondraczek@ww.uni-erlangen.de

Solar Energy Materials & Solar Cells 95 (2011) 1590–1593

Contents lists available at ScienceDirect

Solar Energy Materials & Solar Cells

journal homepage: www.elsevier.com/locate/solmat

Efficient near-infrared downconversion in $GdVO_4:Dy^{3+}$ phosphors for enhancing the photo-response of solar cells

D.C. Yu [a], S. Ye [a], M.Y. Peng [a], Q.Y. Zhang [a,*], J.R. Qiu [a], J. Wang [b], L. Wondraczek [c]

[a] MOE Lab of Specialty Functional Materials and Institute of Optical Communication Materials, South China University of Technology, Guangzhou 510641, PR China
[b] State Key Laboratory of Optoelectronic Materials and Technologies, School of Chemistry and Chemical Engineering, Sun Yat-Sen University, Guangzhou 510275, PR China
[c] Chair of Glass and Ceramics, Department of Materials Science, University of Erlangen-Nuremberg, 91058 Erlangen, Germany

ARTICLE INFO

Article history:
Received 24 September 2010
Accepted 7 January 2011
Available online 21 February 2011

Keywords:
Solar cell
Luminescence
Downconversion
Rare earth ions
Energy transfer

ABSTRACT

Near-infrared (NIR) downconversion (DC) has been observed in a Dy^{3+}-doped $GdVO_4$ phosphor, where one ultraviolet-blue photon can be split efficiently into two NIR photons. Underlying mechanism for the process of NIR-DC is analyzed in terms of absorption spectrum, static and dynamic photoemission and monitored excitation spectra. Internal quantum efficiency is obtained up to 111% on the basis of experimental and theoretical calculation results. This enables the phosphor promising in significant enhancement of spectral response of silicon solar cells, particularly in the range of 200–500 nm.

1. Introduction

Luminescent materials with quantum efficiency (QE) exceeding unity play an important role in novel concepts for solid state lighting, information display and solar energy conversion [1–5]. In a photoluminescence process, QE exceeding unity requires that, following excitation, more photons are emitted than those involved in the excitation process [4–13]. The term near-infrared (NIR) downconversion (DC) refers to a process where a high-energy ultraviolet (UV) or visible (VIS) photon is cut into two (or more) NIR photons. With respect to state-of-the-art Si-based photovoltaic cells, NIR-DC may enable a significant increase in energy conversion efficiency. As of today, even for the most advanced technologies, this efficiency is physically (Shockley-Queisser) limited to about 30% or 68%, respectively, for single- or multiple-junction architectures [10,14]. The reason for this lies in the fact that crystalline silicon (c-Si) solar cells effectively convert only photons with energy close to the band-gap of Si ($E_g \sim 1.12$ eV) and that, additionally, even in the ideal case (no recombination), only one electron can be generated from one photon, regardless the actual photon energy. On the other hand, the incident solar spectrum exhibits its maximum at ~550 nm, and strong contributions from the soft UV to blue spectral region of relatively high photon energy [10], frequently in order to avoid long-term bleaching, these photons are even filtered from the incident light in an actual solar module. Using photoluminescent converter materials to modify the solar spectrum, especially on the high photon energy side, is therefore of significant interest for various aspects [5,15–18]. For the case of splitting one UV or blue photon into two NIR photons, for a single junction solar cell, the Shockley-Queisser limit can be increased to about 40% [19].

Herein, we demonstrate NIR-DC from a polycrystalline Dy^{3+}-doped $GdVO_4$ phosphor. Based on static and dynamic spectroscopic data, the mechanism leading to the conversion of one 200–500 nm photon to two NIR photons will be discussed in detail. Application of the NIR-DC phosphors in silicon solar cells might greatly enhance its photo-response and conversion efficiency.

2. Experimental

$GdVO_4$ and $GdVO_4$:2%Dy^{3+} polycrystals were prepared by a high-temperature solid state reaction at 1000 °C for 10 h, employing NH_4VO_3 (analytical), Gd_2O_3 (99.99%), and Dy_2O_3 (99.99%) as raw materials. X-ray diffraction (XRD, Philips PW1830, Co Kα) was measured for each product and confirmed that the samples crystallized in tetragonal space group of $I4_1/amd$ and no other crystalline phases were present in the materials. Static and dynamic photoluminescent spectra and excitation spectra were recorded with the Jobin-Yvon Triax 320. As excitation source, a 450 W Xe short-arc lamp and an 808 nm laser diode (LD), respectively, were used. For light detection, two photomultiplier tubes, Hamamatsu R5108 and red-sensitive R928, were employed, respectively. Diffuse reflection spectra were collected

* Corresponding author. Tel.: +86 20 87113681; fax: +86 20 87114204.
E-mail address: qyzhang@scut.edu.cn (Q.Y. Zhang).

0927-0248/$ - see front matter © 2011 Elsevier B.V. All rights reserved.
doi:10.1016/j.solmat.2011.01.004

Proceedings

D. Möncke, D. Palles, N. Zacharias, M. Kaparou, M. Papageorgiou, A. Oikonomou, E.I. Kamitsos, L. Wondraczek

Chemical and Spectroscopic Investigation of a Greek Glass Archaeological Collection Spanning the Mycenaean to Roman Period as Probed by SEM/EDS, IR and Raman Techniques

Int. Symp.: History, Technology and Conservation of Ancient Metal, Glasses and Enamels, 16–19 November 2011, Athens, Greece, submitted to Proceedings).

Andreas Roosen, Martin Rauscher and Nadja Straue:

Printing of Particulate Structures in the Micrometer Range for Microelectronic Application

Proc. 12th Annual Meeting of International Union of Materials Research Societies (IUMRS) 2011, Taipei, Taiwan, 19 – 22 September 2011, paper 465

Books

X. Yin, N. Travitzky, P.Greil

Reactive Infiltration Processing of Ti_3AlC_2 and Ti_3SiC_2-Based Composites

Chapter 3 in: MAX Phases: Microstructure, Properties and Applications

ISBN 978-1-61324-182-0 Editors: It-Meng Low and Yanchun Zhou, pp.

© 2011 Nova Science Publishers, Inc.

Patents

B. Faltus, J. Gegner, P. Greil, H. Herbst, J. Hofmann, L. Schlier, N. Travitzky, H. Velde

Rollkörper

Ger. Offen. (2011) 2011E00143 DE

B. Faltus, J. Gegner, P. Greil, H. Herbst, J. Hofmann, L. Schlier, N. Travitzky, H. Velde

Keramikrollen und Keramikliner

Ger. Offen. (2011) 2011E00142 DE

B. Faltus, J. Gegner, P. Greil, H. Herbst, J. Hofmann, L. Schlier, N. Travitzky, H. Velde

Gleitringe für Gleitringdichtungen aus polymerabgeleiteter Keramik

Ger. Offen. (2011) 2011E00394 DE

4. CONFERENCES, WORKSHOPS, SEMINARS, LECTURES, AWARDS

German-Japanese Seminar on Advanced Ceramic Materials

Established in 2010 the cooperation between the Friedrich-Alexander University of Erlangen-Nuernberg (FAU) and the Nagoya Institute of Technology (NITech) centres on education and research in the field of advanced ceramic materials. Topic areas of joint research and training activities include biomaterials, electric functional materials, environmental and engineering materials. Until November 2011 eight students and faculties from NITech and four from FAU have visited the partners laboratories for short term up to several months.

In March 2011 the 1st joint seminar on advanced ceramic materials was organized at Erlangen. The 2nd seminar took place from November 24–25, 2011 and presented more than twenty oral and poster contributions from young researchers and students of NITech and FAU. Microstructure design, processing and property optimization of advanced ceramics to be applied in regenerative medicine, energy conversion, and environmental protection were discussed.

Poster presentation in the technical hall

We want to thank all participants contributing to the seminar program and our faculty colleagues from NITech and FAU for actively supporting the exchange program. The international offices staff of both universities is acknowledged for their organizational help. Finally we want to express our gratitude to the financial support provided from JSPS (Japan) and from DFG (Germany) for making possible the stimulating cooperation.

Conferences organised by members of the Institute

A. Roosen

Member of the Program Committee and Session Chair, Annual Meeting of the Deutsche Keramische Gesellschaft, Saarbrücken, 28th–30th March 2011

A. Roosen

Session Chair, 7th International Conference and Exhibition on Ceramic Interconnect and Ceramic Microsystems Technologies, San Diego, CA, USA, 05th–7th April 2011

A. Roosen

Chair of the Topical Symposia "Multilayer Ceramics", 12th Conference of the European Ceramic Society, Stockholm, Sweden, 19th–23rd June 2011

A. Roosen

General Chair of the DKG-Symposium „Characterization in Ceramics Processing: From Powders to Green Bodies", Erlangen, Germany, 29th–30th November 2011

A. Roosen

Member of the Program Committee and Session Chair, Workshop on "Handling of Highly-Viscous Systems", Eisenach, Germany, 8th–10th October 2011

N. Travitzky

Symposium Organiser: „Additive Manufacturing with advanced materials", EUROMAT 2011 12th–15th Sept. Montpellier, France.

Science Night

Science Night (Lange Nacht der Wissenschaften) on October 22nd, 2011 involved a large number of institutes in the region of Erlangen, Fürth and Nuremberg. From 6 pm up to 1 am the department of material science opened the lab doors to show interested public exclusive experiments and latest research results in a common way. The Chair of Glass and Ceramics offered the following attractions:

- 3D-movie with red/green glasses on cellular ceramic structures
- Use of ultrasonic sensor application in a racing course with remote motor racing cars
- Two glass artists showed their fantastic handcraft in blowing beautiful glass ware.

The technical hall, was illuminated red and green and Prof. Zollfrank's band was playing music.

Gathering audience of interested visitors in the institute's technical hall.

Workshops

4th Advanced Training Course on "Tape Casting and Ceramic Multilayer Technology", University of Erlangen, 15th February 2011

The ceramic multilayer technology offers a number of opportunities for the manufacture of miniaturized and highly integrated parts, layered composite materials as well as complex 3D shapes. The aim of the training course was to explain and demonstrate the manufacture of green tapes. The interrelation between the characteristics of the green tape and the subsequent processing steps were explained (punching, metallization, stacking, lamination, binder burn out and sintering).

Prof. Andreas Roosen, University of Erlangen-Nuremberg, Institute of Glass and Ceramics: Ceramics Multilayer Technology and typical products

Dipl.-Ing. Stefan Schäfer, University of Erlangen-Nuremberg, Institute of Particle Technology: Dispersion process.

Dipl.-Ing. Nadja Straue, University of Erlangen-Nuremberg, Institute of Glass and Ceramics: Preparation of tape casting slurries

Dipl.-Ing. (FH) Ingo Götschel, University of Erlangen-Nuremberg, Institute of Glass and Ceramics: Tape casting process

Dipl.-Ing. Armin Dellert, University of Erlangen-Nuremberg, Institute of Glass and Ceramics: Drying process and green tape properties

Dr. Torsten Rabe, BAM, Berlin: Punching and structuring

Dipl.-Ing. (FH) Frieder Gora, W.C. Heraeus, Hanau: Metallisation via screen printing

Prof. Andreas Roosen, University of Erlangen-Nuremberg, Institute of Glass and Ceramics: Stacking and lamination

Dipl.-Ing. Michael Beck, University of Erlangen-Nuremberg, Institute of Glass and Ceramics: Binder burnout and co-firing

Dr. Michael Frank, Kuraray Europe GmbH, Frankfurt am Main: Mowital, a binder for ceramic tape casting

Invited Lectures

A. Dellert (V), A. Roosen **29.11.11**

Messung von Trocknungsspannungen an Schichten über die Durchbiegung flächiger Substrate

DKG-Symposium „Characterization in Ceramics Processing: From Powders to Green Bodies“, Erlangen, Germany

T. Fey **30.10.11**

Cellular Ceramics

Bremen Gradporenet, Bremen

T. Fey, B. Ceron-Nicolat, P. Greil **23.01.11**

Cell-size effect in cellular Ceramics

35th International Conference and Exposition on Advanced Ceramics and Composites, Daytona Beach, Florida

T. Fey, R. Kaiser, P. Greil **28.03.11**

Berechnung von Packungsdichten (Lee/McGeary/Dinger/Funk) - Vorstellung eines .NET-basierenden Softwaretools

DKG-Jahrestagung 2011, Saarbrücken

P. Greil **02.05.11**

Rapid Prototyping von Keramik

University of Jena, Material Sciences Colloquium

P. Greil **21.06.11**

Advancements in Polymer-Filler Derived Ceramics

ECerS XII Stockholm, Sweden

P. Greil **25.10.11**

Design and generic principles of self-healing ceramic materials

DGM Symposium High Performance Ceramics, Karlsruhe, Germany

D. Möncke, A. Herrmann, D. Ehrt, M. Friedrich, N. Da, L. Wondraczeck, I. Konidakis, E.I. Kamitsos **06.10.11**

Einbau und Bindungsverhältnisse des Indikatorions Mn^{2+} in verschiedensten Gläsern – Korrelation von EPR und Fluoreszenz-Spektroskopie

Sitzung des Fachausschusses I "Physik und Chemie des Glases“, Erlangen, Germany

D. Möncke, D. Ehrt **04.09.11**

Photo-Ionization of Transition Metal doped Glasses

The International Conference on the Chemistry of Glasses and Glass-Forming Melts in celebration of the 300th anniversary of the birth of Mikhail Vasilievich Lomonosov", Oxford, England

D. Möncke, D. Ehrt, E.I. Kamitsos **21.08.11**

Spectroscopic Study of Manganese-Containing Borate and Borosilicate Glasses: Cluster Formation and Phase Separation

Borate 7 "7th International Conference on Borate Glasses, Crystals, and Melts", Halifax, Canada

D. Möncke, D. Palles, E.I. Kamitsos, L. Wondraczek, N. Zacharias,M. Papageorgiou, M. Kaparou, A. Oikonomou **25.09.11**

Glass Structure of Historic Greek samples from the Mycenaean to Roman Period probed by Infrared and Raman Spectroscopy

The Fifth Balkan Conference on Glass Science and Technology and the 17th Conference on Glass and Ceramics, Nessebar, Bulgaria

D. Möncke, D. Palles, N. Zacharias, M. Kaparou, M.Papageorgiou, A. Oikonomou, E. I. Kamitsos, L. Wondraczek **06.11.11**

Chemistry, Structural and Technological Examination of a Greek Glass Archaeological Collection Spanning from the Mycenaean to Roman Period probed by SEM/EDS, IR and Raman Spectroscopy

International Symposium „History, Technology and Conservation of Ancient Metal, Glasses and Enamels"6-19 November 2011, Athens, Greece

A. Roosen (V), A. Dellert **29.11.11**

Partikelformanalyse und deren Bedeutung für die Ermittlung von Schwindungsanisotropien

DKG-Symposium „Characterization in Ceramics Processing: From Powders to Green Bodies", Erlangen, Germany

A. Roosen (V), I. Götschel **09.12.11**

Nutzung des Foliengießverfahrens zur Herstellung mehrlagiger Feuerfest-Verbundwerkstoffe

2nd Freiberger Feuerfestforum, Freiberg, Germany, 9th December 2011

A. Roosen (V), P. Vozdecky **08.10.11**

Verarbeitung nanoskaliger Partikel zu keramischen Folien

Workshop on "Handling of Highly-Viscous Systems", Eisenach, Germany

A. Roosen **07.11.11**

Progress in Tape Casting and Multilayer Processing of Ceramic Materials

Workshop on "Optimized Processing of Multimaterial Architectures", Risø, Denmark

A. Roosen **19.06.11**

Particle orientation in tape cast products and its impact on shrinkage

12th Conference of the European Ceramic Society, Stockholm, Sweden

A. Roosen **19.09.11**

Printing of Particulate Structures in the Micrometer Range for Microelectronic Applications

12th Annual Meeting of International Union of Materials Research Societies (IUMRS) Taipei, Taiwan

A. Roosen **23.09.11**

Tape Casting and Printing as Combinable Techniques to Manufacture Electronic Devices

Colloquium at Cheng-Kung University, Tainan, Taiwan

A. Roosen **27.07.11**

Drucktechnische Herstellung von partikulären Strukturen im Mikrometer-Bereich

Wissenschaftliches Kolloqium, KIT, Karlsruhe

N. Straue (V), A. Roosen **27.10.11**

Die Viskosität: ein entscheidender Parameter bei der Rezepturentwicklung in der Keramik.

5th Workshop Rheology of the chair "Polymer Science", University of Erlangen-Nuremberg

N. Straue **12.01.11**

Keramische Prozesstechnik und ihr Anwendungspotential im Bereich der gedruckten Elektronik

Seminar of the Chair "Multiscale Simulation of Particulate Systems", University of Erlangen-Nuremberg, Erlangen

N. Travitzky **07.11**

Additive Manufacturing of Complex Ceramic Parts

Workshop: "Additive manufacturing of ceramic components", Rheinbach, Germany

Awards

V. Bürger (supervised by A. R. Boccaccini & L. Wondraczek)
Effect of residual stresses on bioactive glass bioreactivity. M.Sc.-Thesis**,**
Oldfield-Award (joint 1st): Award presented at SGT Annual Meeting, Oxford, UK

N. Da
STIBET-fellowship (6 months), DAAD

U. Deisinger, K. Schindler, A. Roosen
Fabrication of complex ceramic 3D structures with internal channels by using cold low pressure lamination
Poster Award, "Multilayer Ceramics", ECERS, Stockholm, Sweden

S. Krolikowski, S. Reibstein, K. Nielsen, L. Wondraczek
Viscosity-temperature-pressure dependence in low-melting glasses
AFPG9 Travel Award to Attend the 9th Conference on Advances in Fusion and Processing of Glasses, presented at the conference, Cairns, Australia

K.H. Nielsen, N. Da, S. Reibstein, S. Krolikowski, D. de Ligny, B. Champagnon, S. Sirotkin, J.-P. Simon, O. Grassme, G. Peters, L. Wondraczek
Struktur-Eigenschaftsbeziehungen in ionischen Sulfophosphatgläsern
Best Poster Award (2nd): 85. Glastechnische Tagung, Saarbrücken

S. Reibstein, D. De Ligny, S. Krolikowski, S. Sirotkin, J.-P. Simon, H. Behrens, B. Champagnon, L. Wondraczek
Heterogeneity and structural relaxation of compressed borate-silicate glasses.
DAAD Travel Grant to Attend the 7th International Conference on Borate Glasses, Crystals, and Melts, Halifax, Canada

A. Roosen
Partikelformanalyse und deren Bedeutung für die Ermittlung von Schwindungsanisotropien
cfi-Best Paper-Award, DKG-Symposium „Characterization in Ceramics Processing: From Powders to Green Bodies", Erlangen, Germany, 29th–30t^{h} November 2011

N. Straue

Continuous Manufacture of Submicron Thick Ceramic Green Tapes and Coatings Demonstrated for TCO Nano Particles

Best Student Paper Award, 7th International Conference and Exhibition on Ceramic Interconnect and Ceramic Microsystems Technologies, San Diego, CA, USA, 5th–7th April 2011

A. Winterstein (supervised by L. Wondraczek & H. Ebendorff-Heidepriem)

Development of Optically Active Germanate Glasses for Photonic Crystal Fibres, M.Sc.-Thesis

Oldfield-Award (2nd) Award presented at SGT Annual Meeting, Oxford, UK

Dr. Y. Gueguen

Professor Position, Université de Rennes1, Rennes, France

W. Zhang

CRC-fellowship (12 months) to conduct research on glasses for solar spectral conversion Chinese Research Council 2011

5. ADDRESS AND MAP

Department of Materials Science - Glass and Ceramics

Friedrich-Alexander University of Erlangen-Nuremberg

Martensstr. 5

91058 Erlangen, GERMANY

Phone: ++49-(0) 9131-852-7543 (Secretary)

Fax: ++49-(0) 9131-852-8311

E-mail: ww3@ww.uni-erlangen.de

Internet: http://www.glass-ceramics.uni-erlangen.de/

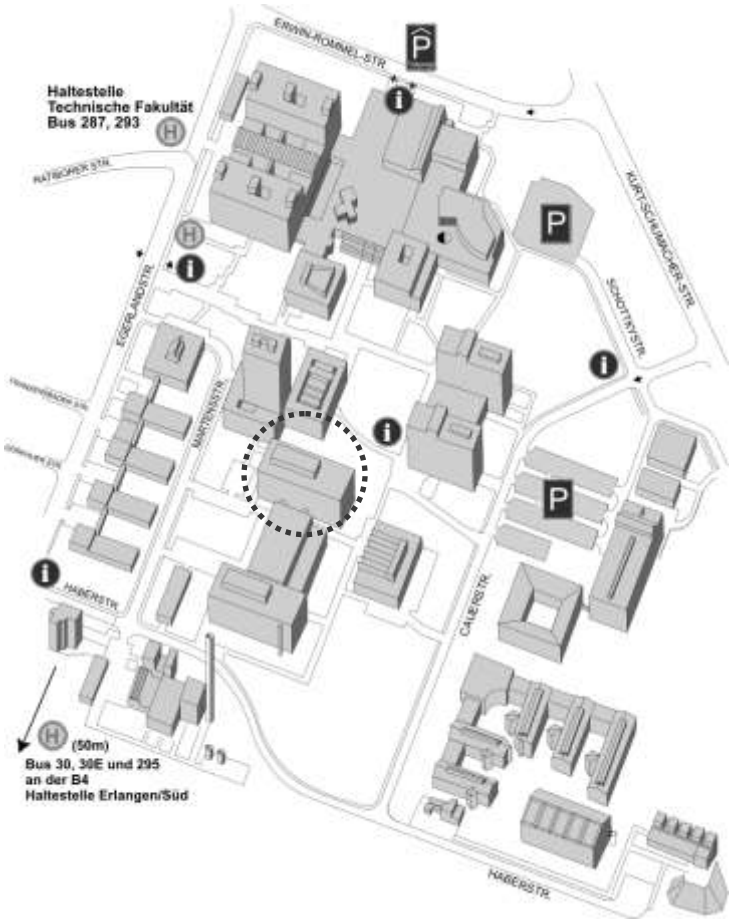

By car:

Highway A3 exit **Tennenlohe**; direction to Erlangen (B4).
Follow the signs **„Universität Südgelände**".
After junction „**Technische Fakultät**" please follow the map.

By train:

Railway station **Erlangen**.
Bus line No. 287 direction „**Sebaldussiedlung**".
Bus Stopp „**Technische Fakultät**".
50 meters to a layout plan; search for „**Institut für Werkstoffwissenschaften**".

http://www.glass-ceramics.uni-erlangen.de/Home/contact.htm

Institute of Advanced Materials and Processes (ZMP)

Dr.-Mack-Strasse 81

Technikum, Ebene 3

D-90762 Fürth

Tel.: ++49-(0) 911-950918-10

Fax: ++49-(0) 911-950918-15

Internet: http://www.zmp.uni-erlangen.de/

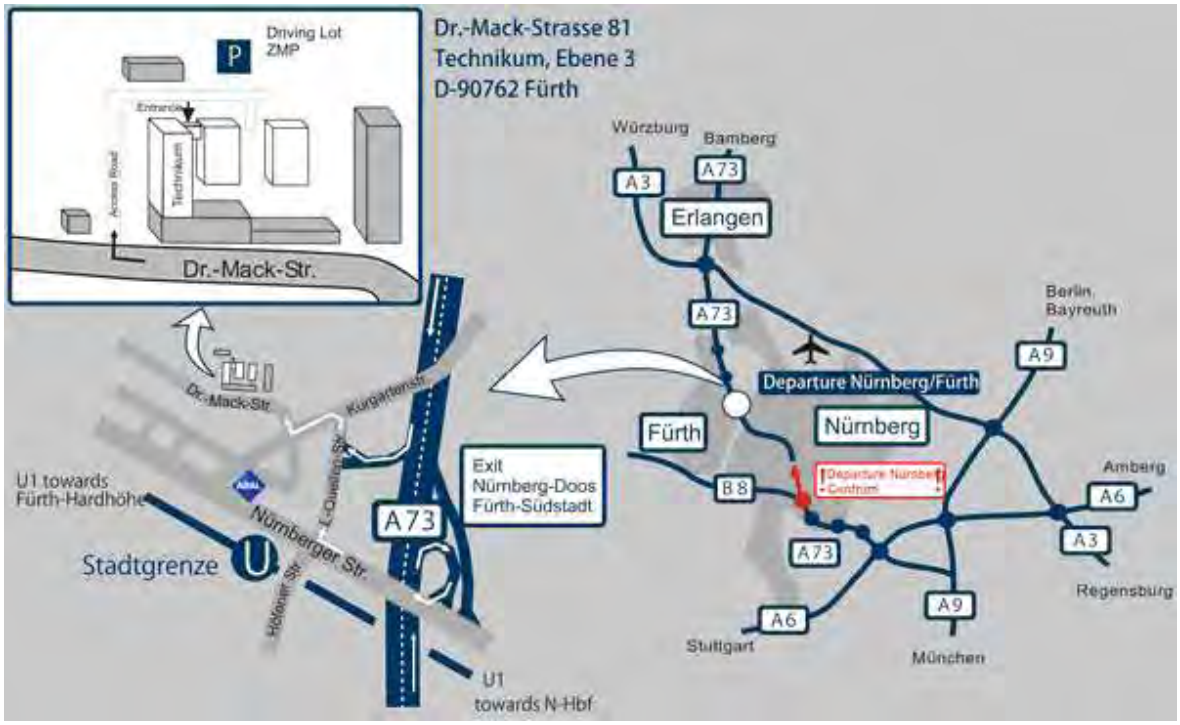

http://www.zmp.uni-erlangen.de/anfahrt/

Pratum Fürth

Friedrich-Alexander University of Erlangen-Nuremberg

Dr. Mack Str. 77

D-90762 Fürth

6. IMPRESSUM

Peter Greil

Department of Materials Science – Institute of Glass and Ceramics

Martensstraße 5

91058 Erlangen